

9-26-2008

Proteomic Analysis of the Response of Pseudomonas Aeruginosa PAO1 to the Cell to Cell Signaling Molecule Trans, Trans-farnesol of Candida Albicans

Shelby L. Jones-Dozier
Georgia State University

Follow this and additional works at: https://scholarworks.gsu.edu/biology_diss



Part of the [Biology Commons](#)

Recommended Citation

Jones-Dozier, Shelby L., "Proteomic Analysis of the Response of Pseudomonas Aeruginosa PAO1 to the Cell to Cell Signaling Molecule Trans, Trans-farnesol of Candida Albicans." Dissertation, Georgia State University, 2008.
https://scholarworks.gsu.edu/biology_diss/84

This Dissertation is brought to you for free and open access by the Department of Biology at ScholarWorks @ Georgia State University. It has been accepted for inclusion in Biology Dissertations by an authorized administrator of ScholarWorks @ Georgia State University. For more information, please contact scholarworks@gsu.edu.

PROTEOMIC ANALYSIS OF THE RESPONSE OF *PSEUDOMONAS AERUGINOSA* PAO1
TO THE CELL TO CELL SIGNALING MOLECULE TRANS, TRANS- FARNESOL OF
CANDIDA ALBICANS

A Dissertation

Presented in Partial Fulfillment of Requirements for the Degree of Doctor of Philosophy in the
College of Arts and Sciences

Georgia State University

2008

by

Shelby Lynn Jones-Dozier

Committee:

Dr. George E. Pierce, Chair

Dr. Sidney Crow, Jr., Member

Dr. Jayne B. Robinson, Member

Date

Dr. P. C. Tai
Department Chair

PROTEOMIC ANALYSIS OF THE RESPONSE OF *PSEUDOMONAS AERUGINOSA* PAO1
TO THE CELL TO CELL SIGNALING MOLECULE TRANS, TRANS- FARNESOL OF
CANDIDA ALBICANS

By

SHELBY LYNN JONES-DOZIER

Under the Direction of Dr. George E. Pierce

ABSTRACT

Nosocomial infections associated with implanted medical- devices are on the rise due to a growing immunocompromised patient population. The organisms of interest in this study are *Pseudomonas aeruginosa* and *Candida albicans*. These organisms are opportunistic pathogens and are frequently implicated as the cause of infection and colonization of medical devices. *P. aeruginosa* is a motile gram-negative bacterium that is able to suppress the growth of *C. albicans*. Quorum sensing mimicry and biofilm formation on the hyphal surface of *C. albicans* by *P. aeruginosa* aids in suppression. *C. albicans* is a dimorphic fungus capable of quorum sensing with *E,E*-farnesol and is a central focus in this work. The goal of this project is to determine changes in protein expression when *P. aeruginosa* is exposed to *E,E*-farnesol using 2D DIGE®. Changes in the cytosolic proteome of *P. aeruginosa* expose metabolic shifts that result in suppression of *C. albicans*. This work summarizes the effect of growth phase and concentration of *E,E*-farnesol on *P. aeruginosa* PAO1 and GSU3. Preliminary results reveal a general response of *P. aeruginosa* to *C. albicans* as changes in relevant metabolic nodes that affect pyocyanin production and the induction of virulence factors that lead to the killing of *C. albicans*. The overall goal of this study was to generate a profile of protein expression where a variety of conditions to further characterize the response could be easily assayed.

INDEX WORDS: *P. aeruginosa*, *C. albicans*, Proteomics,
Nosocomial infections, Quorum Sensing, Attachment, Medical
Devices

PROTEOMIC ANALYSIS OF THE RESPONSE OF *PSEUDOMONAS AERUGINOSA* PAO1
TO THE CELL TO CELL SIGNALING MOLECULE TRANS, TRANS- FARNESOL OF
CANDIDA ALBICANS

by

SHELBY LYNN JONES-DOZIER

A Dissertation Submitted in Partial Fulfillment of the Requirements for the Degree of

Doctor of Philosophy

in the College of Arts and Sciences

Georgia State University

2008

Copyright by
Shelby Lynn Jones-Dozier
2008

PROTEOMIC ANALYSIS OF THE RESPONSE OF *PSEUDOMONAS AERUGINOSA* PAO1
TO THE CELL TO CELL SIGNALING MOLECULE TRANS, TRANS- FARNESOL OF
CANDIDA ALBICANS

by

Shelby Lynn Jones-Dozier

Committee Chair: George E. Pierce

Committee: Sidney Crow, Jr.
Jayne B. Robinson

Electronic Version Approved:

Office of Graduate Studies
College of Arts and Sciences
Georgia State University
September 2008

DEDICATION

I would like to dedicate this work to my parents who always supported me to achieve great things in life and to keep a level head. I would also like to dedicate this work to my grandparents who always told me that I would do great things if I worked hard for it. I would like to dedicate this work to Adam Dozier, Audrey Dozier, and Tyler Dozier who consistently helped me find focus, when it was easy to wander. I would like to dedicate this work to my friends, who did not always understand what I was talking about, but remained interested and helped me to see the big picture.

ACKNOWLEDGEMENTS

With sincere gratitude I would like to thank my advisors, George E. Pierce, Sidney A. Crow, and Jayne B. Robinson. I would also like to thank all of my colleagues, past and present, and lab-mates for helping me through all of the ups and downs of this project. I would like to also extend a special thanks to Dr. Carmen Eilertson for acting as an exceptional mentor to help me find where my passions were hiding and always encouraging me when times got rough.

TABLE OF CONTENTS

DEDICATION		iv
ACKNOWLEDGEMENTS		v
LIST OF TABLES		viii
LIST OF FIGURES		xi
CHAPTER		
1	INTRODUCTION	1
	Background	2
	Nosocomial Medical-Device associated infections	2
	Quorum sensing	7
	Interactions between <i>Pseudomonas</i> <i>aeruginosa</i> and <i>C. albicans</i>	9
	<i>C. albicans</i> and Medical-Devices	14
	<i>P. aeruginosa</i> and Pyocyanin	17
	Farnesol	22
	Quorum-sensing disruption in nature and the potential use in the clinic	27
	Objectives of this work	30

2	MATERIALS & METHODS	31
	Strains and cultivation	31
	Cell cultivation and harvest	33
	Cell disruption	34
	Protein quantification	37
	Protein assay for 2D proteomics	37
	CyDye® labeling	38
	First dimension Isoelectric focusing	43
	Equilibration of IEF gel strips	47
	Second dimension SDS PAGE	48
	Casting SDS PAGE gels	48
	Imaging and analysis	51
	Spot excision	53
	Protein digestion (Trypsinization)	54
	Zip-tipping® and MALDI TOF-TOF	55
	Proteomics experimental set-up	56

	Growth on <i>E,E</i> -farnesol and alternative carbon sources	61
	Low-osmolarity growth	62
	<i>C. elegans</i> virulence assay	63
	MIC assay- Tobramycin	64
	Imaging cell morphology	66
	Pyruvate dehydrogenase activity assay	66
3	RESULTS	68
4	DISCUSSION	99
REFERENCES		116
APPENDICES		136

LIST OF TABLES

Table 1: Microbiological profile of adult Cystic Fibrosis patients	12
Table 2: Matrix of pairing of samples for randomization	40
Table 3: Isoelectric focusing protocol for a 24-centimeter Imoboline pH 3-11 strip, at 50 μ A per strip	46
Table 4: Isoelectric focusing protocol for a 24-centimeter Imoboline pH 4.5-5.5 strip, at 50 μ A per strip	47
Table 5: Sample organization for MIC assay	65
Table 6: Summary of identified proteins by proteomic analysis of <i>Pseudomonas</i> <i>aeruginosa</i> PAO1 exposed to 25 μ M <i>E,E</i> -farnesol in IPG range of 4.5 to 5.5	76
Table 7: Mass-spectrometry identified proteins from proteomics project of <i>P. aeruginosa</i> PAO1 biofilm exposed to 250 μ M <i>E,E</i> -farnesol	85
Table 8: Mass-spectrometry identified proteins from proteomics project of co- culture between <i>P. aeruginosa</i> PAO1 and <i>C. albicans</i> SC5314	87
Table 9: Growth curve of <i>P. aeruginosa</i> PAO1 exposed to 250 μ M <i>E,E</i> - farnesol under low osmolarity conditions	90
Table 10: Effect of <i>E,E</i> -farnesol on <i>P. aeruginosa</i> PAO1 virulence in <i>C.elegans</i> fast killing assay	92
Table 11: Enzyme activity of Pyruvate Dehydrogenase	94

Table 12: The effect of exposure to 250 μ M *E,E*-farnesol on antibiotic susceptibility 96
in *P. aeruginosa* PAO1

LIST OF FIGURES

Figure 1: Interaction between <i>C. albicans</i> and <i>Pseudomonas aeruginosa</i>	13
Figure 2: Stages of biofilm formation in <i>C. albicans</i>	15
Figure 3: Regulatory pathway for the biosynthesis of pyocyanin	21
Figure 4: Molecular structure of <i>E,E</i> -farnesol	22
Figure 5: Molecular regulatory pathways to control dimorphism in <i>Candida albicans</i>	26
Figure 6: Schematic diagram for set-up of microtip sonication for packed cell pellet of <i>P. aeruginosa</i>	35
Figure 7: Diagram sample for randomization of CyDye® labels	39
Figure 8: Workflow for CyDye® labeling	42
Figure 9: Isoelectric point of peptides	44
Figure 10: Overview of approach to identify proteins of interest in DeCyder® version 6.5 and ImageMaster® Platinum version 6	52
Figure 11: Ettan Dalt Spot Picker	53
Figure 12: Diagram of experimental set-up for flow-through biofilm	59
Figure 13: DeCyder image of Flagellin B as identified by proteomic analysis of <i>Pseudomonas aeruginosa</i> PAO1 with 30 µM racemic farnesol in the pI range of 3-11	71
Figure 14: DeCyder image of GMP synthase as identified by proteomic	

analysis of <i>Pseudomonas aeruginosa</i> PAO1 with 30 μ M racemic farnesol in the pI range of 3-11	73
Figure 15: DeCyder image of Dihydrolipoamide dehydrogenase as identified by proteomic analysis of <i>Pseudomonas aeruginosa</i> PAO1 with 30 μ M racemic farnesol in the pI range of 3-11	74
Figure 16: DeCyder image of ATPase PilB as identified by proteomic analysis of <i>Pseudomonas aeruginosa</i> PAO1 exposed to 25 μ M <i>E,E</i> -farnesol	77
Figure 17: DeCyder image of Major porin and structural outer membrane porin OprF precursor as identified by proteomic analysis of <i>P. aeruginosa</i> PAO1 exposed to 25 μ M <i>E,E</i> -farnesol	78
Figure 18: DeCyder image of Amidase as identified by proteomic analysis of <i>Pseudomonas aeruginosa</i> PAO1 exposed to 25 μ M <i>E,E</i> -farnesol	79
Figure 19: DeCyder image of Arginine diminase as identified by proteomic analysis of <i>P. aeruginosa</i> PAO1 exposed to 25 μ M <i>E,E</i> -farnesol	80
Figure 20: DeCyder image of NAD- dependent glutamate dehydrogenase as identified by proteomic analysis of <i>P. aeruginosa</i> PAO1 exposed to 25 μ M <i>E,E</i> -farnesol	81

Figure 21: DeCyder image of Pore region OprF (outer membrane protein and related peptidoclycan-associated (lipo)proteins) as identified by proteomic analysis of <i>P. aeruginosa</i> PAO1 exposed to 25 μ M <i>E,E</i> -farnesol	82
Figure 22: DeCyder image of Aconitase as identified by proteomic analysis of <i>Pseudomonas aeruginosa</i> PAO1 exposed to 25 μ M <i>E,E</i> -farnesol	83
Figure 23: Illustration of proteins found in common in biofilm, co-culture, and planktonic experimental conditions	88
Figure 24: Image of <i>P. aeruginosa</i> GSU3 exposed to 250 μ M <i>E,E</i> -farnesol and 0.8 μ g/ml Tobramycin	97
Figure 25: Image of <i>P. aeruginosa</i> GSU3 exposed to 0.8 μ g/ml Tobramycin	98
Figure 26: Biofilm formation of <i>S. aureus</i> and uptake of ethidium bromide when exposed to <i>E,E</i> -farnesol	109
Figure 27: Antibiotic susceptibility patterns when <i>S. aureus</i> grown in the presence of <i>E,E</i> -farnesol	110
Figure 28: Schematic for proposed role of OprF in sensing activation of t-cells by the detection of IFN-gamma	112

Introduction

The goal of this dissertation was to explore through the use of expression proteomics the dynamic interplay that occurs between *P. aeruginosa* and *C. albicans*. Both of these organisms are important opportunistic pathogens in the health-care setting. *P. aeruginosa* is most notably associated with Cystic Fibrosis patients, in whom it is one of the leading causes of chronic lung infections and death due to damage to the lung tissue (Gilligan, 1991). Infections caused by *C. albicans* are most notably associated with patients undergoing cancer treatment, diabetes mellitus, or infection with human immunodeficiency virus (Kao, *et al.*, 1991). Both of these microorganisms warrant study due to the significant roles they play in device associated nosocomial infections. The variety of infections attributed to these two organisms are linked to the type of indwelling medical- device in place within the patient. Device types such as central-venous catheters, urinary catheters, and mechanical ventilators are commonly colonized and the type of disease they cause is directly linked to the insertion site of the device. For example, blood-stream infections resulting from the colonization of central-venous catheters to ventilator-associated pneumonia in patients requiring mechanical respiration (Pierce, 2005).

A third compelling reason to study the interplay of these organisms is based on clinical data that suggests that *P. aeruginosa* and *C. albicans* may suppress the growth and virulence of one another through a variety of mechanisms (Kerr, 1994; Burns, 1999). A thorough understanding of this complex relationship has the potential to better prevent infections by exploiting the well-developed tactics used by *Pseudomonas* and *Candida* for controlling growth and virulence of competing microorganisms

Background

Nosocomial medical-device associated infections:

Approximately two million nosocomial infections occur each year (Halye, 1985; Bunting, 2005), accounting for roughly 5% of all patients admitted into a hospital resulting in 90,000 to 100,000 deaths annually in the United States (Buntin, 1999; Starfield, 2000). Antibiotic resistant organisms cause approximately 70% of nosocomial infections and the remaining 30% are caused by infections associated with indwelling medical devices (Safdor, 2001; Burke, 2003).

Installation of a urinary catheter, composed of medical grade materials including silicone and latex, is inserted into the urethra until the tip of the catheter reaches the bladder. Upon insertion it is possible to introduce microorganisms from the external surface of the urethra into the deeper and sterile regions of the urinary tract. If there is a urinary tract infection already in progress at the time of insertion, the catheter surface may allow the organisms to penetrate further into the urinary tract or provide a substrate for biofilm formation. Approximately 40% of nosocomial infections are catheter associated urinary tract infections (CAUTI). In the United States, one million cases of UTI were reported, of which 80% were classed as CAUTI.

The Edmond M. SCOPE project (1995-2002) (Wisplinghoff, *et al.*, 2004) identified the causative agents of blood-stream infections (BSI) and ranked them according to rate of incidence. *Candida* species were the fourth most common isolate, responsible for 9% of total patients and *P. aeruginosa* was the seventh most common isolate, responsible for 4.3% of total

patients with a sample size in this study of 20,000 patients. The prevalence of these two organisms in association with multiple device types and a robust ability to form biofilm on medical grade materials are two major reasons for the focus of this study.

Historically, the medical community has viewed hospital- acquired infections as a normal part of medical practice. The perception pervaded that infections of this type were inevitable resulting from immunologically suppressed patients with non-communicable diseases. Innovative medical technology has lead to increased reliance on the use of medical devices and treatment strategies that suppress the immune system. The rate of nosocomial infections and deaths related to these infections increased to the point that questions were asked as to their source. This drew a great deal of scrutiny on the health care delivery system from government regulators, the CDC, private insurance companies, and the general public.

Epidemiological data has provided information about how non-communicable diseases are commonly spread by the health care worker among immunologically suppressed patient populations. This data has transformed the perception that non-communicable infections among hospital patient populations are inevitable into one where nosocomial infections are preventable. Gerberding reported this shift in attitude in 2002 as one of many papers aimed determining the suspected origins of this infection type and approaches towards mitigating the incidence of nosocomial infections.

Nosocomial infections, or health-care setting acquired infections, are the fourth leading cause of death in the United States, following stroke, cancer, and heart disease. Adding to the staggering death toll related to nosocomial infections is the high financial cost. In 2002, \$6.5

billion dollars were spent to treat nosocomial infections and were paid in large part by third party payers, such as Medicare or private insurance companies. (Weinstein, 1998; Jarvis, 2001) In Pennsylvania, the treatment of nosocomial infections cost Medicaid and the State Employee's Benefits plan \$125 million dollars and private insurance companies \$1 billion dollars (Buntin, 2005). In 2007, the New York Times reported that Medicare would no longer pay for the treatment of nosocomial infections after October 2008, as a part of the pay for performance policy that makes health care facilities responsible for the delivery of good health care (Glickman, *et al.*, 2007). In a statement to congress by Mike E. Miller, Ph.D. on behalf of the Medicare Payment Advisory Commission in July 2005, he states the ultimate goal of the pay for performance program is to remove the inequity of equal payment to physicians that provide inadequate care to those who meet or exceed patient needs.

Research has shown that simple changes, like hand washing, improved cleaning protocols of common-use equipment, and improved environmental controls within the health-care environment can play a drastic role at reducing the incidence of nosocomial infections. Professional organizations such as the Association for Professionals in Infection Control and the Society for Healthcare Epidemiology of America include as a part of their mission statement to educate medical professionals and collect accurate data on the incidence of nosocomial infection.

It is crucial to possess a thorough understanding of the biology of the microorganisms that cause device-associated nosocomial infections in order to design effective treatment strategies. In an early study by Elek and Conen published in 1957, it was shown that the inoculum size of a pathogen required to cause infection was much lower when a foreign body, such as a medical device, was present. This work suggested that the presence of the medical device compromises

the primary and secondary defenses of the immune system so that fewer invading organisms are needed to cause an infection. Treatment strategies designed for traditional infections, that do not include the presence of a foreign body, are highly ineffective when an implanted medical-device is present.

Indwelling medical devices present an ecological niche that may be exploited by microorganisms. Major factors that play a role in the incidence of medical -device associated infections include the materials used in the device's construction, the breach of anatomical barriers at the point of placement within the patient, and the type of coatings applied to the device surface (Stone, *et al.*, 1999; Ramage, *et al.*, 2006; Backovic, *et al.*, 2007). The materials used in the construction of medical devices are commonly medical grade latex or silicone. These materials provide a prime substrate that is permissive for the adhesion of host proteins and in the primary attachment of microorganisms that lead to biofilm development. It has been documented that the initial deposition of host proteins on the device surface plays an important role in facilitating the attachment of microorganisms to the device surface (Denstedt, 1998; Trautner, 2004). A second significant factor in the role that medical devices play in the incidence of infection is the breach in primary anatomical barriers that normally prevent entry of microorganisms into sterile regions of the body such as the blood stream, lungs, or bladder (Trautner, *et al.*, 2004).

Shortages in medical staff have been implicated as one possible reason for the oversight of urinary catheters left in place for extended periods of time. A vicious cycle is created where more patients become critically ill from devices left in place beyond the recommended period of use thus, requiring more care and more attention from the medical staff

when the infection could have been prevented. Once an infection has developed in association with the abiotic surface of the medical device these colonizing organisms become extremely difficult to treat with traditional antibiotics. In fact, antibiotics are regarded as one of the least effective methods to treat all types of devices associated infections (Trautner, *et al.*, 2004). The method, recommended by the Centers for Disease Control, to treat these infections involve the removal of the medical devices at regular intervals after 72 hours of use. Due to the refractory nature of microorganisms within a biofilm on the surface of an implanted medical-device to antibiotic therapy the device must be removed and replaced if medically necessary to aid is one major reason to remove the device. It was reported by Kojic *et al.* in 2004 that if a device is not removed it is possible for the infection to reoccur once antibiotic therapy is complete.

Timely removal is another essential element to tackling the problem associated with nosocomial medical-device associated infections. Astonishingly, in a study by Saint *et al.*, 2000, that was directed at identifying the number of non-essential urinary catheters it was reported that 23% of doctors involved in the project did not accurately report which of their patients had urinary catheters in place and how long they were in use. To obtain this data medical students, residents, and attending physicians were each asked which of their patients did or did not have urinary catheters in place. It was possible to quantify how many urinary catheters were inaccurately reported by comparing the response of the doctor to a computer database that tracked the status of each patient.

In summary, medical-device associated nosocomial infections present a high cost both financially and for patient mortality. It has been shown with epidemiological data that a wide variety of microorganisms play a role in causing these infections that can originate from the

normal flora of the patient or can be carried by the health care facility or health care worker.

Multiple approaches have been taken to mitigate the incidence of these infections by improving maintenance of the health care facility, procedures for installing and maintaining the medical devices, and improved surveillance of susceptible patient populations.

Quorum sensing

Quorum sensing is the process by which bacteria and some fungi detect how many microorganisms are present in the surrounding environment. Then dependent on the number of surrounding microorganisms gene expression is altered in order to coordinate gene expression among the microbial community. Known quorum-sensing compounds are chemical compounds such as acylated homoserine lactones (acyl-HSLs), oligopeptides, butyrolactones, furanosyl diester autoinducer-2 (AI-2), and the quinolone signal in *P. aeruginosa* known as PQS (Calfée, *et al.*, 2001; Diggle, *et al.*, 2003; Smith, *et al.*, 2003).

The concentration of the quorum- sensing molecule in the external environment is directly proportional to the number and density of the group at large within a given space. As the population density increases so too does the concentration of the quorum- sensing compound. The central theme of quorum sensing is based on the secretion of signaling molecules by multiple producing organisms into the external environment. Once the signaling molecule reaches a threshold concentration at the point of the effector cells, which can be the same or a different species from the producing organisms. The effector cells then alter their gene expression resulting in community wide alterations in phenotype. Generally, the phenotypic traits altered are involved in virulence and biofilm development.

The processes by which the quorum- sensing compound can interact with the target cell are diverse among different species of microorganisms. The three major mechanisms identified are passive diffusion, active transport (Smith, *et al.*, 2003; Hogan, 2006) and a sensor kinase cascade, as is the case with *Vibrio harveyi* and *Vibrio cholerae* (Taga, *et al.*, 2001). Once these compounds reach a threshold level, regardless of their mechanism of entry, within the cell they influence gene expression.

Initially, quorum sensing was thought to only occur between single species; however, it has been shown that in mixed-species populations quorum- sensing signaling molecules exhibit cross talk (Vlamakis, *et al.*, 2005). Experiments have shown that concentrations are altered resulting in one bacterial species affecting the gene expression in a different species. This was shown to be the case in co-cultures of *E. coli* and *V. cholerae*, two organisms that both utilize autoinducer 2 (AI-2) signals. *V. cholerae* would produce the signal and *E. coli* would uptake the AI-2 molecule causing a change in concentration of AI-2 in the external environment and altering gene expression in *V. cholerae* (Xaiver, *et al.*, 2005). Interestingly, *P. aeruginosa* produces virulence factors in response to AI-2 when it does not produce AI-2 itself (Vlamakis, *et al.*, 2005). Quorum sensing cross-talk increases the complexity of interactions between mixed-species populations. The ability of one microorganism to alter the gene expression of another through quorum sensing presents potential targets for mitigating pathogenesis in organisms that rely on quorum sensing to regulate the expression of virulence factors. The ability to jam the signals and prevent the expression of virulence factors may be another approach to combat difficult to treat or antibiotic resistant infections.

Interaction between *P. aeruginosa* and *C. albicans*

The selection of *P. aeruginosa* and *C. albicans* as the central focus of this work was based on patterns of microbiological colonization of the lungs of Cystic Fibrosis patients. Cystic Fibrosis is a genetic disorder that affects approximately 30,000 Caucasian Americans (Lau, *et al.*, 2004). Cystic Fibrosis is characterized by a defect in the CFTR transport system that is normally responsible for the secretion of chloride ions across the apical surface of secretory cells throughout the body. In individuals that have a defective CFTR channel the amount of chloride ions secreted by the cell is low (Hassett, *et al.*, 2002). The osmotic pressure created by this defect in ion transport induces the formation of thick mucous within the lumen of the airway. Water is retained within the cell and is not properly secreted with the secreted mucous. This has the effect of disrupting one of the primary defense barriers in the lung to capture invading microorganisms and clear them. The cilia that normally remove airway mucous are unable to properly function in clearance because the thick, viscous mucous prevents their movement.

Historically, CF patients have had digestive problems where viscous mucous also accumulated within the secretory ducts and lumen of the small intestine of the digestive tract resulting in poor adsorption of nutrients, in addition to lung infections. Changes in diet that restricted salt were able to mitigate the effects of CF on digestion, improving the ability of patients to obtain nutrients and increased the life expectancy of many CF patients. Also, antibiotics to prevent bacterial infections from progressing within in the lung prolonged the life of most CF patients from an average of 10 years to 25 years of age (Govan, *et al.*, 1993).

The primary cause of death in Cystic Fibrosis patients remains to be lung damage resulting

from chronic infections caused by *P. aeruginosa*. This organism remains to be responsible for 80% of the premature deaths in this patient population due to a progressive loss of pulmonary function. Chronic lung damage is caused by repeated inflammation events in response to bacterial antigens released from chronic biofilms of predominantly mucoid *P. aeruginosa* colonies (Gilligan, 1991; Lau, *et al.*, 2004). Current therapy for *P. aeruginosa* infections in CF patients relies on the combination of different classes of antibiotics. These combinations are typically an aminoglycoside and anti-*Pseudomonas* Beta-lactams or the use of an aminoglycoside with fluoroquinolone. Tobramycin inhaled directly into the lung has been extremely effective in delivering high doses of the drug to the infected areas while keeping the incidence of side-effects low (Hassett, *et al.*, 2002).

Regular monitoring of the microbiological profile of CF sputum has been an important clinical tool to best improve the administration of antibiotics to control rates of infection. From these patient profiles it has been possible to collect statistical data on the rate of clearance of significant pathogens from the lung. This information has revealed an interesting trend in the patterns of colonization by fungal organisms. Typically, in non-CF patients with compromised lung tissue that receive antibiotic therapy an upsurge in the number of isolates of fungal species, most commonly *C. albicans* occur. Interestingly, in Cystic Fibrosis patients where the tissue is compromised and should be favorable for colonization by fungal species this trend is lower than expected.

Data that *C. albicans* is the second most common organism isolated from sputum in adult CF patients suggests that it is not adept at persisting in the CF lung (Table 1). *C. albicans* isolates demonstrate patterns of appearance and disappearance. This suggests that *C. albicans*

repeatedly enters the lung but is cleared before a persistent colonization can occur. An upsurge in *C. albicans* colonization is only apparent when the CF patients with chronic *P. aeruginosa* infections undergo anti-pseudomonal antibiotic therapy. In a study by Burns, *et al.* in 1999 the sputum of CF patients was tested before, during, and after antibiotic therapy. It was found that while the number of *P. aeruginosa* isolates decreased the number of *C. albicans* isolates increased. This finding suggests *P. aeruginosa* is modifying the environment in the CF airway to inhibit of growth in *C. albicans*. In a study by Kerr in 1994 it was found that *P. aeruginosa* and *Burkholderia cepacia* were able to inhibit the growth of *C. albicans* and various fungal species, including *Aspergillus niger*, *Cryptococcus neoformans*, and *Histoplasma capsulatum*. These fungal species were not inhibited by the commonly isolated lung pathogens *Escherichia coli* NCTC 10418, *Staphylococcus aureus* NCTC 6571, and *Haemophilus influenzae* NCTC 11931 (Tripathi, *et al.*, 1969).

Table 1: Microbiological profile of adult Cystic Fibrosis patients

Organism	% Incidence in Patient pop.	CFU per ml aspirate	Persistence rate
<i>P. aeruginosa</i>	83.4	10 ⁷ - 10 ⁹	high
<i>C. albicans</i>	29.4	10 ⁴ -10 ⁷	low, high frequency
<i>S. aureus</i>	24.5	10 ⁴ -10 ⁷	low

Table 1: Bauernfeind, *et al.*, 1987 Infection vol. 15. The persistence rate is determined by how frequently isolates are verified from consecutive analyses of sputum.

P. aeruginosa and *C. albicans* represent an interesting model system for antagonistic bacterial-fungal polymicrobial biofilms (Hogan, *et al.*, 2002; Semighini, *et al.*, 2006). Clinical data has revealed that infections by these organisms tend not to occur concurrently but sequentially. In the host, *P. aeruginosa* is able to suppress the outgrowth of *C. albicans* and allow for clearance of the fungi by the immune system. However, if anti-pseudomonal antibiotics are administered the number of *P. aeruginosa* isolates decline and isolates of *C. albicans* increase (Kerr, 1994; Burns, *et al.*, 1999).

Figure 1: Interaction between *C. albicans* and *P. aeruginosa*

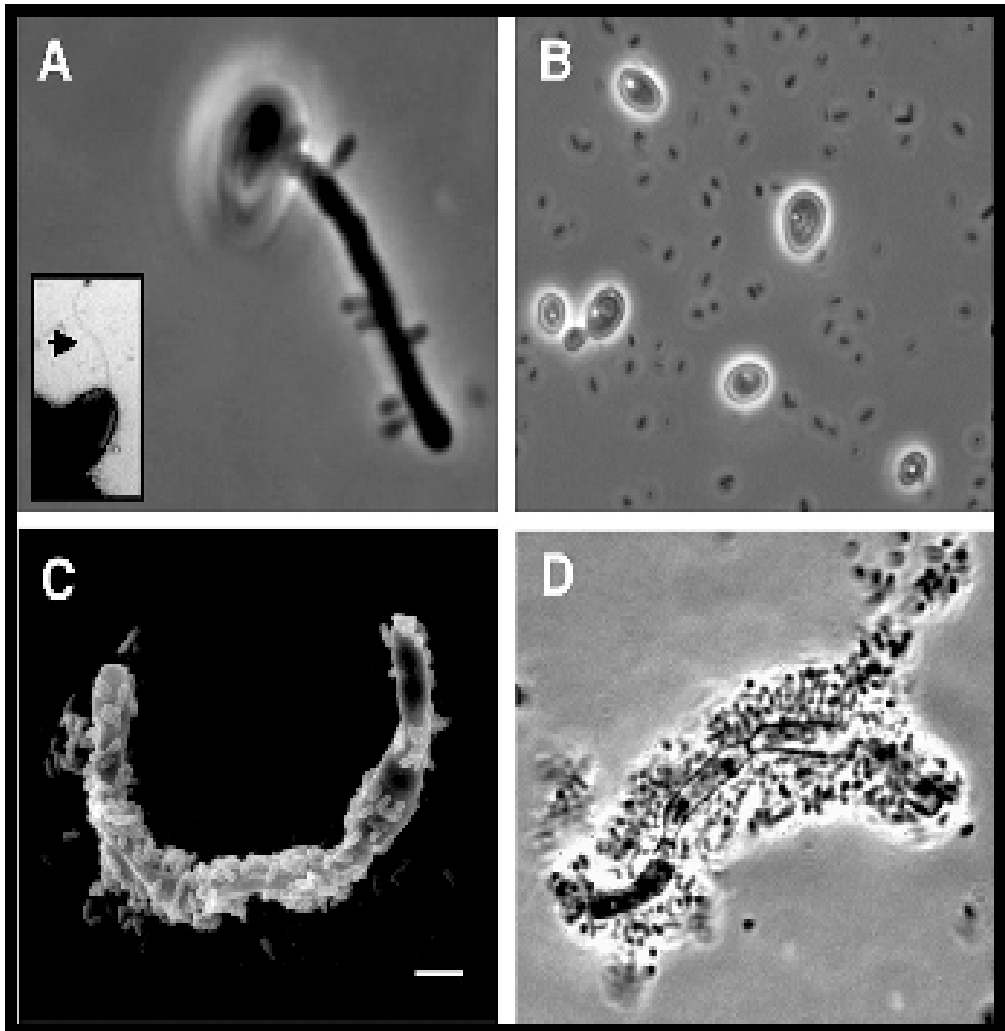


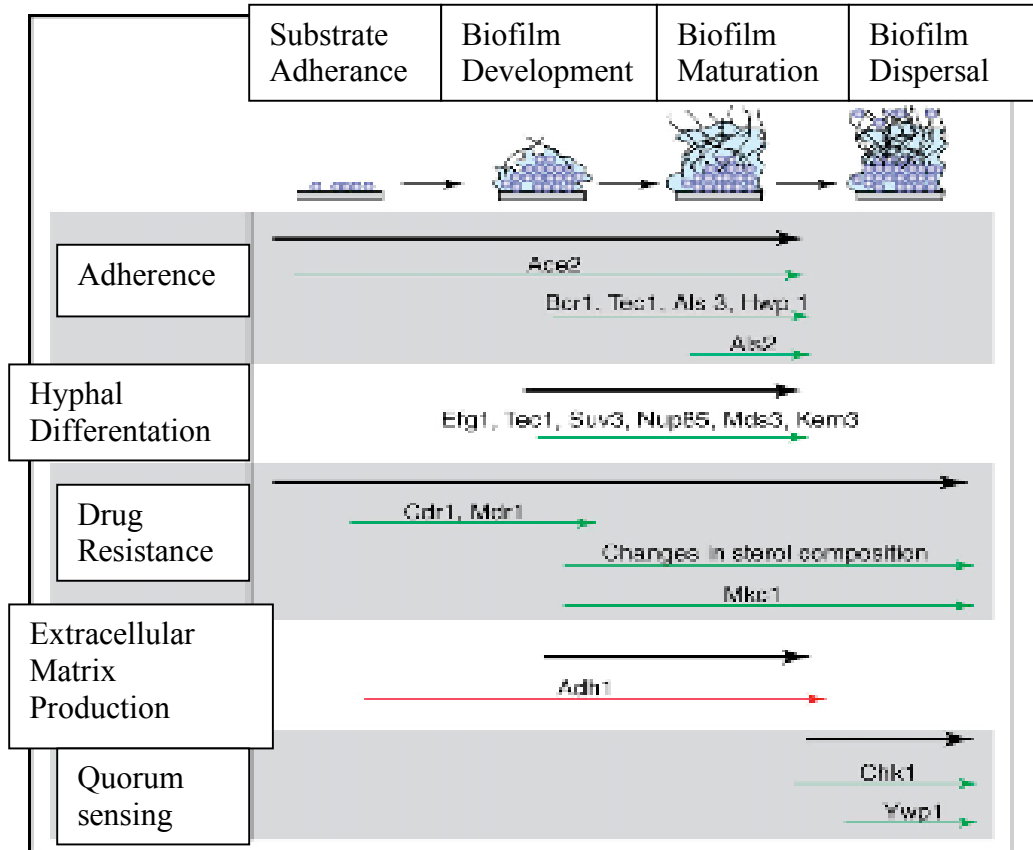
Figure 1: (Source Hogan, *et al.*, 2002) The interactions that occur between *C. albicans* and *P. aeruginosa* according to the morphological properties of *Candida*.

***Candida* and Medical-Devices**

C. albicans is a dimorphic yeast that is a member of the normal flora of humans that is acquired early in life commonly during the passage through the birth canal or from close contact with family members (Odds, 1988). The ability of *C. albicans* to colonize mucosal surfaces and penetrate epithelial tissue is dependent on dimorphic shifts. The dimorphism of *C. albicans* can be defined as an environmentally controlled reversible transition between yeast and a mycelial form. Dimorphism has been shown to rely on initial cell density; this phenomenon is defined as the inoculum size effect and is one of eleven factors that lead to dimorphic shifts (Kulkarni, *et al.*, 1981).

Biofilm formation is a major factor in the pathogenic process for this organism that allows for the colonization of mucosal surfaces, dentures, and medical devices. The initial stages of biofilm formation rely on the ability of *C. albicans* to regulate its morphology. What makes *C. albicans* of special concern is its ability to exhibit dimorphism during the biofilm formation process (Jabra-Rizk, *et al.*, 2004). Physiological regions of the human body where *C. albicans* commonly colonize include the mouth, vagina, lungs, intestine, bronchi, skin, heart, meninges, bones, and joints. The biofilm of *C. albicans* begins on the mucosal surface in the yeast form and once dimorphism has initiated hyphae are formed and this organism is able to penetrate into tissues and gain access to virtually any physiological region of the body, resulting in systemic candidiasis.

Figure 2: Stages of biofilm formation in *C. albicans*



(Source: Jabra-Rizk, *et al.*, 2006 FEMS Yeast Res vol. 6)

P. aeruginosa is thought to inhibit growth and the ability of *C. albicans* to cause a nosocomial infection in patients with a medically implanted device. The exact mechanism of this inhibition is unclear although quorum-sensing molecules are thought to play a role (Pierce, 2005). Supported by data that shows when an antibiotic to suppress a *Pseudomonas* infection is given, a *Candida* infection soon follows (Burns, *et al.*, 1999). This report states that with the use of inhaled antibiotics the number of *P. aeruginosa* isolates decrease and the number of isolates of *C. albicans* increases. The author does not consider *C. albicans* to be a concern for CF patients as a pulmonary pathogen. However, in the NNIS report from May 1999, *C. albicans* is responsible for 4.7% of nosocomial pneumonias.

Candida infections are difficult to diagnose definitively to the species level when associated with an implanted medical device. As more standardized and sophisticated diagnostic tests emerge it is possible to better identify *Candida* species as the causative agent of a device-associated infection. The resultant trend of the use of more accurate diagnostic tools is an increasing incidence of *Candida* species as the cause of device-associated nosocomial infections (Kojic, *et al.*, 2004). Data reported in a NNIS study period from 1986 to 1989 reported the isolation of *Candida* species from urinary isolates of patients in the ICU at 22.1%. In the study period from 1992 to 1997 the rate of urinary isolates from ICU patients was at 31%. The presence of the urinary catheter is a significant factor in the occurrence of this type of infection. It was also reported in the NNIS study that in ICU patients with a urinary catheter 21% of the infections were caused by *Candida* species. In ICU patients without a urinary catheter in place only 13% of patients had urinary tract infections caused by *Candida* species. Other risk factors that play a role in *Candida* growth in the urine include diabetes mellitus, urinary tract

abnormalities, malignancy, and antibiotic use (Kojic, *et al.*, 2004).

Farnesol is secreted by *C. albicans* continuously and functions to control of the morphological state of the entire cell population. The trans, trans conformation was shown to be biologically relevant. *P. aeruginosa* also secretes an analog of farnesol, 3-oxo-C12-HSL (Hogan, *et al.*, 2004). This compound is biologically active in *C. albicans* and is able to inhibit hyphal formation and further biofilm development. The ability of *P. aeruginosa* to mimic this signal causes the morphology of *C. albicans* to remain in the yeast form. This has the effect of reduced efficiency in forming a biofilm on a variety of surfaces including medically implanted devices (Nickerson, *et al.*, 2006). Based on this mechanism the goal of *P. aeruginosa* is to not kill the *C. albicans* cell but to inhibit its ability to form biofilms. However, *P. aeruginosa* does have the ability to kill hyphal form *C. albicans* by physically attaching to the hyphal element and using enzymatic methods to lyse and kill the cell (Hogan, *et al.*, 2002).

***P. aeruginosa* and Pyocyanin**

P. aeruginosa is a ubiquitous gram-negative bacterium and is a member of the normal human microbial flora. *Pseudomonas aeruginosa* does not become a serious threat as a pathogen until the host immune system is suppressed or if a biofilm has the opportunity to develop. Suppression of the host immune system can be due to multiple factors including infection with Human Immuno-Deficiency virus (HIV), chemotherapy, burns, transplants, implanted medical devices, and neutropenia. In the compromised host *P. aeruginosa* is commonly associated with infections of the mucosa and respiratory tract that are difficult to treat and frequently lead to

death (Dickinson, *et al.*, 1989). Once in a biofilm, this organism becomes highly resistant to chemotherapeutic agents due to phenotypic and environmental changes related to the biofilm including reduced growth rate, reduced oxygen tension, and the initiation of membrane efflux pumps that are genetically regulated.

Pyocyanin (PCN) is a secondary metabolite that is produced by *P. aeruginosa*. This compound is a zwitterion that easily penetrates biological membranes and has been found in large concentrations from the sputum and ear-secretions of patients infected with *P. aeruginosa*. PCN is a compound that is a very important virulence factor and is regulated by the Las/Rhl quorum-sensing system. In infected human host tissue, PCN causes cellular damage, inhibition of respiration, inhibition of ciliary function, epidermal cell growth, procyclin release, calcium homeostasis, and the inactivation of alpha-1-protease inhibitor. The inactivation of this inhibitor adds to the imbalance of protease-antiprotease activity that is common in the CF lung. PCN and the precursor phenazine-1-carboxylic acid have also been found to alter the host immune response by modulating levels of RANTES and IL-8 (Lau, *et al.*, 2004).

The antimicrobial action of PCN is dependent on the presence of oxygen (Hassan, *et al.*, 1980). The first stage of PCN antimicrobial activity requires the reduction of PCN to its monovalent or divalent form. PCN must then auto-oxidize in order to continue the process. Interestingly, PCN is able to inactivate the anti-oxidative stress mechanisms catalase and the GSH redox cycle in human epithelial cells (Lau, *et al.*, 2004). In the report by Westwater, *et al.* in 2005, the ability of *C. albicans* to protect itself from oxidative stress by secreting *E,E*-farnesol into the surrounding environment was established. The protective mechanisms of farnesol against oxidative damage could potentially be one mechanism to resist attack by *P. aeruginosa*

and mitigate the harmful effects of PCN.

P. aeruginosa is able to infect a variety of hosts from different phylogenetic backgrounds including humans, plants, nematodes, and insects. Interestingly, the virulence mechanism utilized by *P. aeruginosa* in such divergent hosts is largely the same. The benefit of this broad range of host susceptibility with similar virulence mechanisms is the availability of model organisms that are relevant to the human host. PCN is one of the major virulence mechanisms used in all of the hosts that *P. aeruginosa* is known to infect. The nematode *Caenorhabditis elegans* virulence assay is very useful to better understand the virulence mechanisms used by *P. aeruginosa*. The main mechanism used by *P. aeruginosa* to kill *C. elegans* is through the generation of reactive oxygen species by PCN (Tan, 2000). The *C. elegans* assay can be used to assess two different virulence mechanisms. The fast killing assay is based on the activity of PCN. This assay is based on an accumulation of PCN and requires eight hours to kill the animals. The slow killing assay is based on the ingestion and growth of *P. aeruginosa* in the lumen of the gut of *C. elegans*. Killing occurs after several days when *P. aeruginosa* is able to penetrate the epithelium and kill the worm (Tan, 2000).

The mechanism used by PCN to induce cellular damage has led to the development of new treatment strategies for CF patients chronically infected with *P. aeruginosa*. It has been found that treatment regimens that utilize GSH aerosols and anti-oxidant supplements have improved CF lung functions. Another potential clinical application is to prevent the production of PCN by targeting the enzymes that are a part of the enzymatic pathway that lead to its production. *P. aeruginosa* synthesizes PCN from the shikimate pathway (*aro* pathway). The shikimate pathway is used to synthesize aromatic amino acids, para-aminobenzoic acid, vitamin

K, folic acid, and ubiquinone. This pathway is found in bacteria, yeasts, filamentous fungi, apicomplexan parasites, plastids of plants, and algae. Vertebrates do not possess the enzymes used in this biosynthetic pathway and must acquire the nutrients synthesized through diet (Lau, *et al.*, 2004). The enzymes of the shikimate biosynthetic pathway are a potential target for antimicrobial drugs and also a vaccine target to prevent production of PCN.

Figure 3: Regulatory pathway for the biosynthesis of pyocyanin

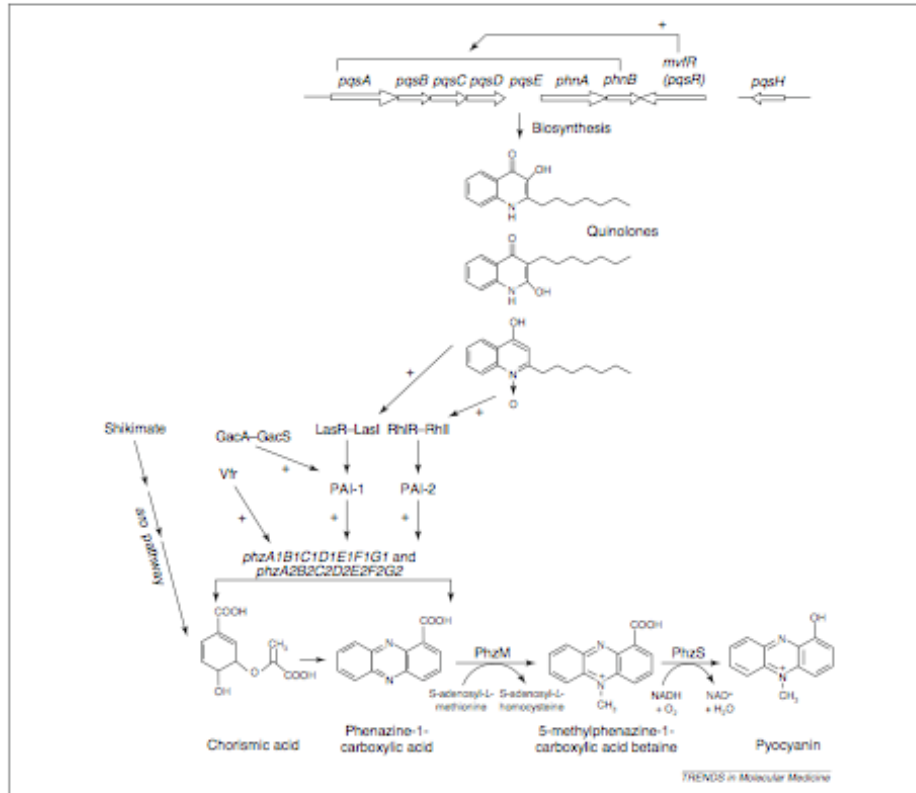


Figure 1. The pyocyanin (PCN) biosynthetic pathway. PCN is synthesized from chorismate by the *phz* operons, as well as by *phzM* and *phzS*, which catalyze the final steps in the synthesis. The synthesis is positively regulated by the *LasR*-like transcriptional activator *MvfR* (*PqsR*) through the synthesis of quorum-sensing quinolone molecules, with additional regulatory signals from the *LasR*-*LasI*, *RhlR*-*RhlI*, *GacA*-*GacS* and *Vfr* regulatory systems.

Figure 3: (Source: Lau, *et al.*, 2004 Trends in Molecular Medicine vol. 10)

Farnesol

Figure 4: Molecular structure of *E, E*-farnesol

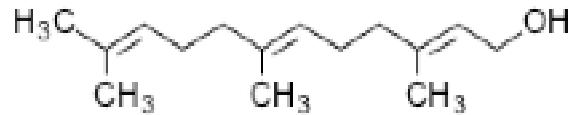


Figure 4: Molecular structure

Farnesol, a sesquiterpene alcohol, is present in essential oils such as citronella, neroli, cyclamen, lemon grass, tuberose, rose, musk, and balsam. Trans, trans-farnesol (*E,E*-farnesol) is synthesized through the ergosterol biosynthetic pathway in *Candida albicans*. *E,E*-farnesol is derived from farnesyl pyrophosphate, a compound integral to the lipid biosynthetic pathway. Four isomers of farnesol are produced but only trans, trans isomer is biologically active (Shchepin, *et al.*, 2003). *E,E*-farnesol has been isolated from the spent medium of *C. albicans* by extraction with organic solvents and identified using gas chromatography-mass spectrometry as 1-hydroxy-3,7,11-trimethyl-2,6,10-dodecatriene (Hornby, *et al.*, 2001)

The synthesis of farnesol begins at the generation of the isoprene unit isopentenyl-PP and dimethylallyl-PP. These two compounds are oriented in a head to tail fashion to generate farnesyl pyrophosphate. The enzymes that are responsible for the synthesis of *E,E*-farnesol from farnesyl pyrophosphate are a Mg²⁺-independent phosphatidate phosphatase and diacylglycerol pyrophosphate phosphatase. These enzymes are encoded by the gene *Lpp1p* and *Dpp1p* respectively in *Saccharomyces cerevisiae* and by the genes *Dpp2* and *Dpp3* in *Candida* (Toke, *et al.*, 1998). Assays to determine the activity of these enzymes were based on cytosolic extracts

where farnesyl pyrophosphate was added as a substrate and the amount of farnesol created was measured.

Farnesol is characterized as a head-to-tail linear sesquiterpene. Isoprenoid compounds have been identified in plants and fungi that yield distinctive odors and flavors. For example, farnesol yields the characteristic odor of Channel No.5 and the original source of purified farnesol was from *C. albicans* (Hornby, *et al.*, 2001). *E,E*-farnesol has also been isolated from the anal scent glands of Nutria, a rodent that is an invasive species in the wetlands of Louisiana. Nutria use scent to establish territory and attract mates. *E,E*-farnesol is thought to be a useful bait compound to improve the efficiency of traps (Lee, *et al.*, 2007). *E,E*-farnesol is also a major constituent of secretions from the temporal gland of male Asian and African Elephants. These scent glands are located on the face lateral to the eye. When male elephants are preparing to become aggressive the secretions of the temporal gland increase and the substance is rubbed on trees to indicate to other males territorial boundaries and to attract potential mates. *E,E*-farnesol has also been isolated from the Nasonov gland of honeybees. This secretion is used to indicate sources of food sources to nestmates (Granero, A.M. *et al.*, 2005).

The fate of farnesyl pyrophosphate, if it is not converted into farnesol, is to form subunits for cell membrane material generated in the lipid synthesis pathway. The mode of action of a majority of anti-fungal chemotherapeutic agents that have been effectively used against *C. albicans* target the enzymes of the lipid biosynthetic pathway that are responsible for synthesizing lanosterol, Zymosterol, and Ergosterol (Carrillo-Munoz, *et al.*, 2006). The blockages of these enzymes lead to an increase in membrane permeability and an increase in farnesol production. As a result, invasive *C. albicans* is no longer able to maintain intracellular

concentration gradients of potassium and other important ions and osmotic pressure leads to lysis of the cell. It is the goal of most anti-*Candidal* drugs to target the lipid pathway and results in a reduction of cell wall integrity. A second effect of the disruption of the lipid biosynthetic pathway is the increase in the production of farnesol. Increased farnesol production causes newly forming cells to remain as yeast and do not readily enter the hyphal form.

E,E- farnesol is synthesized in virtually all eukaryotic cells ranging from fungi to humans. The general interest here is farnesol that is synthesized by the opportunistic fungal pathogen *C. albicans*. It has been demonstrated that farnesol is released continuously from the cell in the amount of approximately 0.13mg/g (dry weight) by the two *C. albicans* strains A72 and CAI-4 (laboratory strains) (Hornby, *et al.*, 2004). It also has quorum sensing capabilities (Hornby, *et al.*, 2001) that have a significant impact on biofilm development and architecture. When levels of farnesol reach a threshold level the ability of the fungus to transition from a yeast form cell into a hyphal form cell is inhibited. This morphological shift, defined as dimorphism, is a significant virulence factor for *C. albicans* infections. When this organism is in the hyphal state, biofilm formation is robust and tissue invasion is possible.

The ability of farnesol to inhibit the hyphal state and lead to more yeast-form cells to develop results in a less robust biofilm and reduced tissue invasion. This inhibition occurs at the genetic level where there is a repressor that is activated that leads to the blockage of transcription factors that lead to the synthesis of genes responsible for triggering hyphal differentiation. It has been shown that, in a developing biofilm, cells that have already committed to the hyphal state are resistant to the effects of farnesol. Only newly developing cells will be susceptible to the hyphal-inhibiting effects of farnesol (Mosel, *et al.*, 2005; Ramage, *et al.*, 2002) In general,

morphological transition from the yeast to hyphal form is triggered by increased concentrations of carbon dioxide, increased temperature, alkaline pH, serum, or the presence of N-acetylglucosamine (Hornby, *et al.*, 2004). It has been shown that three independent signal transduction pathways mediate the transition into the hyphal state. Each pathway depends on specific environmental triggers. It has been shown that farnesol is able to inhibit all three of these pathways. It is still unclear if the inhibition is general or specific for each trigger.

Figure 5: Molecular regulatory pathways to control dimorphism in *C. albicans*

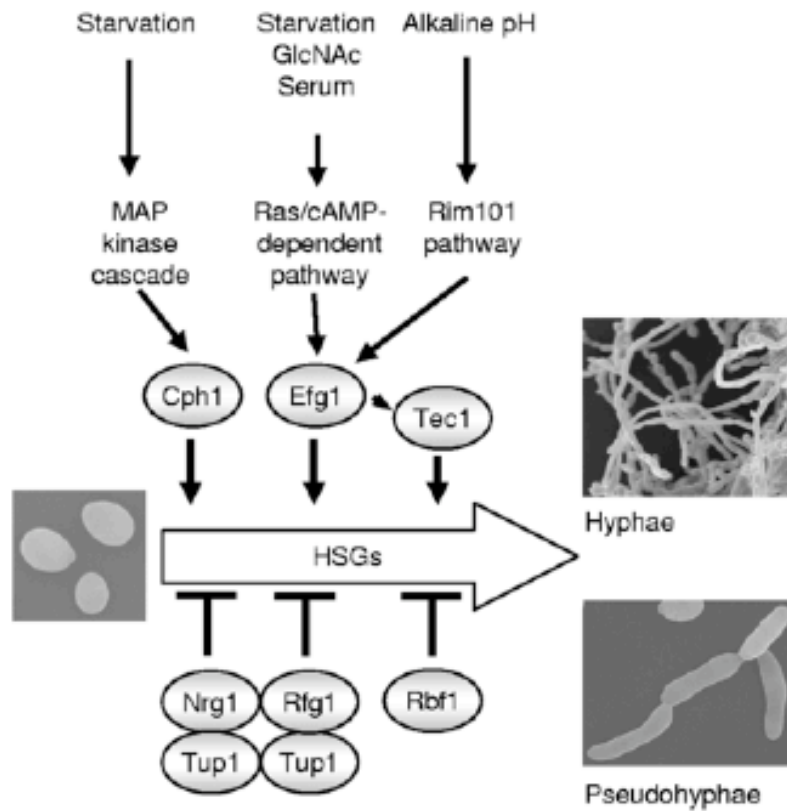


Figure 5:

Source: Nickerson, K.W., A.L. Atkin, J.M. Hornby. 2006. Quorum Sensing in Dimorphic Fungi:

Farnesol and Beyond. *Applied and Environmental Microbiology*. 72(6):3805-3813.

The importance of farnesol in the microbial world is becoming increasingly apparent. It has been demonstrated that farnesol is instrumental in controlling dimorphism in the fungus *Candida albicans*. *E,E*-farnesol has also been shown to aid *C. albicans* in competition with other fungal species that may attempt to occupy the same niche. In a study with *Aspergillus nidulans*

it was shown that *E,E*-farnesol induced apoptosis (Seminghini, *et al.*, 2006). It was also shown that *E,E*-farnesol protected *C. albicans* from attack by reactive oxygen species (Westwater, *et al.*, 2005). Preliminary 2D DIGE results indicate that farnesol secreted by *C. albicans* influences the expression of virulence factors in *P. aeruginosa* and alters quorum sensing systems by suppressing homoserine lactone production and increasing PQS quorum sensing. The strains *P. aeruginosa* PAO1 and *C. albicans* SC5314 were chosen for use in this study because their genomes have been completely sequenced and annotated.

Quorum sensing disruption in nature and the potential use in the clinic

Traditional antibiotics that inhibit the ability of bacteria to grow within the human body has historically been an effective strategy in preventing infectious disease. However, the emergence of resistant organisms has caused treatable diseases to become a more formidable challenge to the medical community. The extreme pressure that growth-suppressing drugs has on bacteria has an equally strong ability to create resistance through active selection, thus increasing the incidence of resistance. The development of an anti-pathogenic drug is an emerging area that is based on knowledge of the regulation of virulence factors by quorum sensing mechanisms. According to the anti-pathogenic drug principle drugs that target quorum sensing systems will prevent the ability of bacteria to adapt to the human environment and block virulence and pathogenic traits (Hentzer, *et al.*, 2003). Quorum sensing virulence factors in *P. aeruginosa* include the secreted compounds elastase, alkaline protease, rhamnolipids, phenazines, cyanide, lectins, and chitinases. The response of the immune system, when challenged with quorum

sensing deficient mutants of *P. aeruginosa*, has been shown to be faster overall exhibiting increased strength of oxidative bursts from PMN and faster accumulation of antibodies (Givskov, *et al.*, 2006). Virulence studies with *C. elegans* and quorum sensing deficient mutants of *P. aeruginosa* have also demonstrated increased rates of survival in the animals challenged with the mutant strains. The mechanisms used to kill the animals are quorum sensing regulated compounds.

Potential targets for anti-pathogenicity drugs involve three components of the quorum sensing system: the signal generator, the signal molecule, and the signal receptor. In nature, the use of quorum sensing disruptors has been found to be an effective strategy to prevent infection and competitive advantage. A plant infected with the tissue degrading plant pathogen *E. carotovora* will increase the pH surrounding the wound site. The alkaline pH causes the lactone ring of AHL to open and degrades the signal. The end result of the blockade of quorum sensing signal is the reduction in tissue damage (Byers, *et al.*, 2002). The marine alga *Laminaria digitata* produces and secretes hypochlorous and hypobromous acids. These compounds are used industrially to prevent biofouling, act as the active sanitizer in swimming pool products, and are generated by activated neutrophils. These compounds react with oxidized acyl-homoserine lactones and provide a competitive advantage to the alga. There are enzymes that degrade AHL by catalyzing lactonolysis and reduce the concentration of active AHL. These enzymes, called AiiA, have been isolated from *Bacillus* species. Homologues of these enzymes have also been found in *Agrobacterium tumefaciens*, *Arthrobacter sp.*, *Klebsiella pneumoniae*, *Comamonas sp.*, and *Rhodococcus sp* (Givskov, *et al.*, 2006).

The development and maintenance of the biofilm and the induction of most virulence factors are both under the control of quorum sensing regulated genes in some organisms such as *P. aeruginosa*. Quorum sensing mutants have been shown to be deficient in biofilm formation and the establishment of a robust infection. A growing area of research to develop novel ways to prevent infection by pathogenic microorganisms is to take advantage of quorum-sensing systems and the potential disruption of these systems (Bjarnsholt, 2007).

A drawback in the further development of this form of therapeutic is the uncertainty in establishing protocols for clinical trials and gaining FDA approval. There is concern about denying patients in clinical trials antibiotics with infectious disease in order to test the efficacy of quorum-sensing inhibitor drugs. The pharmaceutical industry, scientists, and government regulators are at a critical cross-roads that could decide the fate of this form of treatment for infectious disease (ASM Cell-Cell Communication in Bacteria meeting, Austin TX Oct. 7-10 2007). The science behind this developing area of therapy for infectious disease is based on stemming the lines of communication among pathogens to derail the pathogenic process and dampen the virulence of the invading pathogen.

With the use of quorum sensing disruptors it may be possible to prevent the formation of biofilms on biotic and abiotic surfaces or to prevent the production of toxins and virulence factors that are quorum-sensing regulated. A major focus of this study was to look at the ability of a cell-signaling compound produced by *C. albicans*, *E,E*-farnesol to interfere with the quorum-sensing ability of *P. aeruginosa*.

Objectives of this work

The goal of this study was to identify proteins that are differentially expressed under different growth conditions in *P. aeruginosa* when exposed to *E,E*-farnesol or whole cells of *C. albicans*. 2D DIGE[®] based proteomics was used to explore the effects that varying doses of *E,E*-farnesol had on planktonic *P. aeruginosa* strains PAO1 and GSU3. Several proteins of interest were identified in this study that can be grouped into the categories Membrane-associated, Motility associated, Metabolism associated, and Stress associated. Subsequent studies that were based on 2D SDS PAGE proteomics found proteins that grouped within the same categories as in the DIGE[®] based study. These studies altered the growth conditions and method of exposure to elements of *C. albicans*. This project provided a launch-point to design further studies to dissect the intricacies of the relationship between *P. aeruginosa* and *C. albicans*.

Materials and Methods

Strains and Cultivation

The strains of *P. aeruginosa* used were PAO1 and GSU3 obtained from 50 % glycerol stocks maintained at Georgia State University. *P. aeruginosa* PAO1 is a sequenced laboratory strain and *P. aeruginosa* GSU3 is a clinical isolate from a case of bilateral keratitis that was identified and named at Georgia State University. The strain of *C. albicans* used was SC5314 and is a sequenced strain that was obtained from ATCC. All strains were maintained in 1 ml aliquots of 50 % glycerol: standardized cell suspension at -80°C in cryovials (Nalgene catalog no. EF6835A). The cell suspension stocks were made in order to insure fresh cultures for each experiment. In order to revive the cells for use, the cryovial was defrosted at room temperature and then mixed by vortexing until the cells were evenly suspended. Then 100 µl of the stock was added to 10 ml of sterile LB- Miller medium in a sterile 15 ml Falcon tube and vortexed to mix thoroughly. The cells were first grown on LB-Miller agar (15% w/v). The plates were inoculated with a 10 µl disposable loop using the quadrant streak technique and incubated overnight at 37°C. The volume of working liquid culture depended on the total volume of the flask. Typically, a 250 ml baffled flask was used with 100 ml of fresh sterile LB-Miller broth. Two to three isolated colonies from the LB-Miller plate were used as inoculum to start the working liquid flask cultures. These liquid cultures were grown at 37°C and shaking at 130 RPM

in an Innova 4080 (New Brunswick Scientific) environmental rotary shaker. After growth for 16 hours the optical density was recorded (absorbance at 600 nm) and this was used to inoculate experimental conditions with a known density of cells. The flasks employed in the farnesol experiments were 50 ml flasks containing 10 ml of pre-warmed (to 37°C) LB-Miller broth. These flasks were shaken in the environmental shaker at 300 RPM.

Growth Phase: Growth phase was determined by measuring OD₆₀₀ of 1 ml samples using the Turner spectrophotometer (model SP-830). The growth phase in the farnesol experiments were based on values provide by [personal communication] Dr. Jayne Robinson at the University of Dayton (Dayton, Ohio) to determine mid-logarithmic growth. The starting OD₆₀₀ was 0.05 and the ending OD₆₀₀ was 0.7. The optical density was adjusted as required by adjusting the volume of culture added to fresh media.

Preparation of farnesol: *E,E*-farnesol was stored at -20°C until need. Once the bottle was opened, the bottle was flushed with nitrogen to purge any air /oxygen. Due to the hydrophobic nature of *E,E*-farnesol it was necessary to add methanol to increase its solubility. The 3.8 M stock of *E,E*-farnesol was diluted into 100% methanol according to the concentration needed in each experiment. (In the experiments reported here, 25 µM and 250 µM concentration of *E,E*-farnesol were utilized). The following volumes were based on the total volume of media used in the experiment. A 38 mM stock was made by adding 10 µl of the 3.8 M straight from the bottle into 990 µl of methanol. Then 66 µl of this was added to 10 ml of the culture media to yield a final volume of 25 µM. In the 250 µM experiment, 100 µl of stock *E,E*-farnesol was added to 900 µl of methanol. Then 66 µl of this solution was added to 10 ml of culture media. It was important to note that the final volume of the *E,E*-farnesol: methanol ratio was the same although

the concentration was different. DMSO was also used to solubilize *E,E*-farnesol and was used in the same proportions as described in the previous section with methanol. DMSO was used for the biofilm experiment and the antibiotic susceptibility experiment.

Cell cultivation and harvest

The appropriate cell stock were removed from glycerol stocks and grown overnight on agar plates (see previous section on strains and cultivation). Isolated colonies were then selected with a disposable loop and added to 250 ml flasks containing 100 ml of fresh pre-warmed (37°C) LB-Miller media and shaken overnight at 130 RPM. The optical density was recorded and the volume of culture necessary to inoculate a culture of 0.05 OD₆₀₀ was then added to six 50 ml flasks containing 10 ml of fresh pre-warmed LB-Miller. The cultures were incubated until they reached an OD₆₀₀ of 0.7 at 37°C and 300 RPM. The appropriate volume of cell suspension from the first set of six 50 ml flasks was then added to a second set of six flasks containing either 25 µM or 250 µM of *E,E*-farnesol in 10 ml of pre-warmed LB broth, and these flasks were incubated at 37°C and 300 RPM. These cultures were allowed to grow until they reached an OD₆₀₀ of 0.7.

Once the cells reached the appropriate OD₆₀₀ (approximately 6 hours following inoculation) they were transferred into sterile 15 ml conical tubes (Falcon®) and placed on ice. Once chilled, the samples were placed into a tabletop centrifuge (Beckman Coulter Allegra 64R Centrifuge, Fullerton, CA.) that was cooled to 4°C. The cell suspension was spun at 10,000 x rpm for 10 minutes. The supernatant was removed and the cells were washed in a wash buffer appropriate for proteomics (see appendix for magnesium based wash buffer). This cycle was

repeated three times. At the end of the third centrifugation, the supernatant was removed and the cell pellet was resuspended in 1 ml of wash buffer and transferred into a sterile 1.5 ml Eppendorf® tube. The cells were again centrifuged at 10,000 X G for 10 minutes in an Eppendorf Microfuge® unit. Then the supernatant was removed and the cell pellet was flash frozen in an acetone and dry ice bath and placed in the -80°C freezer until disruption. The packed cell weight of each pellet was recorded to insure thorough disruption.

Cell Disruption

The packed cell pellet was removed from the -80°C freezer and allowed to thaw at room temperature. Once the pellet began to thaw, the appropriate lysis buffer for proteomics (see appendix) was added to the pellet with a sterile pipette tip. The pellet was vortexed to disperse it into the lysis buffer. If the pellet was difficult to disperse, a pipette was used to aspirate the liquid until the cell pellet was not longer visible. Once the pellet was dispersed, the entire contents were transferred to a sterile, 15 ml conical tube (Falcon®) and placed on ice. Once the liquid was chilled, the Falcon® tube was placed under the sonicator tip. The tip of the sonicator was placed in the center of the liquid as closely as possible in all directions. It is important to note that the tip was not too close to the surface as foaming would occur. The level of the tip was as close to the center of the total volume as possible with careful attention paid that the tip does not touch the walls of the tube. The Falcon® tube was then placed in a beaker of ice water on top of a stir plate. A stir bar in the bottom of the beaker allowed for the ice water to stir and most effectively remove heat from the cell lysate.

Figure 6: Schematic diagram for set-up of microtip sonication of packed cell pellet of *P.*

aeruginosa

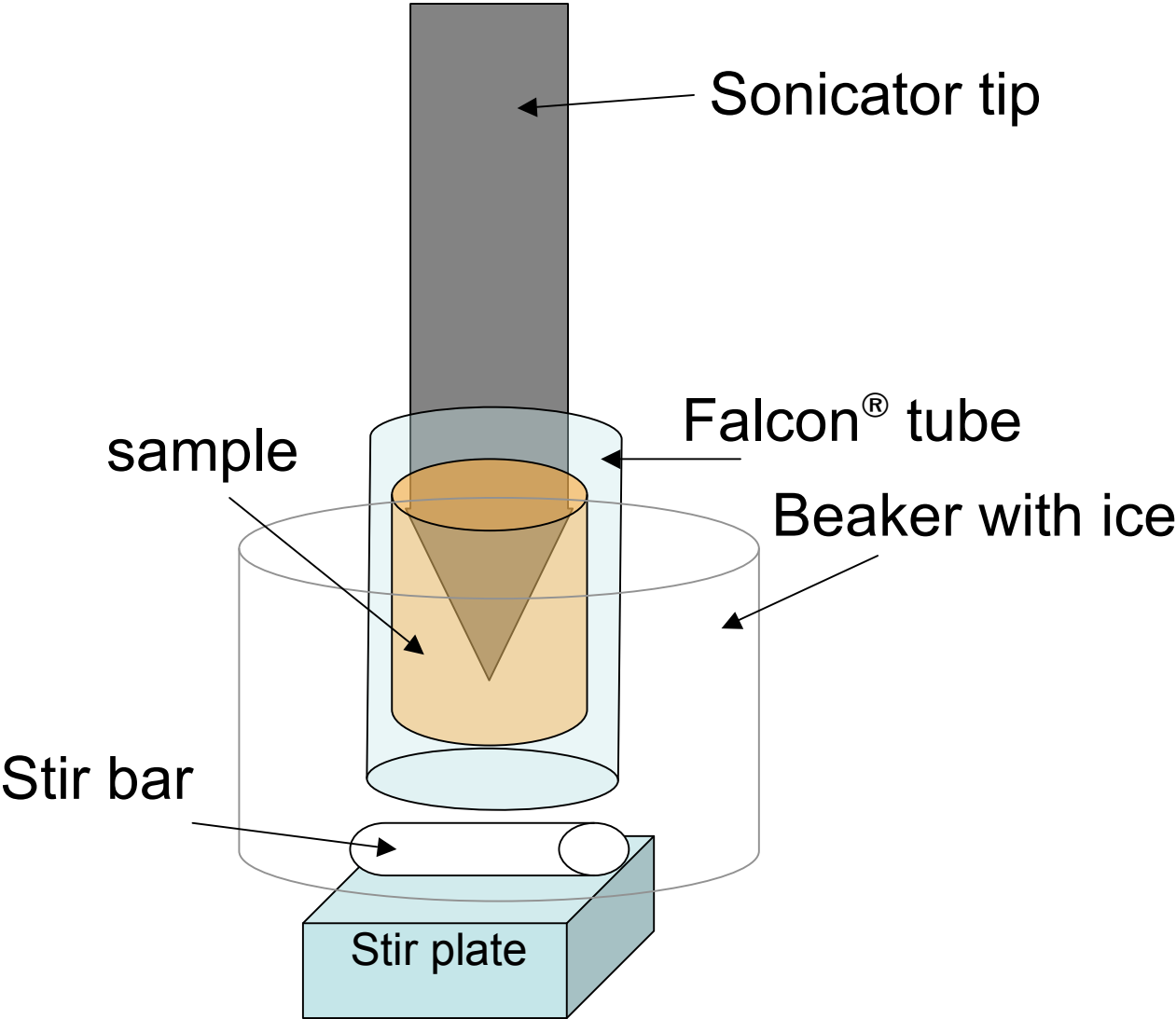


Figure 6: Diagram depicting the setup for protein pellet lysis by micro-tip sonication.

Sonication was used to disrupt the cell membrane and liberate the protein containing cytosol. The sonicator used was the Misonix Sonicator Ultrasonic Processor XL 2020. The microtip was a 1.5 cm tip and the maximum power level reached was 3. The cycle used was a total run of three minutes with one-second power on and 0.5 seconds power off. The optimum power for sonication was reached when the liquid visibly cavitated around the microtip when the peak power was reached during the pulse. The pitch was very important for this step also; the sound was not sharp, it was a smooth grinding sound. Early indications that air was getting into the liquid was a “sucking” sound if this did occur the power should be reduced to prevent foaming. In the event that foaming did occur, the Falcon[®] tube was removed from the sonicator tip and placed in a centrifuge and spun at a low speed for less than five minutes to get the foam out. Then the sample was recorded in the lab notebook and then sonication completed. Once sonication was complete, the lysate was transferred to a lo-bind[®] Eppendorf tube and centrifuged at 10,000 x g to sediment any cell membrane materials or whole cells. Then the protein containing lysate was removed and aliquoted into 50 to 100 μ l fractions. Once labeled and aliquoted, the lysate was stored in the -80°C freezer until ready for use.

The same procedure was used to disrupt the membrane for *C. albicans* with the exception that the time for sonication was extended to 20 minutes and glass beads (approximately 200 mg per cell pellet) (Sigma G1277- acid washed) was added. During the sonication optimization process the lysate was sampled periodically throughout the sonication and centrifuged to determine if cells were lysing properly and efficiently. A quick and easy way used to determine if cells were lysed properly is that the color of the supernatant following centrifugation appears

amber in color. If the supernatant appeared clear then more sonication was necessary.

Protein Quantification

To quantify protein present in the sonicated lysate, a frozen sample was removed from the -80°C freezer, and allowed to thaw at room temperature. Once defrosted, the supernatant was ready for quantification. Quantification was a critical step in the proteomics workflow and a great deal of attention was paid to accurately quantitate all samples (biological replicates) to be studied. The lysis buffer used for proteomics presents some challenges in quantification so a modified Lowry protein quantification kit was used (2D Quant Kit- GE Healthcare Piscataway, NJ.)

Protein assay for 2D proteomics

Traditional protein assays such as the Bradford based assays utilize Coomassie Brilliant blue binding by the protein. The CHAPS present in the lysis buffer will also bind to the Coomassie and provide an inaccurate result. The traditional Lowry assay, which relies on the reduction of cupric ions to cuprous ions, cannot be used due to dithiothreitol (DTT) and thiourea present in the lysis buffer that will form complexes with the cupric ions and provide inaccurate results. The modified Lowry assay takes advantage of the binding of cupric ions that bind to the polypeptide backbone following precipitation and resuspension in an appropriate alkaline buffer. Once the ions have bound to the protein in the sample, a colorimetric agent is used that binds to unbound cupric ions. This assay creates an inverse relationship between the degree of color change and the concentration of protein present. This assay employs a 0-50 µg BSA standard curve and is linear in the range of zero to 50 µg of protein and the volume range of one to 50 µl

of sample can be used. It is important to test multiple volumes of sample in order to most accurately quantify the amount of protein present in the sample lysate. It is important to perform the standard curve at the same time and every time a sample lysate is quantified. Environmental conditions in the room can affect the optical densities, thus the most accurate standard curve should reflect the conditions in the lab at the exact time the sample is also quantified. Once the standard curve is completed, the curve should be entered into an Excel[®] spreadsheet (Microsoft, Seattle Wa.) and a regression line should be placed on the graph. The equation for the regression line is then used to determine how much protein is present in the sample. The optical density of the sample is placed in the y value. The total volume of the sample assayed was divided by x (the protein concentration in $\mu\text{g}/\mu\text{l}$) to give the total amount of protein present in the sample in units of $\mu\text{g}/\mu\text{l}$. It is imperative that a minimum concentration of $5 \mu\text{g}/\mu\text{l}$ be used in order to have a sufficient quantity of sample for labeling with CyDyes[®] and identification by mass-spectrometry. If this protein quantity is not met it is necessary to revisit the disruption method used and possibly consider concentration of the sample lysate prior to quantification.

CyDye[®] labeling

The goal of this stage is to label each sample with a CyDye[®] fluor and create the pool of samples that will act as the internal standard. Several steps are necessary in this stage. The first is the randomization of the samples. This can be accomplished by drawing a circle that has smaller circles that make up its circumference. There should be one smaller circle for each sample in the experiment. A sample label for each sample should be placed in the small circles randomly. The next step is to pair each of the small circles randomly. Drawing an arrow is useful. The base of the arrow can act as the Cy3 labeled sample and the point of the arrow can

act as the Cy5 labeled sample. It is important that each sample have one Cy3 and one Cy5 pairing.

Figure 7: Diagram sample for randomization of CyDye® labels

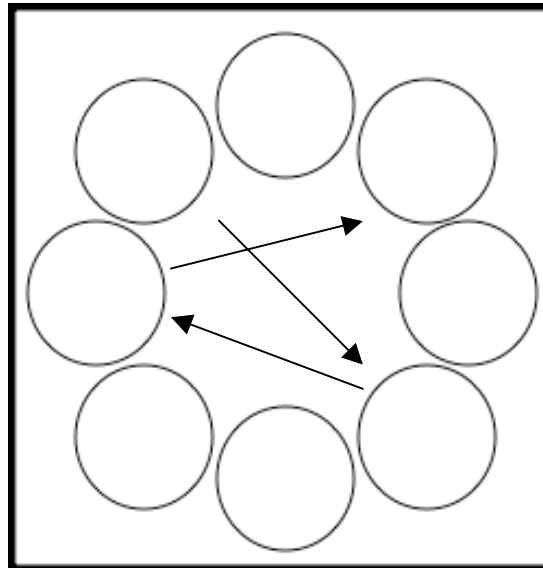


Figure 7: Schematic diagram for method of randomization of samples to organize CyDye® labeling and pairing on 2D SDS PAGE gels. Concept adapted from Tracy Ashcroft from the University of Georgia Core Proteomics Facility Athens, GA.

The next step is to create a table for which samples will be on which gel and what dye will be used. Once again it is important that each of these samples are labeled with both dyes and they are randomly paired on each gel.

Table 2: Matrix of pairing of samples for randomization

Samples	Gel 1	Gel 2	Gel 3	Gel 4	Gel 5	Gel 6
Control 1	Cy3			Cy5		
Control 2		Cy3			Cy5	
Control 3			Cy3			Cy5
Test 1	Cy5				Cy3	
Test 2		Cy5		Cy3		
Test 3			Cy5			Cy3

Table 2: Method to graphically represent cross-labeling and randomization of all samples for a robust 2D DIGE based study.

The next step is to determine how much protein is available for labeling and how much total protein will be loaded onto each gel. The more concentrated the CyDyes[®] used to label the samples the more signal the low abundance proteins will receive. The suggested range is between 200 and 1000 pM CyDye[®]/ μg of protein. The most limiting factor in determining how much total protein to load onto the gel is your least concentrated sample. This least concentrated sample will determine the maximum amount of protein that is available for the three gels that must be present. There are two analytical gels and one preparative gel. It is important that a sufficient amount of protein is present on the preparative gel so that each spot, even the low abundance ones, have enough protein present to be identified positively by mass-spectral analysis.

The labeling process itself is not difficult but great attention must be paid to accurate pipetting. It is important that the samples are kept on ice and in the dark. Each of the samples is labeled individually in their own lo-bind[®] Eppendorf tube. However, the standard should be created at this step by combining equal concentrations of each sample that will be present in the study. This pooled sample will contain all replicates and the control and experimental samples in one lo-bind tube and will be labeled at the same time. The protocol should be closely adhered to in order to ensure that appropriate labeling has occurred. Once labeling is complete, the Cy3, Cy5, and Cy2 samples are combined according to the randomized scheme designed above.

Figure 8: Workflow for CyDye® labeling

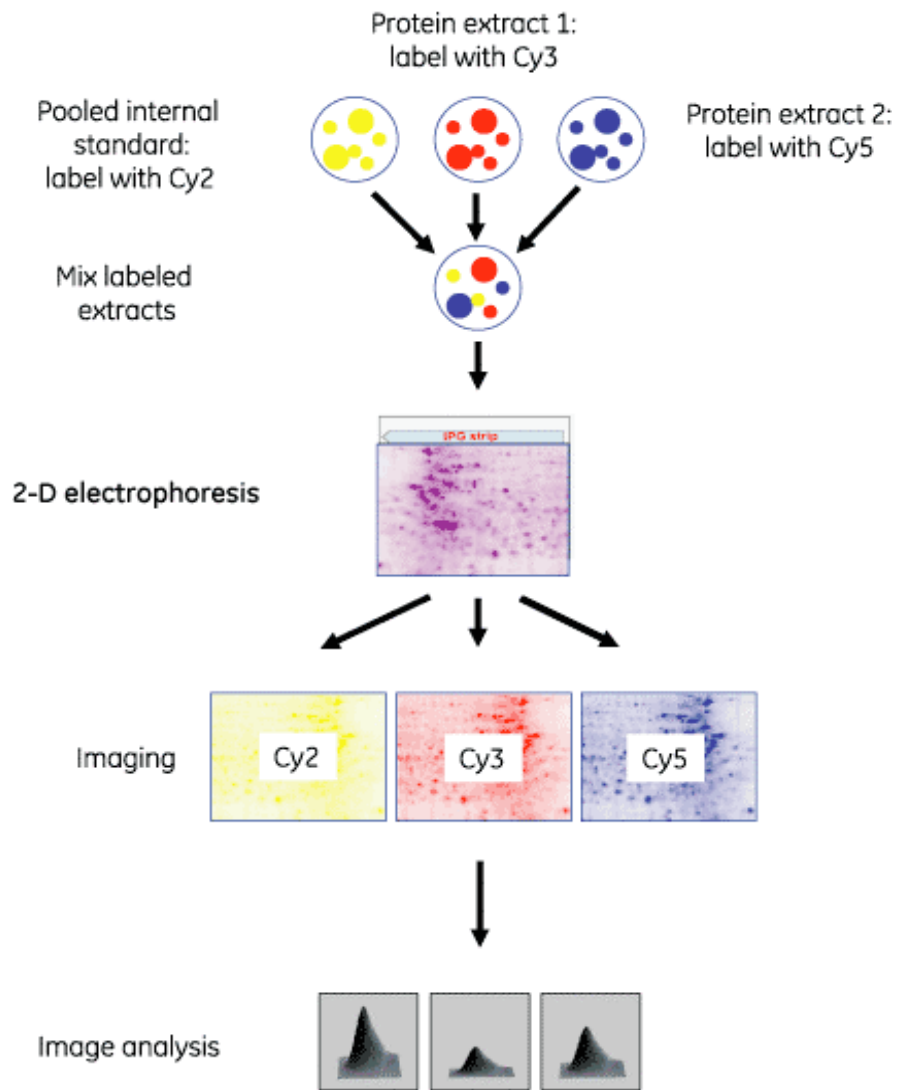


Figure 8: Depiction of workflow scheme to label samples and combine into one single gel. Source: GE Healthcare-Proteomics revision 3, 2006.

First dimension isoelectric focusing (IEF)

Isoelectric Focusing (IEF) is based on the separation of proteins according to pI. This value is determined by the net electronegativity of the side chain of each amino acid in a peptide chain. As the pH of a peptide increases so to does its pI. Strip gels are utilized that have a pre-formed immobilized pH gradient and when sample is added to the strip and with an electric current, the peptides will migrate until they reach a neutral point this neutral point coincides with that peptide's pI. The graph below depicts how the protein's pH coincides with the pI (Figure 9).

Figure 9: Isoelectric Point of Peptides

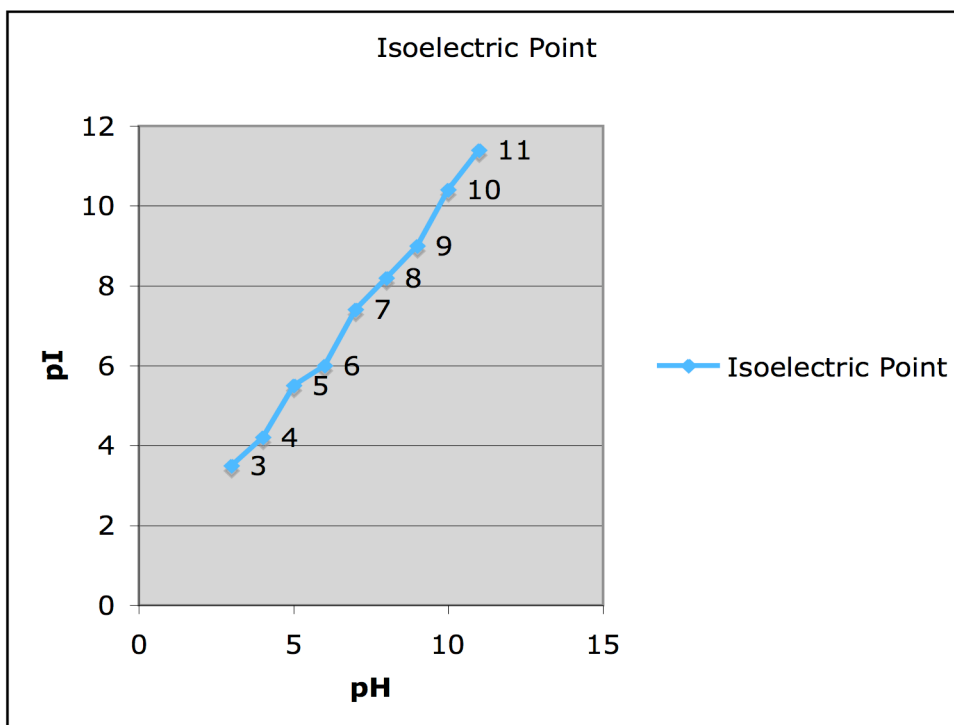


Figure 9: Graphical depiction of pH where peptides reach their respective pI, or the isoelectric point where no electrical force is able to cause movement of the peptide. Graph generated by Shelby L. Jones-Dozier adapted from 2-D Electrophoresis: Principles and Methods (GE Healthcare, Piscataway NJ)

This technique is useful in a 2D SDS PAGE because it allows for separation of peptides on a physical property distinctly from the different peptide's molecular weight. The presence of CyDyes[®] does not significantly change the pH of a peptide so it is possible to label the protein prior to any separation.

This step is very sensitive to salts, contaminants, and detergents that may be present in the sample lysate. The first step in Isoelectric focusing (IEF) is to rehydrate the first dimension strips. The first dimension strips are rehydrated in a buffer that contains IPG ampholites appropriate for the strip pI. The rehydration buffer also contains urea and thiourea to keep the proteins in solution. It is important to note that the urea is present at 8 M. In order to prevent crystallization, it is important to keep the strips out of contact with the air. This is accomplished with the application of the mineral-oil based DryStrip[®] cover fluid. There are several options in IEF concerning how the sample is applied. Typically, analytical gels utilize the cup-loading method to introduce the proteins into the gel following strip rehydration. Preparative gels typically utilize in-gel rehydration in order to load more protein in to the gel itself. The cup-loading method produces fewer streaks, in highly abundant proteins, and allows for better resolution of low-abundant spots that may be near high abundant proteins. The in-gel rehydration method is used for preparative gels because the higher protein loads that are necessary for a preparative gel can clog the cup.

The protein samples were first reduced with dithiothreitol (DTT) containing solubilization buffer at 4°C for 30 minutes. The samples were then combined with the appropriate amount of Destreak[®] solution (GE Healthcare, Piscataway NJ.) for each strip. The samples were added to each well for each dried strip. The strips were applied to the well face down so that the protein samples could be absorbed into the gel as it reswelled. The strips were then covered with DryStrip[®] Cover Fluid (GE Healthcare, Piscataway, NJ) and allowed to sit for approximately 24 hours at room temperature. Once the samples had been adsorbed into the gel, the gel strips were placed into the ceramic gel-boats. The strips were placed face up so that the wicks and

electrodes came into direct contact with the gel surface. The amount of current applied depends on the length of the strip and the pI range of the strip. In this study, 24-cm strips were used and the amount of power applied was altered depending on the pI range of the strip.

Table 3: Isoelectric focusing protocol for a 24 centimeter Imoboline® pH 3-11 range strip, at 50 μ A per strip

Step Voltage mode	Voltage	Time (h:min)
Step and Hold	500	1:00
Gradient	1000	8:00
Gradient	8000	3:00
Step and Hold	8000	3:45

Table 3: Protocol adapted from GE Healthcare Handbook for 2D Electrophoresis, revision 2007.

**Table 4: Isoelectric focusing protocol for a 24 centimeter Imoboline® pH 4.5-5.5 range strip,
at 50 μ A per strip**

Step Voltage mode	Voltage	Time (h:min)
Step and Hold	500	2:00
Gradient	1000	5:00
Gradient	8000	3:00
Step and Hold	8000	10:30

Table 4: Protocol adapted from GE Healthcare Handbook for 2D Electrophoresis, revision 2007.

Following IEF, the gel strips were individually placed into equilibration tubes, wrapped in foil to protect from light, and stored at -80°C until ready for use.

Equilibration of IEF gel strips

Two solutions are made in order to equilibrate the 1D strips following IEF and prior to SDS PAGE at room temperature. The strips are first exposed to 0.5% DTT for 15 minutes with shaking. The strips are laid on their side on a shaker at 85 RPM. The speed should be adjusted so that the solution fully covers the strip. The DTT solution is then discarded and placed into hazardous waste containers and the strips are then covered with a 4.5% iodoacetamide solution and incubated for 15 minutes at 85 RPM at room temperature. The strips are then washed with

1X SDS electrophoresis buffer and attached to the surface of the SDS PAGE gel with agarose gel (see appendix). The IEF gel is placed on the top of the SDS PAGE gel so that no bubbles are present. The agarose is then allowed to solidify before the gels are placed into the electrophoresis tank.

Second dimension SDS PAGE

Second dimension sodium dodecyl sulfate polyacrylamide gel electrophoresis (SDS PAGE) is based on the separation of proteins by their molecular weight. This is a commonly used technique to separate proteins and when coupled with IEF can be a highly robust tool to separate a high quantity of proteins from a sample. The degree of resolution in SDS PAGE can be controlled by the percentage of acrylamide in the gel. For this study, a 1-mm thickness gel was used with a single percentage of 12% that is effective for separating proteins in the molecular weight range of 14- 200 kilo-daltons (KDa).

Casting SDS PAGE gels

The gels were prepared in the lab for each run. The protocol for plate washing was critical to ensure that mass-spec analysis was not contaminated with keratin, dust, or residue from other studies. The plates were first scraped with a plastic Wonder-Wedge[®] tool to remove any residual gel. The plates were then soaked for no more than 6 hours in Contrad 70 (Decon labs catalog no. 1003) detergent. The plates were then scrubbed with a soft plastic scrubber sponge to ensure any material and debris is removed. The plates are then rinsed with deionized water, washed with Decon[®] a second time, rinsed with deionized water and rinsed a final time with double-deionized water. The plates are then soaked in 1 % Hydrochloric acid for 2 hours at 25 RPM on a shaker

Innova Platform Shaker (New Brunswick). The plates are then rinsed again with deionized water and double-deionized water. The plates are then allowed to dry on the Ettan[®] plate holders and covered to protect from dust as the gels air dry. The face of the plate that is to be used to attach the gel to should be determined. It is possible to attach the gel to the top plate or the bottom plate (with spacers). However, consideration must be made at the time of scanning to ensure that the robotic picker picks the proper region of the plate. The gel face that the gel is adhered to is placed on a Lab-Soaker face up and is covered with 4 ml of Bind-Silane[®] solution (see appendix). The solution is spread with a dust-free KimTech[®] Crew Pure CL4 wipes (Kimberly Clark, 7605) and allowed to air dry. The solution is allowed to cure for one hour then the reference markers are placed on the plate. They should be approximately 10.5 cm from the bottom of the plate and 1.5 cm from the outside edge of the plate. The plate is allowed to sit for an additional hour before use. The acrylamide gel solution was prepared and allowed to de-gas for 10 minutes before use. The gel solution was prepared in a vessel that has a pour spout or a bottle with an easy pour ring. Once the plates have cured for two hours they are wiped with 200 proof ethanol with a crew wipe and allowed to sit for 10 minutes to allow complete removal of all volatile components. The gel sandwiches were then assembled in the gel caster. The assembly protocol for the Ettan Dalt[®] six or the twelve gel caster is the same. First a thin plastic spacer is placed at the back of the caster unit. Then a back plate is placed and firmly pushed to the bottom left hand corner. Then the top plate is placed and firmly pushed to the bottom left hand corner and the wonder wedge is used to ensure that the plates are as far as they can go to the bottom left. Then a second thin plastic spacer is put on top of the top plate. This process is repeated until all six or twelve gel sandwiches are assembled. The thick plastic spacers were

then used to fill in the remaining space to ensure a tight fit once the cover plate for the caster was put into place. The gel solution was then poured slowly into the gel caster to ensure that no excess bubbles were formed. The gel solution was poured until the top level was 1 cm above the desired level of the gel. Then 1 ml of water saturated butanol solution (see appendix) was placed on top of each gel with a 1 ml pipette. The pipette tip was run along the entire length while the butanol solution was slowly released in even volumes. The gel caster was then covered with a piece of cellophane until the gels solidified. This took approximately two hours. The gels were then removed from the caster, inspected for defect, and the butanol solution on top of the gel was washed off with double-deionized water and then placed on its side in the gel rack to allow all of the water to drain from the top of the gel. Then the gels were covered in gel-storage solution (see appendix) taking special care to cover the top of the gel where the IEF gel will seat). The gels were laid horizontally at room temperature to allow complete polymerization to occur. Prior to running the second dimension the top of the gels was washed again to remove any residual gel storage solution and allowed to sit on its side in the gel storage rack. The power used for most gel runs was based on an overnight run where 1.5 watts per gel was applied with the Ettan Dalt[®] six or twelve system. A 2X electrophoresis buffer (see appendix) was used in the upper cathodic buffer chamber and a 1X electrophoresis buffer (see appendix) was used in the lower anodic buffer chamber.

After the gel run was complete the gels were prepared according to the dyes used for imaging. If the CyDyes[®] were used, the gels were washed with water to remove any excess electrophoresis buffer and placed into a light-protected box with water and transported immediately to the Typhoon[®] Variable-Mode Imager 4900 for imaging. In the event that a

saturation dye was used, the top plate was carefully removed from the gel sandwich and the gels were placed into individual containers with fixing solution (see appendix) and allowed to sit for 2-24 hours at 4°C. The protocol for each saturation stain should be followed. Post-staining of CyDye® gels also followed the saturation stain protocol.

Imaging and analysis

Gels were imaged with the Typhoon Variable Mode Imager model no. 4900. ImageQuant® (Molecular Dynamics, version 5) was used to view the gel images. This software was used to crop the gel images and convert them to the correct electronic format for the downstream analysis software. Gels that were stained with CyDyes® were analyzed using DeCyder® version 10. Gels that were saturation stained with Coomassie, Deep Purple®, or silver were analyzed using ImageMaster Platinum version 6. Both of these software programs follow the same guidelines to generate a list of significant proteins.

Figure 10: Overview of approach to identify proteins of interest in DeCyder[®] version 6.5 and ImageMaster Platinum version 6

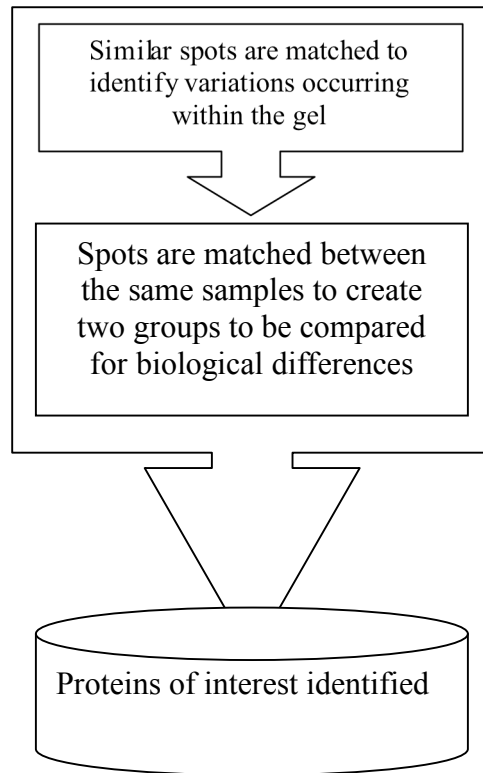


Figure 10: Graphical depiction of workflow for the detection of proteins of interest in 2D DIGE projects.

Spot excision

A pick-list is generated within the analysis software that creates a text (.txt) file that is moved to the computer that operates the Ettan Dalt[®] Spot Picker (GE Healthcare, Piscataway NJ) that is depicted below in Figure 10.

Figure 11: Ettan Dalt[®] Spot Picker



Figure 11: Image obtained from GE Healthcare product catalog 2008

After the text file is imported into the Spot Picker control software, the location of the reference markers, the thickness of the gel, and the location of the microtiter plate that will hold the gel plug are determined. Once these parameters were set, the program was initiated and the protein

spots were excised. Stains that were visible with the naked eye were inspected to ensure that the desired spots were excised. Stains that emitted only a fluorescent signal were imaged again with the Typhoon imager to ensure that the correct spots were excised. After this was verified, the protocol to proteolytically degrade the peptides and extract them from the gel was initiated.

Protein digestion (Trypsinization)

Proteins immobilized within the acrylamide gel matrix are exposed to trypsin that causes proteolytic degradation. Trypsin is a serine protease that degrades peptides at the carboxyl side chains of the amino acids lysine and arginine. Porcine trypsin from Promega was used in this study. The sample gel plugs are exposed to 100 μ l of a 50 mM ammonium bicarbonate/ 50% acetonitrile solution for 20 minutes at room temperature. The solution is then removed by careful pipetting so as not to disturb the gel plug then fresh 50 mM ammonium bicarbonate/ 50% acetonitrile is allowed to sit for an additional 20 minutes. The 50 mM ammonium bicarbonate/ 50% acetonitrile is again carefully removed by pipetting then replaced with 75% acetonitrile. The 96-well plate is then placed in the Eppendorf Vacufuge[®] (Model no. 22331 Hamburg, Germany) unit for 30 minutes with no heat. The dried and dehydrated gel plugs were then exposed to approximately 7 μ l of a 20 μ g/ ml solution of trypsin. Sufficient volume of the trypsin solution is added to cover the entire gel plug. The trypsin is kept at 4°C until added to the gel plug. The 96- well plate was placed on ice for 30 minutes once the trypsin was added to allow the trypsin to become adsorbed into the gel before proteolytic digestion began. After 30 minutes, the plate was wrapped thoroughly with Parafilm to prevent drying prior to placing into the 37°C incubator overnight. Following the overnight incubation, 100 μ l of a 50% acetonitrile/

0.1% trifluoroacetic acid (TFA) solution is added to the gel plug in order to extract the peptides from the gel matrix. The extraction solution was added in two fractions. First 60 μl of the 50% acetonitrile/ 0.1% TFA solution was added to the gel plug and allowed to sit for 20 minutes at room temperature. Then the solution was removed by pipette and placed into a fresh Lo-Bind Eppendorf[®] tube and 40 μl of the 50% acetonitrile/ 0.1% TFA was added to the gel plug. This solution was allowed to sit for 20 minutes at room temperature. Following incubation, the 40 μl was combined in the same Eppendorf[®] tube with the original 60 μl that was removed in the first set. The Eppendorf[®] tubes were then placed in the Eppendorf Vacufuge[®] for 2 hours or until the liquid was completely evaporated. The samples were then stored at -20°C until ready for use. The maximum storage time is one week.

Zip-Tipping[®] and MALDI TOF-TOF

Samples were removed from the -20°C and allowed to come up to room temperature for 5 minutes. Then 1.5 μl of neat formic acid was pipetted into each sample tube and vortexed briefly. Then 8.5 μl of 0.1% trifluoroacetic acid (TFA) was pipetted into each sample tube and the sample was vortexed at low speed for five minutes at room temperature. The samples were then centrifuged briefly to bring all of the liquid down into the bottom of the Eppendorf[®] tube. The Zip-Tip[®] (Millipore) was then prepared by first wetting and then aspirating with 0.1% TFA. The sample was then bound to the C-18 column and washed with 0.1% TFA. The sample was released from the column with the elution solution and spotted onto the MALDI plate. Once the sample dried, the alpha-cyano-4-hydroxycinnamic acid matrix was applied (Agilent Technologies, catalog no. G2037A). The MALDI plate was then placed at 4°C until ready for

analysis. The samples were analyzed at the Emory Microchemical Facility, Atlanta GA.

Proteomics experimental set-up

Overview: Each experiment varied in the experimental treatment with farnesol. The growth of working cultures, downstream harvest, and preparation for 2D proteomics followed the methods described in the previous sections.

Experiment 1: *P. aeruginosa* PAO1 exposed to 30 μM racemic farnesol, IPG range 3-11

The protocol to initiate this experiment followed the procedure introduced in the cell cultivation and harvest section found earlier in the Materials and Methods section. The concentration of the farnesol stock solution was altered so that 66 μl of racemic farnesol at a final concentration of 30 μM was added to the culture media.

Experiment 2: *P. aeruginosa* PAO1 and GSU3 exposed to 25 μM and 250 μM *E,E*-farnesol, IPG range 3-11

The protocol to initiate this experiment followed the procedure introduced in the cell cultivation and harvest section found earlier in the Materials and Methods section. The concentration of the farnesol stock solution was made exactly as indicated in this section so that only 66 μl of farnesol and methanol was added. The concentration of the stock solution varied so that the final concentration was either 25 μM or 250 μM in the culture media.

Experiment 3: *P. aeruginosa* PAO1 exposed to 25 μM *E,E*-farnesol, IPG range 4.5-5.5

The protocol to initiate this experiment followed the procedure introduced in the cell

cultivation and harvest section found earlier in the Materials and Methods section. The concentration of the farnesol stock solution was made exactly as indicated in this section so that only 66 μ l of farnesol and methanol was added and the final concentration of farnesol was 25 μ M.

Experiment 4: *P. aeruginosa* PAO1 catheter lumen biofilm exposed to 250 μ M *E,E*-farnesol, IPG range 3-7

The initial cultivation of cells followed the method outlined in the materials and methods section however no farnesol was added at this stage. A flow-through system was setup up where fresh LB Miller media maintained at 37°C and was passed through the lumen of a Bard Bardex® Foley All-Silicone 16 French urinary catheter. A schematic of the experimental setup is presented in figure 10. First the lumen was inoculated with 5 ml of mid-log phase cells of *P. aeruginosa* PAO1 with an approximate OD₆₀₀ nm of 0.7 with a sterile syringe. A sterility check was performed of the effluent to ensure that only *P. aeruginosa* was present in the lumen. Following seeding, fresh sterile media was passed in one direction through the lumen. The flow rate was adjusted so that the cells were unable to grow upstream of the catheter segment with a Masterflex® pump (Cole Parmer model 7518-10) set at a flow rate of 20 ml/min with Masterflex® Tygon tubing (06409-15). All connections were maintained with tubing clamps that insured no liquid media leaked. The urinary catheter was allowed to sit for two days to allow the cells to develop a mat along the lumen of the catheter before exposure to farnesol occurred. Once the biofilm had fully developed the catheter containing the biofilm was removed from the flow-through system and was connected to two sterile 10 ml syringes that contained 250 μ M *E,E*-

farnesol. One of the syringes was completely filled with medium and the other was completely empty. In order to expose the cells to the farnesol without disturbing the biofilm, the media was slowly released from the full syringe and equal pressure was used to suction the media into the empty syringe. Once the previously empty syringe was full with approximately 10 ml of media the process was repeated in the other direction. This process was repeated once every 10 minutes for two hours. At the completion of the two-hour exposure the media was forcefully pushed from the syringe through the catheter and the cells were expelled into a 50 ml falcon tube. The media was then drawn up again and was used to forcefully wash the cells from the lumen of the catheter. The cells that remained in the lumen were removed by placing the catheter segment into a fresh 15 ml falcon tube with 11 ml of sterile PBS and vortexing until the thin layer of cells were removed. The lumen segment was removed and the tube was centrifuged at 10,000 RPM for 10 minutes to pellet the cell material that was washed from the lumen. This pellet was then combined with the previously acquired aspirate from the lumen. The protocol for cell harvesting, as outlined previously in the materials and methods section, was followed to prepare the cells for lysis and proteomic study.

Figure 12: Diagram of experimental set-up for flow-through biofilm

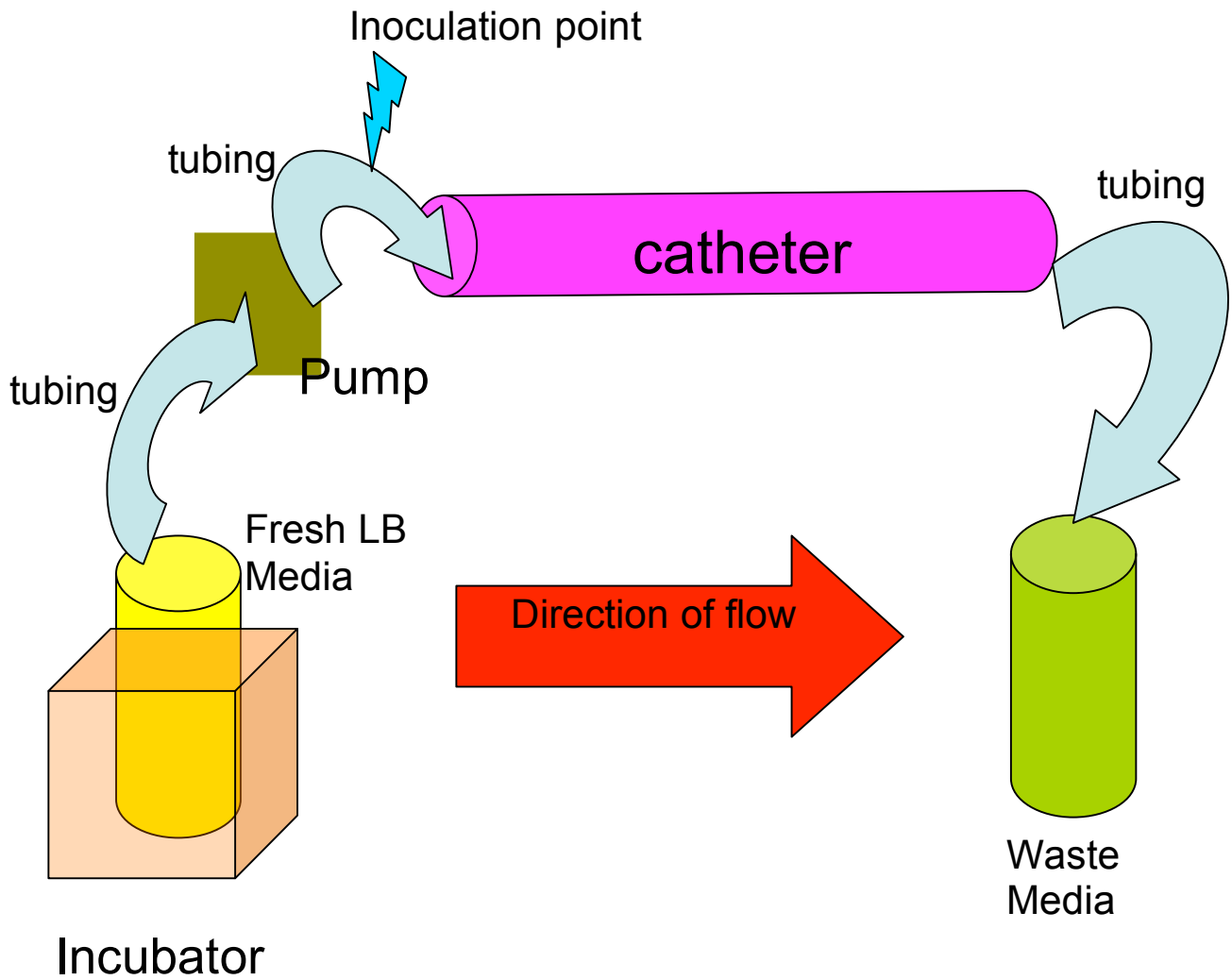


Figure 12: Graphical depiction of the experimental set up for the flow through biofilm model. The flow of media was in a single direction to ensure that fresh media was continuously provided to the developing biofilm.

Experiment 5: *P. aeruginosa* PAO1 co-cultivation with *C. albicans* whole cells, IPG range 3-7

The cells used in this experiment were removed from glycerol stock and initial cultures were established according to the procedures outlined previously in the Materials and Methods section. Both organisms used, *P. aeruginosa* PAO1 and *C. albicans* SC5314, were initially grown in LB Miller broth at 37°C and 130 RPM. First both strains were grown to mid-log phase (an OD₆₀₀ of 0.7 for PA and an OD₆₀₀ of 1 for CA) and 1 ml was removed from each culture. This sub-sample was centrifuged at 10,000 RPM for 10 minutes at 4°C. Following centrifugation the supernatant was discarded and was replaced with fresh PBS, at which time the pellet was dispersed with vortexing. This process was repeated three times to remove any residual medium. The cell pellets were resuspended in 500 µl of sterile PBS. 250 µl of each organism was used to inoculate a common flask with 100 ml of pre-warmed sterile LB Miller media that contained both *P. aeruginosa* and *C. albicans* after inoculation. Then the remaining 250 µl was used to inoculate a second flask, which also contained 100 ml of pre-warmed sterile LB Miller media that was only *P. aeruginosa* or *C. albicans* after inoculation. These flasks were allowed to grow for 8 hours at 37°C and 130 RPM and were then immediately put on ice following the 8 hour incubation. The cells were then harvested according to the harvesting protocol described previously and the resulting cell pellets were placed on ice for one hour to ensure thorough chilling. After one hour, the individual pellets of *P. aeruginosa* and *C. albicans* were combined by first resuspending the pellet in 2 ml of chilled sterile PBS and then the slurry

was combined into one centrifuge bottle and centrifuged at 4°C at 10,000 RPM for 10 minutes. The supernatant was removed and the wet weight of each pellet from the combined cultures was measured. The cells were then lysed according to the procedure outlined previously in the Materials and Methods section to prepare the samples for proteomic analysis. The sonication was optimized to preferentially lyse the bacterial cells without complete lysis of the yeast cells. In order to fully lyse yeast cells extended sonication times with the presence of glass beads are required.

Growth on *E,E*-farnesol and alternative carbon sources:

Two experiments were performed to determine the ability of *P. aeruginosa* to grow on *E,E*-farnesol as a sole carbon source. Second to determine the ability of different long chain carbon compounds to prime the metabolism of *P. aeruginosa* to utilize *E,E*-farnesol as a carbon source. Liquid media and solid media were prepared with Stanier's minimal medium to which alternate carbon and nitrogen sources were added. The carbon sources assayed for growth were: glucose, sorbitol, sodium- acetate, hexanoic acid, hexanoamide, and octanoic acid. The nitrogen source used was ammonium sulfate. Both plates and liquid media were made with 1000 ppm carbon source and 1000 ppm nitrogen source. *P. aeruginosa* PAO1 was tested for the appearance of colonies for plates and turbidity for liquid media. PAO1 cells were removed from glycerol stocks and allowed to thaw. Once thawed, 10 µl was removed and placed into 10 ml of sterile LB Miller media. The media was vortexed to allow even dispersion of cells in the liquid media. 10 µl was then pipetted into LB Miller plates and spread with a sterile glass spreader. The plates were allowed to incubate at 37°C overnight. The following morning the plates were checked for sterility, scraped, and used to inoculate liquid Stanier's medium with glucose as the

carbon source. 200 ml of liquid Stanier's medium was inoculated with one loop full of *P. aeruginosa* PAO1 and allowed to shake at 150 RPM and 37°C for 8 hours or to an OD₆₀₀ of 0.8 to create a working culture. For the solid media experiments 10 µl was removed from the working culture and spread on the surface of each medium type. The plates were allowed to incubate overnight at 37°C. They were rated according to the density and number of colonies present on the plate surface present following overnight growth. For the liquid media experiments, 10 µl was removed from the working culture and was inoculated into 990 ml of test media. Three replicates were made of each media type. The baffled flasks were allowed to incubate overnight at 37°C and 150 RPM for approximately 16 hours. The flasks were assayed for turbidity and the OD₆₀₀ was determined using with 1 ml samples. The 16 hour culture was diluted into fresh test medium and the OD₆₀₀ was measured hourly to generate a growth curve. Each flask was inoculated with a starting OD₆₀₀ of 0.02 and was allowed to incubate at 37°C and 150 RPM.

Low-osmolarity growth:

P. aeruginosa PAO1 was inoculated from glycerol stocks with 10 µl into 10 ml of sterile LB Miller media. The media was vortexed until the cells were fully dispersed. 10 µl of the first past stock was used to inoculate 99 ml of LB Miller media. The baffled flask was allowed to incubate at 37°C and 150 RPM overnight for approximately 16 hours. The low osmolarity medium was based on LB medium and contained tryptone and yeast extract but no sodium chloride. After 16 hours the *P. aeruginosa* cells were exposed to 250 µM farnesol or to the methanol only as a control for 8 hours. The cultures were then split where half of the cells in

each condition were exposed to high osmolarity LB and low osmolarity LB. There were three replicates for each media condition.

***C. elegans* virulence assay**

The assay for fast killing of *C. elegans* by *P. aeruginosa* requires a high salt growth medium. The high osmolarity PGS media was used (see appendix), and fast killing was scored after 8 hours. *E. coli* 0P50 that does not kill *C. elegans*, was used as a control. Glycerol stocks of *E. coli* 0P50 were obtained from Dr. W.W. Walthall's collection at Georgia State University and were grown according to the method described in the strains and cultivation section. *P. aeruginosa* and *E. coli* cultures were first grown overnight in 100 ml of LB-Miller broth at 130 RPM and 37°C. A 10 µl disposable inoculating loop was used to create a lawn of bacterial cells on the high osmolarity PGS agar plates. The plates were allowed to incubate at 37°C for 16 hours and 24 hours at 25°C. Then the plates were seeded with 20-30 L4 stage *C. elegans* (provided by Dr. W.W. Walthall, Georgia State University). The plates were observed under a dissection scope to quantify the exact number of *C. elegans* present on each plate. The plates were then allowed to incubate at 25°C for eight hours in the dark. After eight hours the number of live *C. elegans* were quantified. Live *C. elegans* were defined as exhibiting movement across the bacterial lawn or movement once touched with a hair-thin metal probe. *C. elegans* were counted as dead if they exhibited no movement upon stimulus. The number of survivors at the end of eight hours was used to determine the percent mortality when compared to deceased.

MIC assay- Tobramycin

A stock solution of Tobramycin (Sigma T-1783) with a concentration of 100 mM was made in 50 ml of sterile water. The stock solution was then aliquoted into 5 ml volumes and stored at -20°C until thawed for use. A working solution of 50 mM was made just before use in the assay with sterile water. Cells of *P. aeruginosa* GSU3 were removed from glycerol stock and inoculated into 100 ml of sterile LB Miller media and allowed to incubate for 16 hours at 37°C and 150 RPM. The MIC assay was performed in Costar® (catalog no. 3473) 24 flat bottom microtiter plates. The total volume for each well was 1 ml. In each well the final volume was adjusted with sterile LB Miller media. The volume of DMSO + *E,E*-farnesol working solution was made by making a 1:10 dilution of 3.8 M stock *E,E*-farnesol solution (100 µl into 900 µl of DMSO). The two conditions tested were, GSU3 cells exposed to 250 µM *E,E*-farnesol solubilized in DMSO and GSU3 cells that were only exposed to DMSO (66 µl) . Each condition was exposed to a range of Tobramycin concentrations that were shown in the literature to be effective in inhibiting the growth of GSU3. The concentrations tested were 0.5 µg/ml, 0.75 µg/ml, 1 µg/ml, 1.5 µg/ml. One row was used to test the effects on growth of no Tobramycin on each condition. One row was used to determine the changes in OD that may be caused by compositional changes in the culture medium for each condition. All components were present without any cell culture. The wells were set-up as reported in the following table:

Table 5: Sample organization for MIC assay

Row	Dilution <i>μg Tobramycin / ml</i>	Volume Tobramycin <i>μl working solution</i>	Volume DMSO + <i>E,E</i> -farnesol: 250 μM stock <i>(μl)</i>	Volume blank media <i>(ml)</i>	Volume inoculum <i>(μl)</i>
1	0	0	6.6	990	5
2	0.5	5	6.6	984	5
3	0.75	7.5	6.6	981	5
4	1	10	6.6	978	5
5	1.5	15	6.6	974	5

Table 5: Organization of samples in a 24 well microtiter plate for incubation and growth in the Tobramycin MIC assay. Each row had different concentrations of Tobramycin while the volume for farnesol and inoculum remained the same.

Imaging cell morphology

Cells from the tobramycin MIC assay were imaged to better capture observed changes in morphology that occurred during the assay. The cells (*P. aeruginosa* GSU3) were imaged in 24-well microtiter plates. These plates were imaged by Dr. Simmons (Georgia State University) using the DeltaVision[®] microscope system, (Applied Precision, LLC., Issaquah, WA.)

Pyruvate dehydrogenase activity assay

Cells of *P. aeruginosa* were lysed according to the proteomics protocol with the exception that the lysis buffer used was sterile 50 mM phosphate buffered saline and were stored at -80°C. The cells were thawed at room temperature and kept on ice once completely thawed. The concentration of total protein was quantified using the 2D Quant Kit (GE Healthcare, Piscataway NJ) following manufacturers protocol and the final concentration was adjusted to 1 µg/µl with 50 mM PBS for each sample. 500 µg of total protein was used for each sample that was tested. Three conditions were set up to establish adequate controls: reaction mixture without pyruvate and 500 µg sample protein, reaction mixture with 50 mM pyruvate and 500 µg sample protein, reaction mixture with 100 mM pyruvate and 500 µg sample protein. The reaction mixture was composed of 2.5 mM NAD, 0.2 mM thiamine pyrophosphate, 0.1 mM Coenzyme A (Sigma Aldrich), 0.3 mM DTT, 1 mM Magnesium chloride (Sigma Aldrich), .6 mM INT (Iodonitrotetrazolium violet) (Sigma Aldrich). This solution was made up in 10X solution to accommodate small masses of additives and the solution was stored at 4°C until ready for use. A stock solution of 5 mM pyruvate was also made and stored at 4°C until ready for use. The same volume of crude enzyme extract was added into each reaction vial (3 replicates per sample).

Then a base line absorbance at OD₅₀₀ was recorded before the pyruvate was added. This value was subtracted from each sample to determine the difference in slope between the control and experimental conditions. To start the reaction an appropriate volume of 5 mM pyruvate was added. In order to get the correct concentration of the reaction mixture, pyruvate solution, and protein concentration the solutions were made up in the following manner. Total working volume in each reaction vial was 1.5 ml. A sterile clean 5 ml test tube was used. First 150 µl of the 10X reaction mixture was added to the test tube. Then 375 µl of the 4X pyruvate solution was added to the test tube. Then the volume of crude sample needed to add the same concentration of total protein to each vial was calculated and added. The total volume of reaction mixture, pyruvate solution, and crude protein solution used was added together and this value was subtracted from 1.5 to determine the volume of water to add to make the total volume of each sample 1.5 ml. Before the pyruvate solution was added the optical density was recorded of one of the samples to obtain a blank base-line value. Once the reaction was started, 300 µl was removed and placed into a 96-well plate the absorbance was read at OD₄₉₀ in the Victor (Perkin-Elmer, Wellesley, MA) and 1 ml was assayed for absorbance in the Turner at OD₅₀₀. The Victor was programmed to take an OD reading every second for three minutes for each individual well. The reading in the Turner was taken every 10 seconds for three minutes. All timing for reactions began once the reaction mixture was added.

Results

Overview

The goal of this project was to determine the effects exposure to *E,E*-farnesol had on the expression proteome of *P. aeruginosa*. The approach taken was to utilize two-dimensional gel electrophoresis based proteomics to identify proteins which showed significant differences in abundance as a result of exposure to *E,E*-farnesol within the cytosol of *P. aeruginosa*. Two studies employed Differential In-Gel Electrophoresis (DIGE) techniques while the remainder were based on a two-dimensional Sodium Dodecyl Sulfate Polyacrylamide Gel Electrophoresis (SDS-PAGE). Once proteins of interest (those proteins that showed a significant change {P-value ≤ 0.05 } in abundance {average ratio $\pm \leq 0.05$ }) were found, assays to validate the findings were used to put the results from the proteomics data into physiological context. In each of the proteomics studies, the goal was to identify spots that corresponded to proteins that exhibited a statistically significant and biologically relevant change in abundance. Protein spots that exhibited an average value of $\pm .05$ and a p-value of .05 or less were considered to be statistically significant.

The statistical tests to obtain an average value and a p-value were performed using the statistical tool function provided in ImageMaster[®] or in DeCyder[®]. The p-value was employed to establish statistical significance of the change in abundance across all of the biological and experimental replicates. The average value is a measure of the change in abundance of a

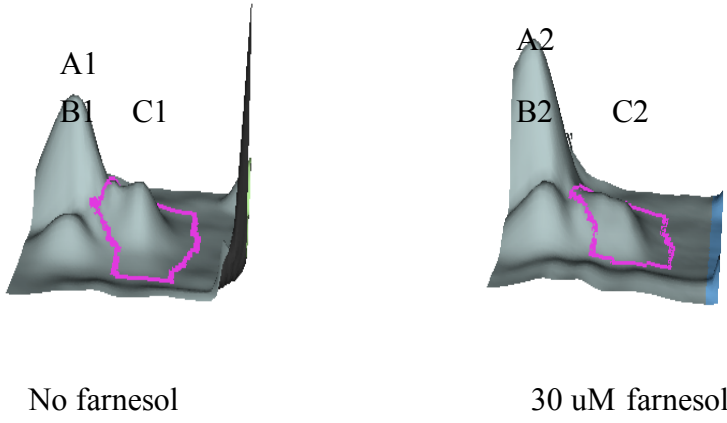
particular protein spot. A positive average value indicates an increase in abundance while a negative average value indicates a decrease in abundance.

The results reported from the image analysis software were in the form of 3D topographical images. The graphical image of the gel was generated by DeCyder[®] version 5. (The 3-D graphical image is a topographical representation of pixel intensity present in the gels that were excited by the specific wavelengths for the particular CyDye[®] label used. The 3D images are provided to better visualize the differences in abundance as peak height and volume, and to provide a visual comparison of adjacent protein spots. Also included in the data report from the spots identified with DeCyder[®] version 6.5 was the distribution graph that displayed the change in abundance in all of the samples within the data set. The x-axis of the distribution graph reports the particular condition that was tested, and the y-axis reports the standardized log abundance. The standardized log abundance is calculated from the Cy2 standard that is present in each DIGE study. With the 3D topographical image and distribution graph it is then possible to easily visualize the relationship between each individual gel. The mean is also present in the distribution graph to highlight the overall trends present in the data for a particular condition to more easily visualize increases or decreases in abundance.

Experiment 1: Exposure of *P. aeruginosa* PAO1 to mixed isomers of 30 μ M farnesol in the pI range of 3-11

Figure 13 reports a protein of significance from the initial proteomics study with farnesol. This study focused on the effect of *P. aeruginosa* PAO1 exposed to 30 μ M farnesol. The farnesol used was a racemic mixture and was not solubilized in a solvent prior to addition to the broth culture of *P. aeruginosa*. Protein peak C2 shows a significant decrease in abundance even though the nearest neighbors show an increase in abundance (A2 and B2) when compared to the control that was not treated with farnesol. Peak C2 decreased in peak height as well as peak volume as compared to peak C1. This protein was selected for MS analysis because its average ratio was $> \pm 2.0$ and exhibited a p-value less than .05. MALDI TOF-TOF analysis identified peak C2 as Flagellin type B from *P. aeruginosa*.

Figure 13: DeCyder image of Flagellin B as subsequently identified by proteomic analysis of *P. aeruginosa* PAO1 with 30 μ M racemic farnesol in the pI range of 3-11



Flagellin type B

Average Volume	-2.07
p-value	7.10E-06

Figure 13: 3D image from DeCyder that displays a decrease in abundance in *P. aeruginosa* PAO1 exposed to 30 μ M racemic farnesol.

Experiment 2: *P. aeruginosa* PAO1 and GSU3 exposed to 25 μ M and 250 μ M *E,E*-farnesol, pI 3-11

The results presented in figure 14 were generated in the DIGE study where two different concentrations of farnesol (25 μ M and 250 μ M) and two different strains of *P. aeruginosa* (PAO1 and GSU3) were analyzed. Peak A2 demonstrates an increase in abundance in peak height and in peak volume. The most evident change in abundance is the peak base area. The increase in A2 is evident despite the decrease in abundance of the near neighbor peak B2 as compared to the control B1. The protein spot (identified by MS analysis to be GMP synthase) exhibited an increase in abundance (1.62) in the cells of both strains that were exposed to farnesol, at both doses. There was no statistically significant difference in GMP synthase abundance levels between the two different strains when exposed to either 25 or 250 μ M *E,E*-farnesol. At 250 μ M levels of *E,E*-farnesol the mean lines for both strains cross indicating no significant difference in abundance between the two strains.

Figure 14: DeCyder image of GMP synthase as subsequently identified by proteomic analysis of *P. aeruginosa* PAO1 and GSU3, pI 3-11.

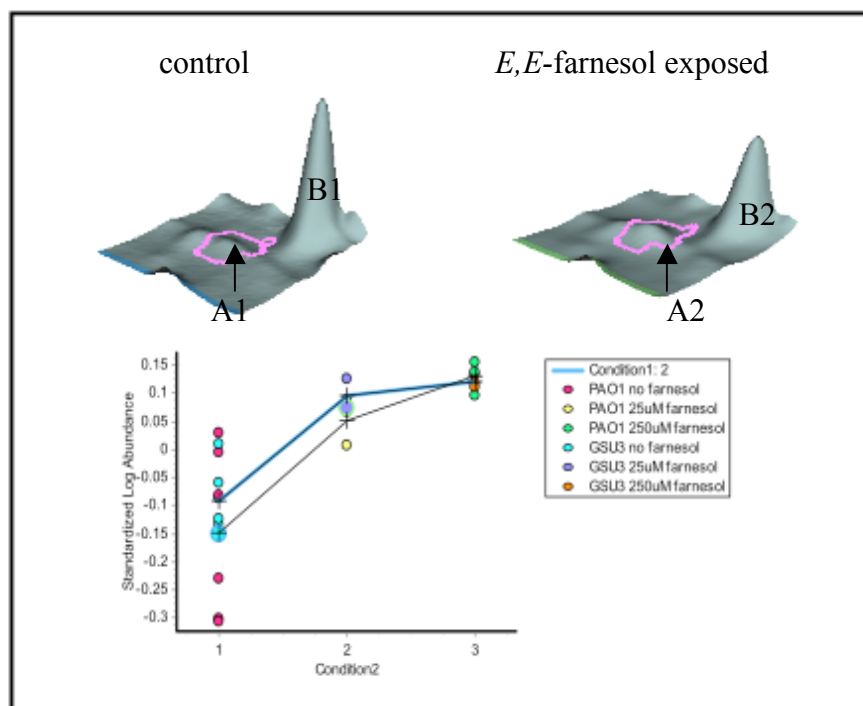


Figure 14: Results from DeCyder[®] version 5 to determine the effects that 250 μ M *E,E*-farnesol has on two strains of *P. aeruginosa* PAO1 and GSU3. These results show that there is a statistically significant increase in both strains for GMP synthase as compared to cells of the same type that were not exposed to *E,E*-farnesol. The average ratio was 1.62 and the p-value was .002.

The results presented in figure 15, which are also from experiment 2, show the change in abundance for the protein spot (that was later identified by MS analysis to be dihyrolipoamide dehydrogenase). This protein exhibited an average value of -1.19 and a p-value of .007.

Interestingly, the trend appears when observing the distribution graph that a closer grouping of

decrease in abundance is present in the cells of PAO1 and GSU3 that were exposed to 25 μM *E,E*-farnesol seen when the cells were exposed to 250 μM *E,E*-farnesol do not present as condensed results and some of the biological replicates show a less marked decrease in abundance when compared to the control.

Figure 15: DeCyder image of Dihydrolipoamide dehydrogenase identified by proteomic analysis of *P. aeruginosa* PAO1 and GSU3.

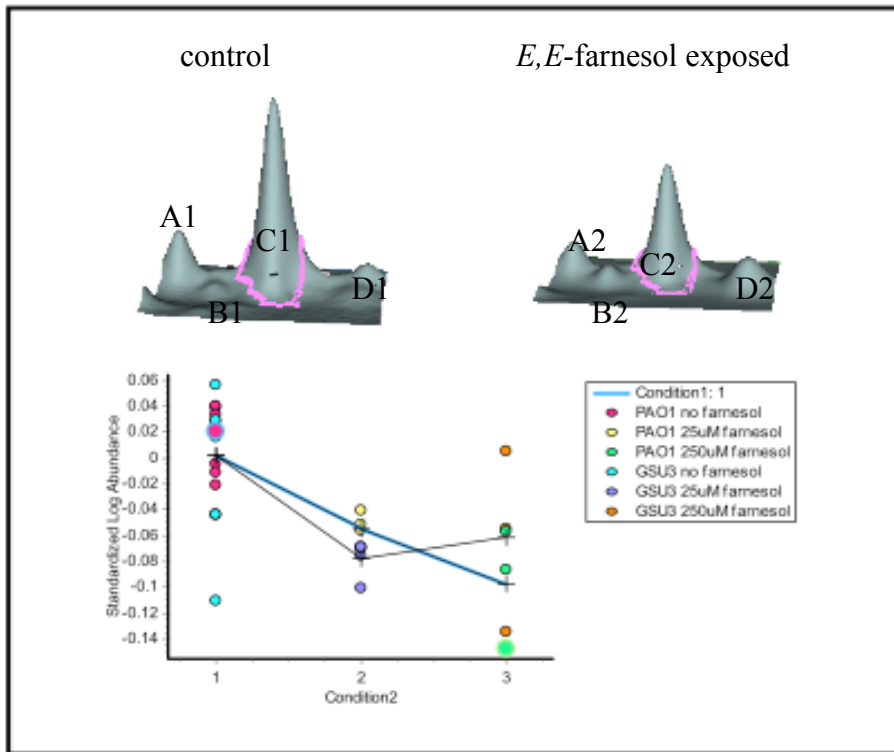


Figure 14: Results from DeCyder[®] version 5 to determine the effects that 250 μM *E,E*-farnesol has on two strains of *P. aeruginosa* PAO1 and GSU3. These results show that there is a statistically significant decrease in both strains as compared to cells of the same type that were not exposed to *E,E*-farnesol. The average ratio was -1.19 and had a p-value of .007.

Experiment 3: Planktonic *P. aeruginosa* PAO1 exposed to 25 μ M *E,E*-farnesol, pI range 4.5-5.5

The data presented in table 6 are a summary of all protein spots that were identified as proteins of interest in the DIGE study that focused on the pI range of 4.5-5.5 for the effects of *E,E*-farnesol on *P. aeruginosa* and which were subsequently identified through MS. Table 6 reports the name and accession number for each protein along with the p-value, average ratio, theoretical pI, theoretical molecular weight, and a summary of its function within the cell. Statistical graphs and 3D topographical views of these proteins of interest identified through MS analysis were a) ATPase PilB, b) major porin and structural outer membrane porin OprF precursor, c) Aconitase B, d) amidase, e) NAD-dependent glutamate dehydrogenase, f) Chain A, structure of Arginine Deiminase, g) outer membrane protein and related peptidoglycan-associated (lipo)proteins and are shown in Figures 1-5 respectively.

In each of the graphical images, the 3D image shown on the left is from the control samples and the 3D image on the right was from the *E,E*-farnesol exposed cells. The statistical graph provides the experimental conditions on the x-axis and the standardized log abundance on the y-axis. Also present on the graph is the mean of standardized log abundance of each of the samples in the study. Each individual circle on the graph represents one gel and the standardized log abundance of the matched spot.

Table 6: Summary of identified proteins by proteomic analysis of *P. aeruginosa* PAO1 exposed to 25 μ M *E,E*-farnesol in IPG range of 4.5 to 5.5

MS ID	p-value	Average ratio	pI	MW (Da)	FXN
ATPase PilB, Type II secretory pathway, ATPase PulE/Tfp pilus assembly ZP_00972151	.0099	-2.50	4.85	56424.28	Cell motility and secretion
Pyruvate dehydrogenase complex, dehydrogenase component E1 ZP_00971965	.0049	-1.83	5.72	41629	Metabolism
Major porin and structural outer membrane porin OprF precursor COG2885 gi 84321510	.0083	-1.97	5.0	37640	Secretion and membrane stability
COG1049: Aconitase B ZP_0097612	.024*	1.78	5.37	94185.43	Central metabolism TCA cycle
peptidoglycan-associated (lipo)proteins gi 84321510 COG2885	.016*	-1.63	4.42	23594.86	Membrane spanning region of OprF
hypothetical protein PaerPA_01001051 [<i>Pseudomonas aeruginosa</i> PACS2]	.014*	-1.65	Unk	Unk	Unk
amidase gi 15599358	.0023	1.52	5.8	38000	metabolism
hypothetical protein PaerP_01000692 [<i>Pseudomonas aeruginosa</i> PA7]	.0048	1.50	Unk	Unk	Unk
ABC-type multi-drug transport system, ATPase and permease components ZP_00968441	.0039	-1.51	5.25	67620	Defense mechanism
NAD-dependent glutamate dehydrogenase [<i>Pseudomonas aeruginosa</i> PAO1] gi 15598264	.0023	-1.53	4.8	48000	Amino acid metabolism
Chain A, Structure Of Arginine Deiminase gi 42543632	.039*	-1.53	5.08	46069.98	Metabolism of amino acids and related molecules
COG2885: Outer membrane protein and related peptidoglycan-associated (lipo)proteins [<i>Pseudomonasaeruginosa</i> C3719] gi 84321510	.015*	-1.54	4.42	23594.86	Membrane spanning region of OprF
hypothetical protein PaerPA_01000945 [<i>Pseudomonasaeruginosa</i> PACS2]	.0023	-1.59	Unk	Unk	Unk

Table 6: Table summarizing proteins identified by DeCyder and MS analysis that was statistically significant. This table reports the MS identity, average ratio, p-value, pI, molecular weight, and summarized function. Shaded rows indicate proteins that are presented more in-depth in Figures 1-5.

Figure 16: DeCyder image of ATPase PilB identified by proteomic analysis of *P. aeruginosa* PAO1 exposed to 25 μ M *E,E*-farnesol.

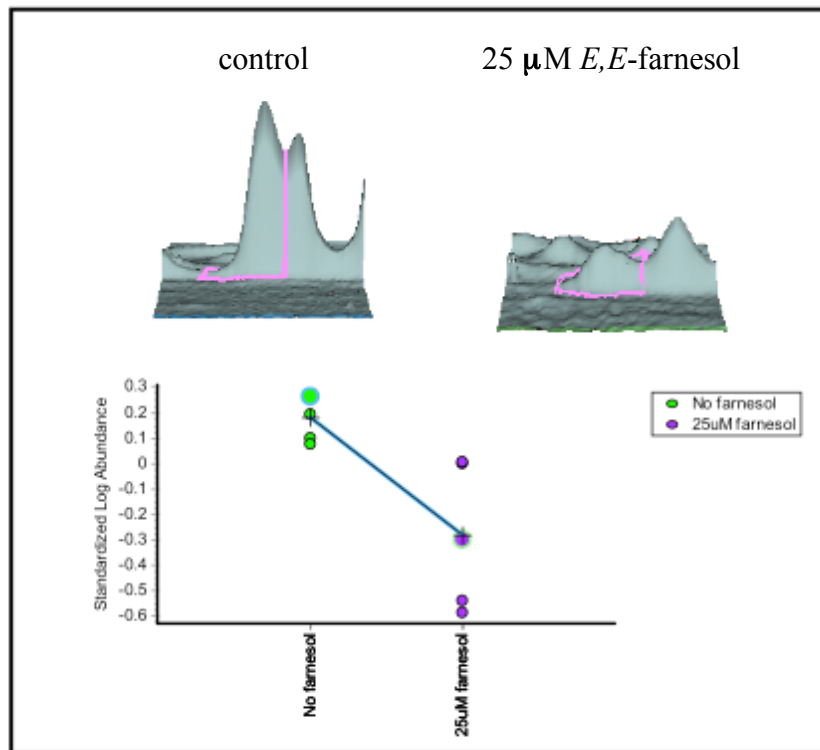


Figure 16: 3D topographical image and standardized log abundance generated by DeCyder[®] version 6

Result show that 25 μ M *E,E*-farnesol affected planktonic *P. aeruginosa* PAO1. These results showed a statistically significant decrease (p-value .0099) and (fold change -2.5) in ATPase PilB as compared to PAO1 cells that were not exposed to *E,E*-farnesol. The mean of the experimental values is approximately -0.3 while the mean of the control values is approximately 0.2.

Figure 17: DeCyder image of Major porin and structural outer membrane porin OprF precursor as identified by proteomic analysis of *P. aeruginosa* PAO1 exposed to 25 μ M *E,E*-farnesol.

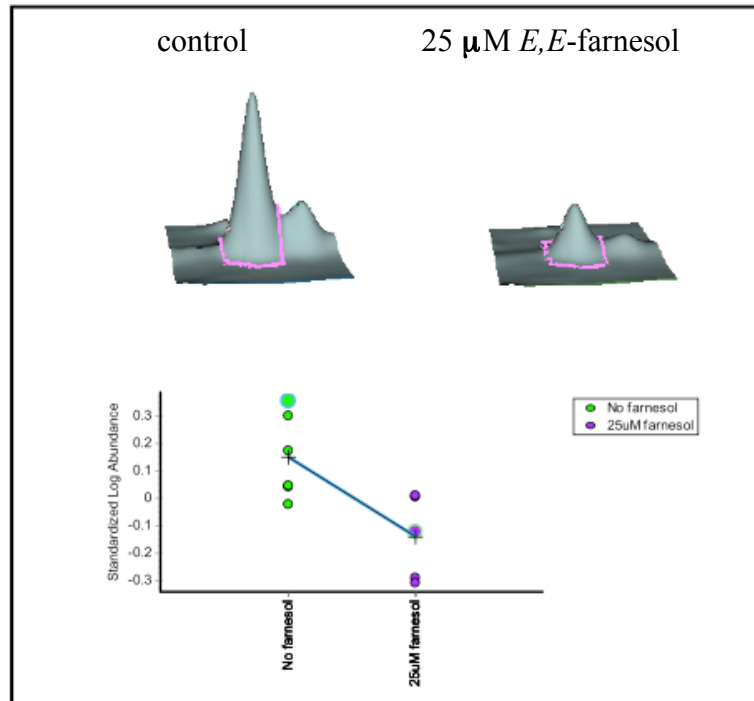


Figure 17: 3D topographical image and standardized log abundance generated by DeCyder[®] version 6

Result show that 25 μ M *E,E*-farnesol affected the abundance of OprF precursors within the cytosol in planktonic *P. aeruginosa* PAO1. These results showed that there is a statistically significant decrease (p-value .0083 and fold change of -1.97) in OprF precursor as compared to cells of the same type that were not exposed to *E,E*-farnesol.

Figure 18: DeCyder image of Amidase as identified by proteomic analysis of *P. aeruginosa*

PAO1 exposed to 25 μ M *E,E*-farnesol

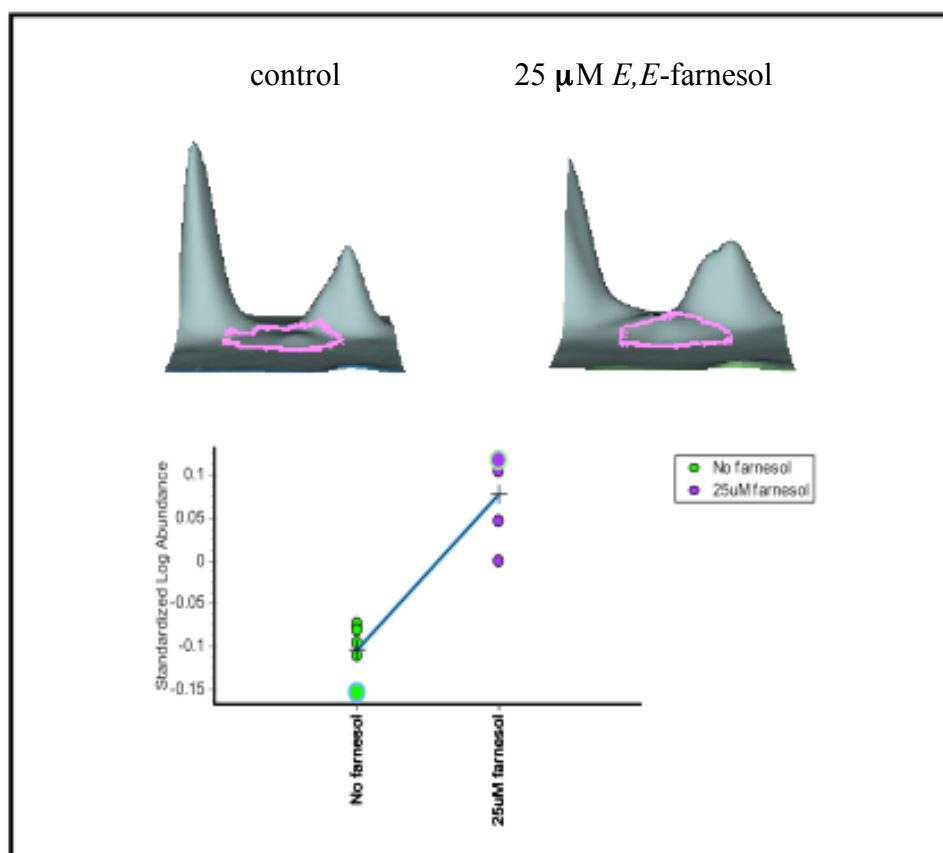


Figure 18: 3D topographical image and standardized log abundance generated by DeCyder[®] version 6

Result show that 25 μ M *E,E*-farnesol affected the abundance of amidase within the cytosol in planktonic *P. aeruginosa* PAO1. These results showed that there is a statistically significant increase (p-value .0023) and fold change (+ 1.52) in amidase as compared to cells of the same type that were not exposed to *E,E*-farnesol.

Figure 19: DeCyder image of Arginine diminasase as identified by proteomic analysis of *P. aeruginosa* PAO1 exposed to 25 μ M *E,E*-farnesol

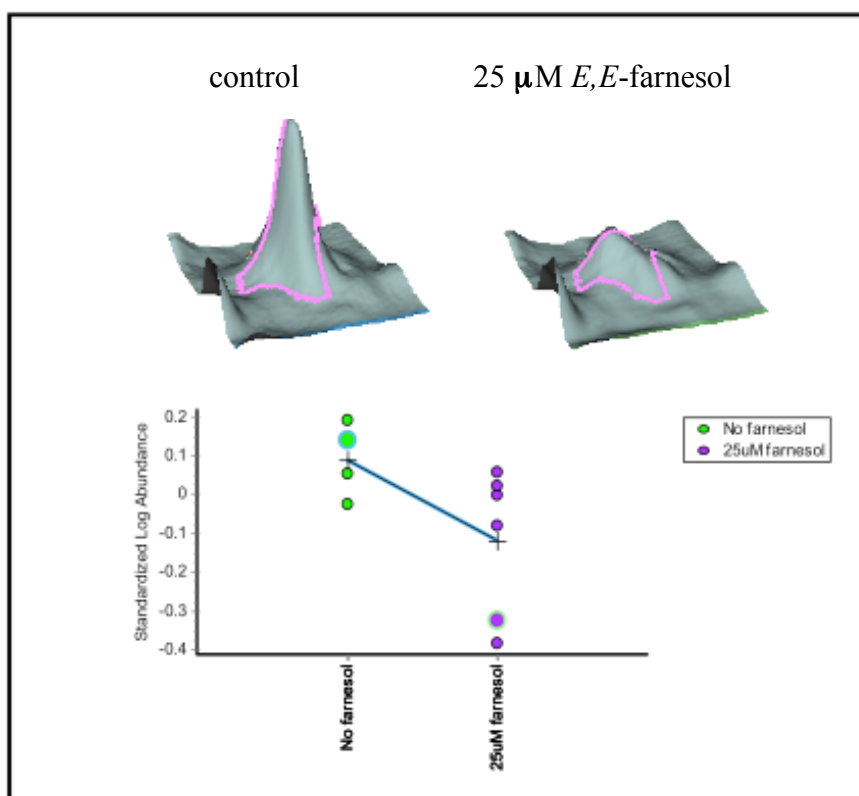


Figure 19: 3D topographical image and standardized log abundance generated by DeCyder[®] version 6

Result show that 25 μ M *E,E*-farnesol affected the abundance of arginine diminasase within the cytosol in planktonic *P. aeruginosa* PAO1. These results showed that there is a statistically significant decrease (p-value .039) and fold change (-1.53) in arginine diminasase as compared to cells of the same type that were not exposed to *E,E*-farnesol.

Figure 20: DeCyder image of NAD-dependent glutamate dehydrogenase as identified by proteomic analysis of *P. aeruginosa* PAO1 exposed to 25 μ M *E,E*-farnesol

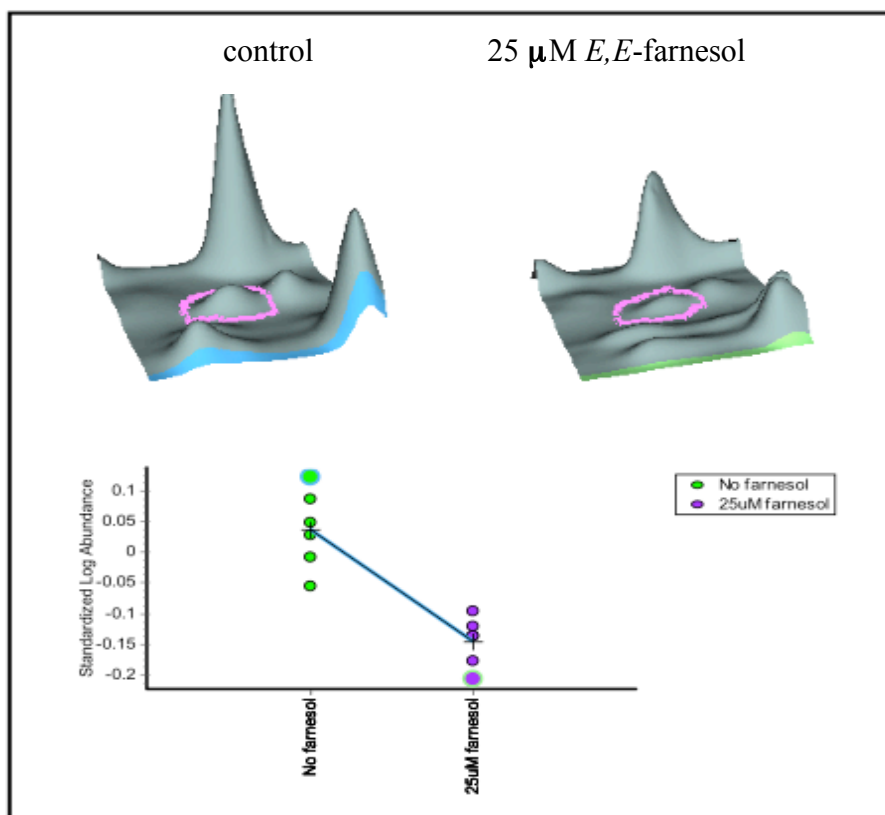


Figure 20: 3D topographical image and standardized log abundance generated by DeCyder[®] version 6

Result show that 25 μ M *E,E*-farnesol affected the abundance of NAD-dependent glutamate dehydrogenase within the cytosol in planktonic *P. aeruginosa* PAO1. These results showed that there is a statistically significant decrease (p-value .0023) and fold change (-1.53) in NAD-dependent glutamate dehydrogenase as compared to cells of the same type that were not exposed to *E,E*-farnesol.

Figure 21: DeCyder image of Pore region OprF (Outer membrane protein and related peptidoglycan-associated (lipo)proteins as identified by proteomic analysis of *P. aeruginosa* PAO1 exposed to 25 μ M *E,E*-farnesol

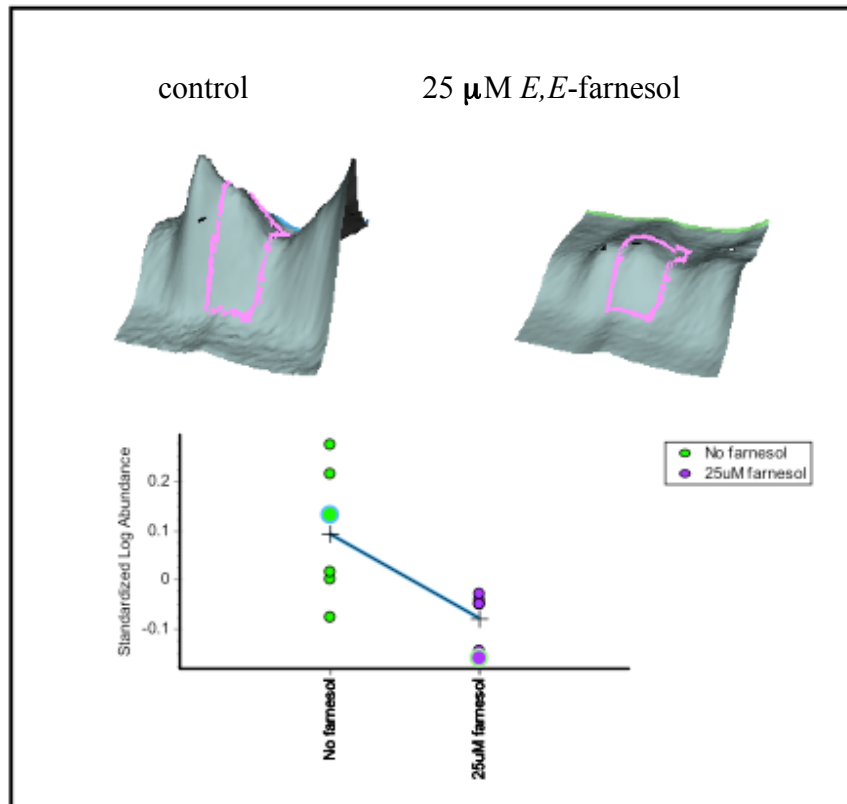


Figure 21: 3D topographical image and standardized log abundance generated by DeCyder® version 6

Result show that 25 μ M *E,E*-farnesol affected the abundance of pore region of OprF within the cytosol in planktonic *P. aeruginosa* PAO1. These results showed that there is a statistically significant decrease (p-value .015) and fold change (-1.54) in pore region OprF as compared to cells of the same type that were not exposed to *E,E*-farnesol.

Figure 22: DeCyder image of Aconitase as identified by proteomic analysis of *P. aeruginosa* PAO1 exposed to 25 μ M *E,E*-farnesol

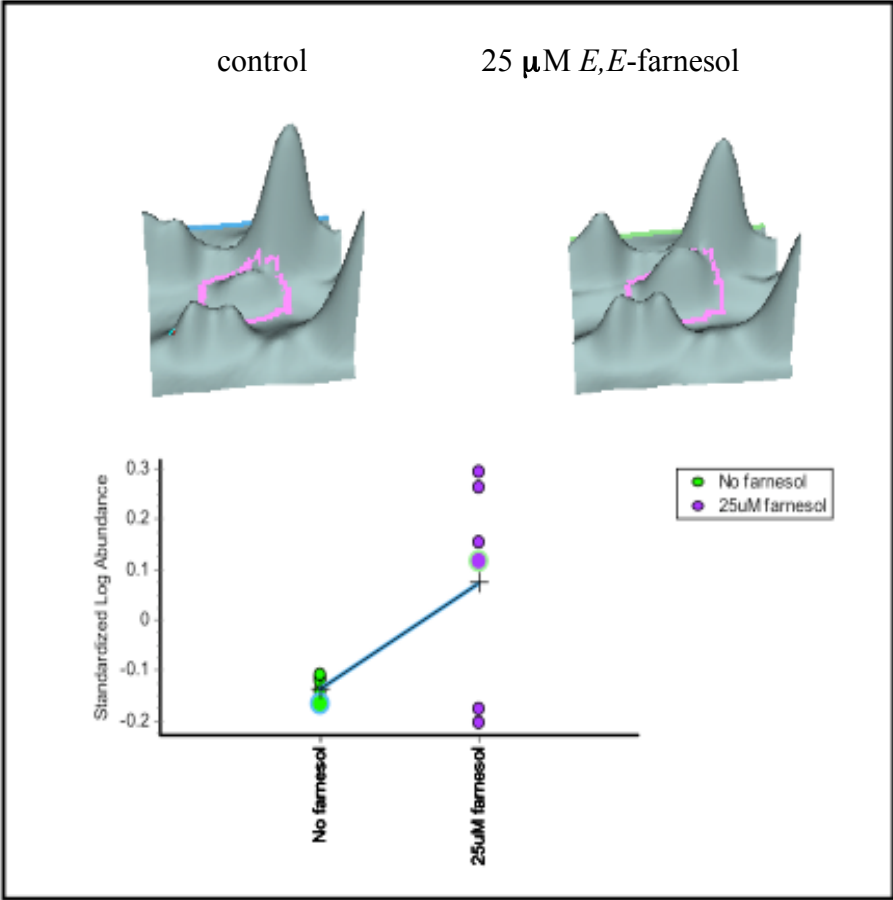


Figure 22: 3D topographical image and standardized log abundance generated by DeCyder[®] version 6

Result shows that 25 μ M *E,E*-farnesol affected the abundance of aconitase within the cytosol in planktonic *P. aeruginosa* PAO1. These results showed that there is a statistically significant decrease (p-value .015) and fold change (-1.54) in aconitase as compared to cells of the same type that were not exposed to *E,E*-farnesol.

Experiment 4: Exposure of Biofilm *P. aeruginosa* PAO1 to 250 mM farnesol in the pI range of 3-11

Table 7 presents the results from the proteomics experiment where *P. aeruginosa* PAO1 cells were grown as a biofilm in the lumen of a Bard Bardex[®] All-Silicone Urinary Foley catheter. The fully developed biofilm, as defined by a consistent blanket of cell growth on all sides of the lumen, was exposed to fresh media containing 250 μ M *E,E*-farnesol. The proteins were extracted using the proteomics protocols detailed in the materials and methods section and were analyzed for abundance changes using 2D SDS PAGE gels. The gels were analyzed using ImageMaster[®] Platinum (GE Healthcare). The proteins of interest were identified using the histogram function to identify proteins that exhibited an increase or decrease in pixel intensity as compared to the control gels. A limited number of gels were available for analysis due to sample loss from gel structural integrity failure. Full statistical data was not available due to the limited number of samples (< 6). The histogram function allowed for a general comparison between the control and experimental conditions. The 3D topographical image was used to assist in the determination that the match was accurate and that the reported fold change was accurate. Proteins of interest were removed from the gel and identified by mass-spectrometry.

In table 7 the identity of each protein of interest is reported in the left column with the header MS Identity. Identities were determined using MASCOT to search matches from the identified amino acid sequence. The relative change in abundance is reported in the right hand column and the respective fold change is reported as a downward green arrow or an upward

orange arrow. A total of six proteins of interest were positively identified and are reported in table 7.

Table 7: Mass-spectrometry identified proteins from proteomics project with *P. aeruginosa* PAO1 biofilm exposed to 250 μ M *E,E*-farnesol.





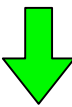

MS Identity	Relative change in abundance exhibited in cells exposed to 25 μ M <i>E,E</i> -farnesol as compared to the control
E3 subunit dihydrolipoamide dehydrogenase	
Arginine deiminase	
Succinyl-CoA synthetase beta-chain	
GroEL	
Elongation factor Tu (GTPase)	
Outer Membrane porin OprE	

Table 7: Proteins identified by MALDI-TOF-TOF MS and MASCOT database search. Protein spots of interest identified with ImageMaster Platinum analysis software.

Experiment 5: Proteomic analysis of Co-culture of *P. aeruginosa* PAO1 with *Candida albicans* in the pI range of 3-11

Table 8 presents results from the proteomics experiment where *P. aeruginosa* PAO1 cells were grown in co-culture with *C. albicans*. Pure cultures of both microorganisms were grown to a specific OD₆₀₀ nm (see materials and methods section for details) then the cultures were mixed in fresh medium. The co-cultured cells were harvested and their proteins extracted according to the proteomics protocol and were analyzed for abundance changes using 2D SDS PAGE gels. The gels were analyzed using ImageMaster[®] Platinum (GE Healthcare). The proteins of interest were identified using the histogram function to identify proteins that exhibited an increase or decrease in pixel intensity as compared to the control gels. The 3D topographical image was used to determine that the match was accurate and that the reported fold change was accurate. Proteins of interest were removed from the gel and identified by mass-spectrometry. The name of the protein is reported in the left column with the header MS Identity. This was determined using MASCOT to search matches from the identified amino acid sequence. The relative change in abundance is reported in the right hand column and the respective fold change is reported as a downward green arrow or an upward orange arrow. The proteins that exhibited a decrease in abundance in the experimental condition have a downward green arrow. The proteins that exhibited an increase in abundance in the experimental condition have an upward orange arrow. A total of four proteins of interest were positively identified and are shown in table 8.

Table 8: Mass-spectrometry identified proteins from proteomic analysis of co-culture between *P. aeruginosa* PAO1 and *C. albicans* SC5314.





Putative copper transport outer membrane porin OprC precursor	
COG2235: Arginine deiminase	
COG1064: Zn-dependent alcohol dehydrogenase	
Conserved hypothetical protein	

Table 8: Proteins identified by MALDI-TOF-TOF MS and MASCOT database search. Protein spots of interest identified with ImageMaster Platinum analysis software.

Figure 23: Illustration of proteins found in common in Biofilm, Co-culture, and Planktonic experimental conditions

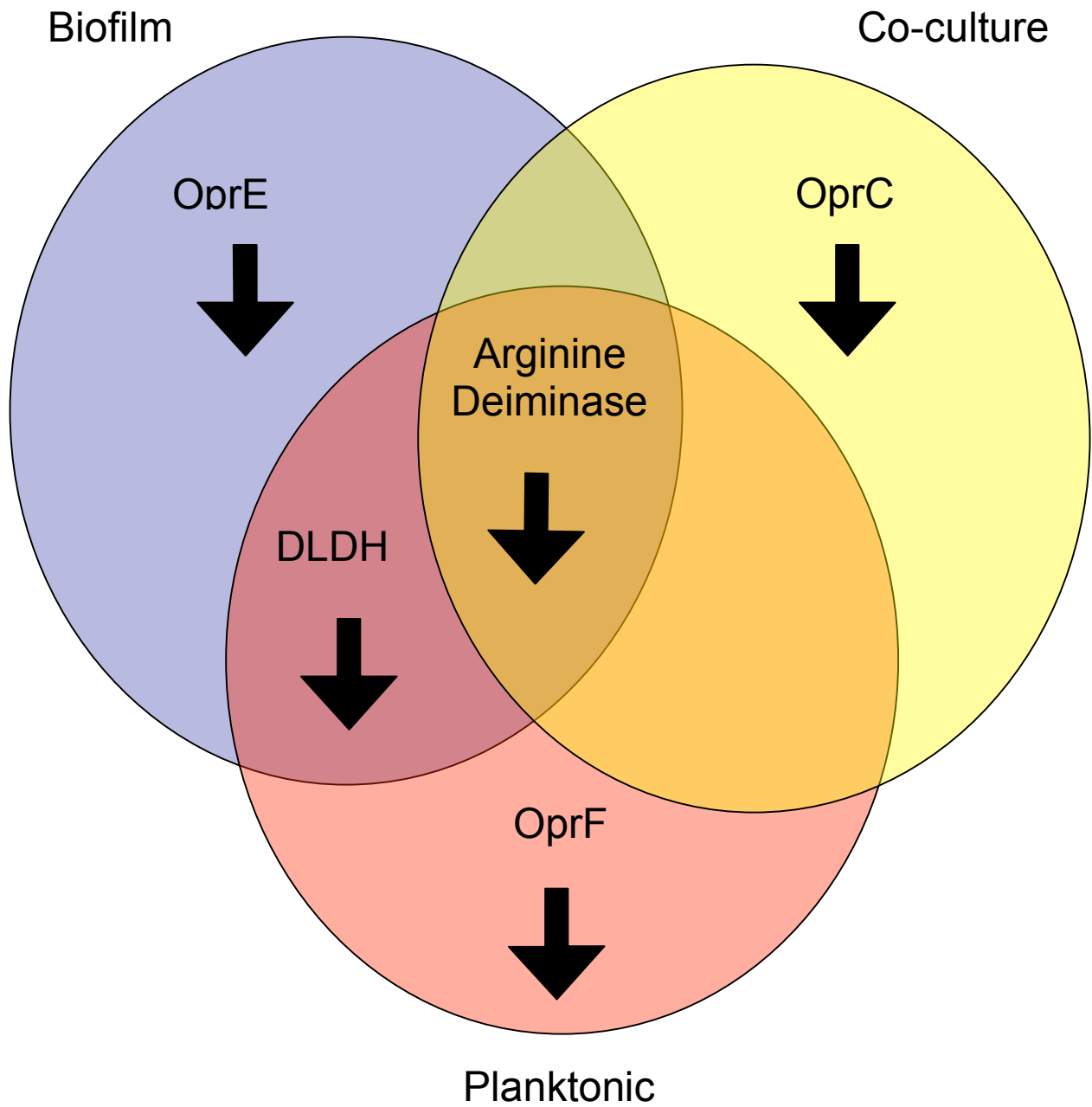


Figure 23: Proteins identified that were present in two or more physiological conditions. The direction of the black arrow indicated the change in abundance.

Physiological tests to validate proteomics findings

Osmotic Stress Assay

To place the proteomics findings in a physiological context the effect that *E,E*-farnesol had on the ability of the cell to withstand osmotic stress was assayed. The purpose of this assay was to determine if the decrease in abundance of porin precursors in the cytosol could lead to a destabilization of the outer cell membrane and structural integrity of the cell wall. This test was based on placing logarithmic growth phase *P. aeruginosa* cells into low osmolarity LB medium. The ability of the cells to withstand stress was assayed using optical density at 600 nm. A growth curve was recorded on samples in triplicate for each condition for six hours. Over the course of the assay there was not a significant difference in growth patterns in the control cells that were not exposed to 250 μ M *E,E*-farnesol.

Table 9: Growth curve of *P. aeruginosa* PAO1 exposed to 250 μ M *E,E*-farnesol under low osmolarity conditions

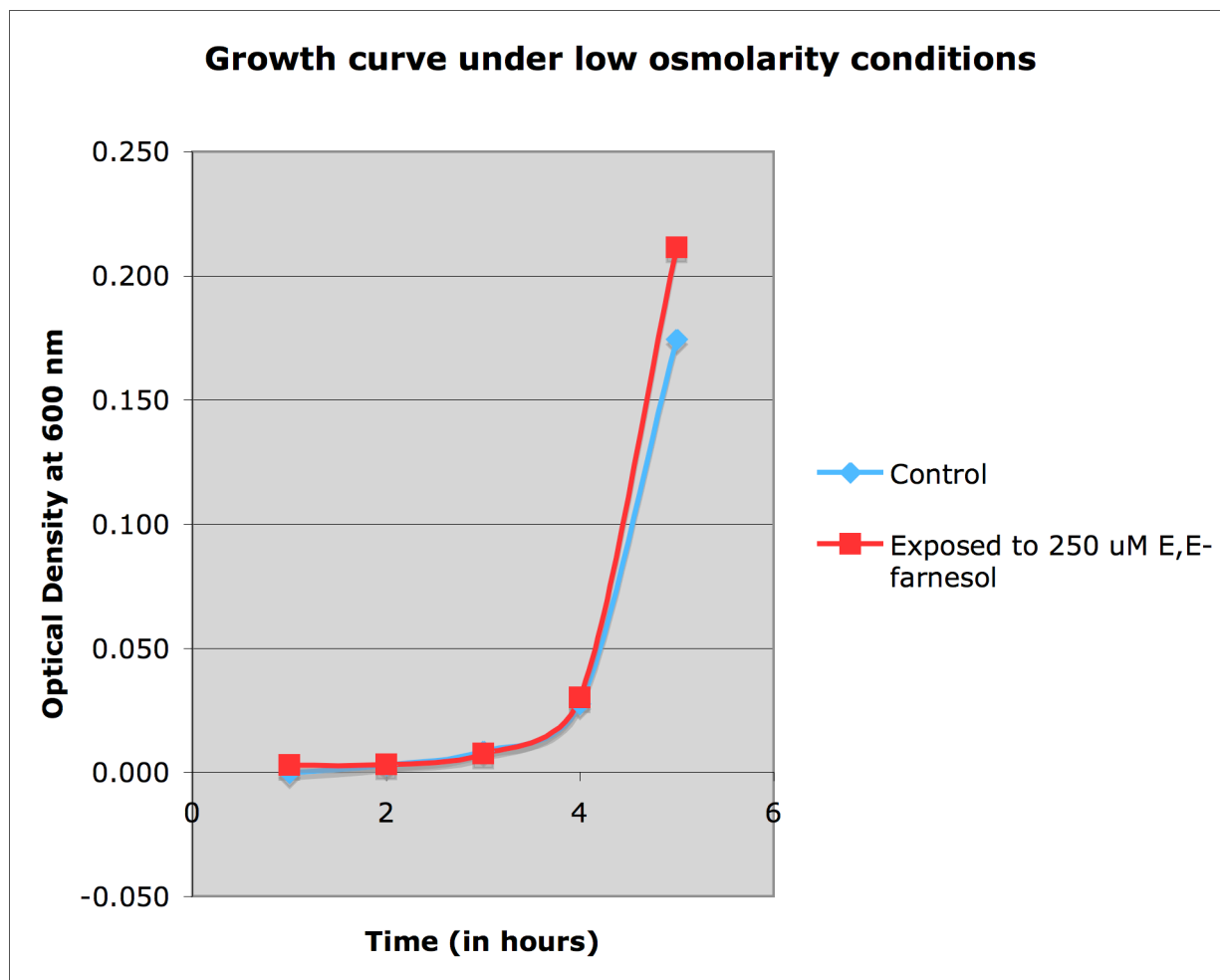


Table 9: Growth curve of *P. aeruginosa* PAO1 exposed to 250 μ M *E,E*-farnesol. The change in turbidity was determined using a spectrophotometer at 600 nm.

Fast killing virulence assay in C. elegans

The effect of exposure to farnesol on the virulence of *P. aeruginosa* was assayed using the *C. elegans* plate virulence assay. The two plate types used were those made with spent medium from *C. albicans* and those without. In order to determine the percent mortality from the *C. elegans* plate assay the number of animals that survived was subtracted from the initial inoculum value. Then the percentage of those that did not survive was determined from the number of survivors. The results presented in table 30 represent the percent mortality for the assay. *P. aeruginosa* PAO1 cells that were grown without any components from *C. albicans* caused a mortality rate in *C. elegans* of 56 %. When *P. aeruginosa* was grown on plates that did have components from *C. albicans* the mortality rate was slightly higher than the control but was significantly lower than the *P. aeruginosa* cells alone. The mortality rate for the control strain *E. coli* cells was on average 18.5 % this was due to the animals sticking to the edge of the plate. Based on these results the presence of farnesol containing spent medium from *C. albicans* does have a role in reducing the virulence of *P. aeruginosa* in the fast killing *C. elegans* assay.

Table 10: Effect of *E,E*-farnesol on *P. aeruginosa* PAO1 virulence in *C. elegans* fast killing assay

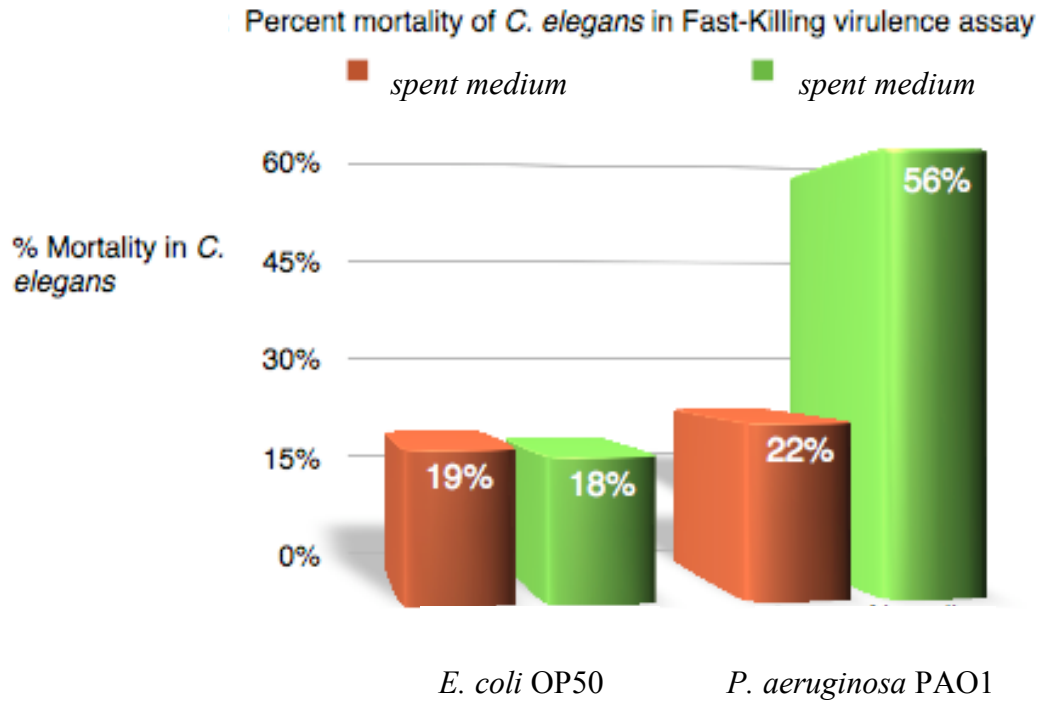


Table 10: Results from fast killing assay with *C. elegans*. Agar plates were made that were spiked with spent medium from *C. albicans* or were only LB Miller agar. *C. elegans* animals were inoculated and counted. After eight hours the animals were counted again and the number of live and dead animals were quantified. The plates that were spiked with spent medium from *C. albicans* did decrease the mortality of *P. aeruginosa* in the fast killing assay.

Validation of activity of Dihydrolipoamide dehydrogenase

In order to validate the proteomics results for dihydrolipoamide dehydrogenase, a component of the pyruvate dehydrogenase enzyme complex. The activity of pyruvate dehydrogenase was quantitated using a colorimetric assay to detect enzyme kinetics (Table 11). The activity of pyruvate dehydrogenase was detected at the rate that iodinitrotetrazolium violet was reduced and caused a color change. The slope of the line was used to determine if the kinetics for cells exposed to 25 μM *E*, *E*- farnesol were significantly lower than those cells that were not. The results show that there was not a significant difference in the slope of the line for the two conditions.

Table 11: Enzyme Activity of Pyruvate Dehydrogenase

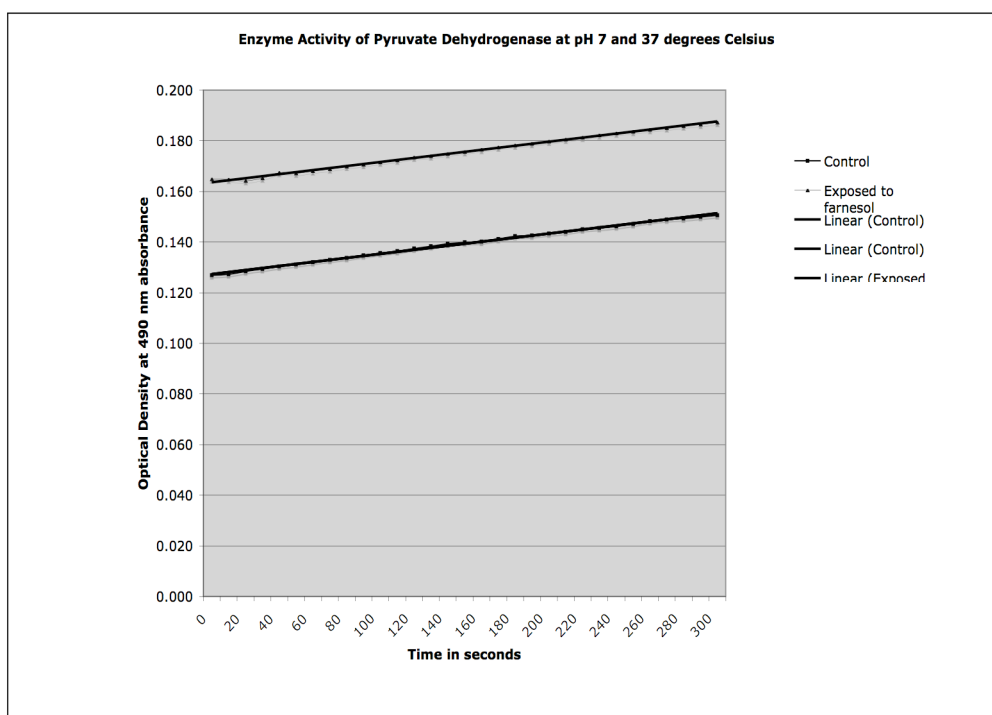


Table 11: This table reports the data from the Pyruvate dehydrogenase activity assay. The enzyme kinetics is based on the slope of the line. The absorbance of this assay is measured at 37 degrees Celsius and pH 7 at 490 nm using the Victor spectrophotometer. The assay begins colorless and as NADH is produced tetrazolium purple is reduced and causes a darker color change that can be measured. The greater the degree of color change in less time is the greater the speed of the enzyme. The slope of both lines was determined to be .0008 using Excel's regression tool. The similarity in slope of both conditions does not show any difference in the enzyme activity of Pyruvate Dehydrogenase in either condition.

Antibiotic susceptibility to tobramycin in P. aeruginosa cells exposed to E,E-farnesol

In order to validate the results for a decrease in abundance of OprF the ability of *E, E*-farnesol to affect the susceptibility of *P. aeruginosa* GSU3 to Tobramycin was assayed. This assay tested *P. aeruginosa* against a range of concentrations from .2 to 1.5 $\mu\text{g}/\text{ml}$ of

Tobramycin. The red line represents the control where cells were not spiked with *E, E*-farnesol during the experiment. The blue line represents the experimental condition where cells were exposed to 250 μM *E, E*-farnesol. The ability of the cells to survive was determined by turbidity measurements at 600 nm using the Victor spectrophotometer. It appears that at lower concentrations the turbidity of the cultures exposed to *E, E*-farnesol is higher than the control. However, at approximately 0.8 $\mu\text{g}/\text{ml}$ the turbidity experiences a dramatic drop and the cells that were exposed to farnesol are more susceptible to Tobramycin than the control.

Table 12: The effect of exposure to 250 μ M *E,E*-farnesol on antibiotic susceptibility in *P. aeruginosa* PAO1

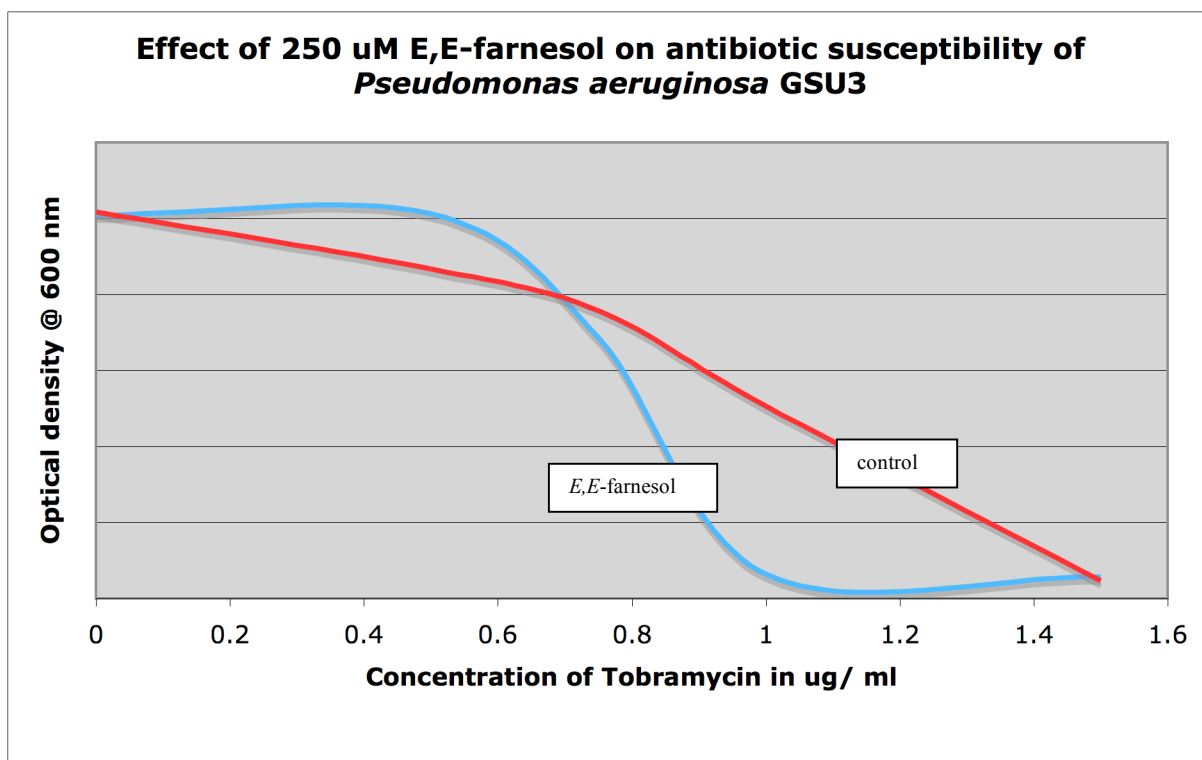


Table 12: Minimum inhibitory concentration assay to test level of susceptibility of *P. aeruginosa* GSU3 to Tobramycin.

Microscopy of P. aeruginosa cells exposed to tobramycin with or without E,E-farnesol

At the completion of the MIC assay it was apparent that the colonial morphology of the cells in the two different treatment conditions exhibited distinct differences. The colonies floating on the surface were imaged by microscopy by Dr. Robert Simmons at Georgia State University. The cells exposed to 250 μ M *E,E*-farnesol exhibited a very diffuse morphology while the control cells had a very condensed group of cells at the center of the broth.

Figure 24: Image of *P. aeruginosa* GSU3 exposed to 250 μ M *E,E*-farnesol and 0.8 μ g/ ml Tobramycin

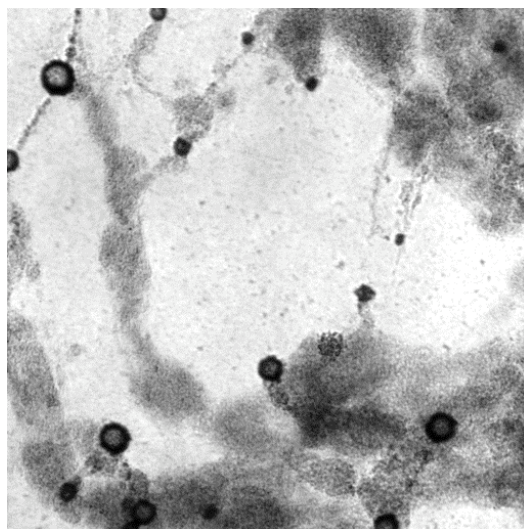


Figure 24: Microscopic image of colonial morphology of cells in broth containing 250 μ M *E,E*-farnesol and 0.8 μ g/ ml Tobramycin

Figure 25: Image of *P. aeruginosa* GSU3 exposed 0.8 $\mu\text{g}/\text{ml}$ Tobramycin

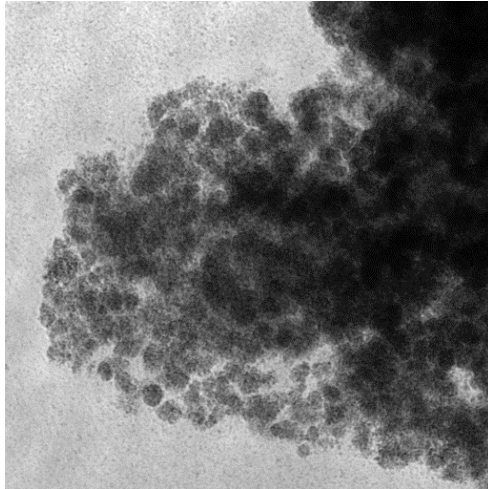


Figure 25: Microscopic image of colonial morphology of cells in broth 0.8 $\mu\text{g}/\text{ml}$ Tobramycin

Discussion

Overall proteomics results

The expression proteome data for proteins with a pI range of 3-11 in *P. aeruginosa* cells exposed to *E,E*-farnesol at 25 and 250 μ M *E,E*-farnesol did not show a highly robust change (fold change in average ratio > 3) in abundance. This outcome was seen in all of the experiments in this study, regardless of the mode of exposure to *E,E*-farnesol or whole cells of *C. albicans*. However, proteins of interest were identified that showed a statistically significant change in abundance (a fold change in average ratio greater or equal to 2). Proteomics techniques have the power to identify modest changes in protein abundance. This is possible due to the rigor of experimental design when taking full advantage of CyDyes[®] to stain the samples and DeCyder[®] software to image the gels. To determine the validity of the average ratio, in terms of statistical significance, the p-value provided a test to demonstrate the relevance of the observed results. This made it possible to identify proteins that exhibited a modest change in abundance but potentially had greater physiological implications within the biological system. A great deal of effort was placed in regulating the cell lysis and downstream protein isolation procedure in order to reliably compare results between experiments.

In the third proteomics project, the IPG range of 4.5 to 5.5 was studied several proteins identified had a theoretical pI that fell just outside the IPG range of the strip. Proteins that were acidic had a pI of 4.4 (peptidoglycan –associated lipoprotein and outer membrane protein and related peptidoglycan- associated protein). The identification of these proteins in the mass-spec analysis could be due to modifications within the cell that shifted the experimental pI of the

protein closer to 4.5. Although these proteins were picked from two distinct protein spots on the gel they were identified with the same MS ID. Upon inspection of the gel the two resolvable spots have the same molecular weight but exhibit a shift in pI, thus suggesting modifications made to the protein while still present within the cytosol. The function of peptidoglycan – associated lipoprotein within the cell is to form the channel region within one of the porins, most commonly OprF, which is discussed in further detail later. Two proteins were also identified that had a theoretical pI that was higher than the IPG range of the strip used in the experiment, suggesting modifications that made the proteins more acidic in the experimental condition. With a pI of 5.7, pyruvate dehydrogenase subunit E1 was identified and with a pI of 5.8, amidase was identified. Both of these proteins are important to metabolism within the cell and modifications were made to the protein that altered the experimentally the pI of these proteins was below the theoretical pI.

A potential reason for the modest change in abundance of the proteins of interest may have been the proportion of cells that were able to come into contact with *E,E*-farnesol directly. *E,E*-farnesol is a hydrophobic compound and was very difficult to effectively solubilize without a solvent present in the solution. Methanol and DMSO were used to increase the solubility of *E,E*-farnesol. Numerous discrete and easily visible micelles were noted upon addition of the *E,E*-farnesol and solvent mixture to liquids, indicating the inability to fully solubilize *E,E*-farnesol into the broth even in the presence of a solvent. Therefore, the proportion of cells within the sample culture that had physical contact with *E,E*-farnesol may have been reduced as compared to a compound that would easily solubilized and evenly diffuse throughout the sample medium.

Individual proteins showing statistically relevant change

In order to put the results into a context that could begin to explain the response that cells of *P. aeruginosa* has when exposed to *E,E*-farnesol a literature search was performed to determine the role that each protein has been documented to play in normal physiology of the cell and in virulence. Each protein of interest is introduced in terms of its function within the cell, any significant roles in virulence, and how the findings in this study fit into the overall story of the interaction between *Pseudomonas* and *Candida*.

GMP Synthase

Guanine Monophosphate synthase (GMP synthase) belongs to the functional class of enzymes for amino acid biosynthesis and metabolism and for purine biosynthesis and metabolism. In this study this protein exhibited an increase in abundance (+ 1.62) (Figure 14). The overall function of anthranilate synthase is to act as the first biosynthetic step in tryptophan biosynthesis. GMP synthase can be found in plants, fungi, and bacteria. In plants, anthranilate synthase is important for the production of secondary metabolites that provide the plant protection through the production of metabolically derived compounds such as endogenous auxin (Niyogi, *et al.*, 1992).

A second anthranilate synthase gene has been found in *P. aeruginosa* (Calfee, *et al.*, 2001). This second anthranilate synthase has been shown to be the first step in phenazine

production. The role of GMP synthase in anthranilate synthase activity is very intriguing because anthranilate synthase is very important in the production of phenazine compounds. The function of anthranilate synthase is to convert chorismate into anthranilate. The mechanism of GMP synthase, as a subunit of anthranilate synthase component II, acts as a potential phenazine modifying enzyme converting phenazine-1 carboxylate → phenazine 1-carboxamide (Farrow, *et al.*, 2007). Anthranilate can then go on to feed the need for either tryptophan synthesis or phenazine production.

In order to better understand the role of this enzyme in amino acid metabolism, purine synthesis and metabolism, or even phenazine production physiological tests will be utilized to pinpoint the exact node of action for this enzyme and how *E,E*-farnesol could influence its abundance within the cytosol. It was demonstrated by Cugini *et al.* in 2007 that exposure to farnesol can inhibit PQS signaling and prevents the production of pyocyanin. The data presented here suggests a potential pathway by which farnesol could be influencing the metabolic shifts within the cell to influence the production of pyocyanin. It is possible that the cell is increasing the abundance of GMP synthase in order to overcome suppression lower in the metabolic pathway that leads to the production of pyocyanin in an attempt to continue production. Future work to better understand the relationship between exposure to *E,E*-farnesol and abundance of GMP synthase to the production of pyocyanin would be to determine if GMP synthase is a regulatory check point that can be regulated at the level of the gene, RNA transcripts, or at the protein.

Dihydrolipoamide dehydrogenase

Data from MS analysis of statistically significant spots in 2D DIGE SDS-PAGE gels revealed a decrease in the enzyme dihydrolipoamide dehydrogenase in cells exposed to 25 and 250 μM *E,E*-farnesol in both PAO1 and GSU3 as compared to control cells that were not exposed (Figure 15). Dihydrolipoamide dehydrogenase (DLDH) is a homodimeric flavoprotein that reoxidizes dihydrolipoamide via NAD reduction, catalyzing the electron transfer between pyridine nucleotides and disulfide compounds (Carothers, *et al.*, 1989). DLDH has been found to be an integral part of many multi-enzyme processes to fulfill the aerobic and anaerobic metabolic needs of the cell. DLDH is present in several multi-enzyme complexes responsible for the conversion of 2-oxo acids to acyl-coA derivative. DLDH containing multi-enzyme complexes include: pyruvate dehydrogenase as the E3 subunit where its function is to oxidize pyruvate, 2-oxo glutarate dehydrogenase where its function is to oxidize alpha-ketoglutarate, 2-oxo acid dehydrogenase complexes where its function is to oxidize branched-chain alpha-ketoacids, glycine cleavage multienzyme complex as the L protein, acetonin dehydrogenase complex. This system, although not present in *Pseudomonas*, is found in gram-positive organisms such as *Bacillus subtilis*, and *Clostridium magnum* (Weiland, 1983; Deitrich, 1990; Kruger, *et al.*, 1994; Oppermann, 1994; Berg, 1997; Aevansson, *et al.*, 1999; Huang, *et al.*, 1999).

DLDH is present in organisms that lack 2-oxo acid dehydrogenase complexes such as *Trypanosoma burcei* and archeobacteria (Danson, *et al.*, 1987; Danson, 1988b) but the function is still not fully understood. Richarme and Heine reported in 1986, and Richarme reported in

1989, that organisms that possess 2-oxo acid dehydrogenases, such as *E. coli*, also utilize DLDH in the metabolism and transport of sugars such as galactose, maltose, and ribose across the membrane. In *S. pneumoniae*, defective DLDH was linked to decreased capsule production that was thought to be due to disrupted alpha-galactoside metabolism and galactose transport (Smith, *et al.*, 2002) cell cycle progression in fission yeast (Jang, *et al.*, 1997), and acts as a highly immunogenic surface antigen in *Neisseria meningitidis* (de la Sierra, *et al.*, 1997; Exposito, *et al.*, 1999).

One goal of the project was to validate a decrease in Pyruvate dehydrogenase (PD) activity in PAO1 cells grown in the presence of 25 μ M *E,E*-farnesol. The PD enzyme is composed of three subunits: E1 pyruvate decarboxylase, E2 lipoyl reductase, and E3 dihydrolipoyl dehydrogenase. Physiological tests to evaluate the role of dihydrolipoamide dehydrogenase were performed by measuring the overall activity of the intact enzyme complex pyruvate dehydrogenase. The results from the assay indicated that there was no difference in the enzyme kinetics in cells that were exposed to 25 μ M *E,E*-farnesol as compared to cells that were not exposed. The conclusion can be made that the change in abundance of the E3 subunit caused by exposure to 25 μ M *E,E*-farnesol does not have an impact on the overall activity of pyruvate dehydrogenase. According to the literature, dihydrolipoamide dehydrogenase does play an important role in alpha-ketoglutarate, 2-oxoglutarate dehydrogenase, and branched chain alpha-keto acid degradation. It is possible to exclude the role that DLDH plays in pyruvate dehydrogenase as a point where a decrease in abundance of DLDH in response to exposure to *E,E*-farnesol would have an affect. This finding is also supported in the literature because it has been demonstrated that exposure to farnesol does not affect the survivability or growth rate of *P.*

aeruginosa. If there were a decrease in pyruvate dehydrogenase activity this would severely impact the ability of cells to utilize glucose as a source of carbon. If this enzyme were affected there should be measurable shifts in growth rate as the cell had to adjust its metabolism to obtain carbon from other sources than glucose.

Future directions to determine the role of a decrease in abundance of DLDH are to explore the functionality of other enzymes that rely on DLDH as a subunit. A strong candidate is 2-oxoglutarate dehydrogenase that is important in the degradation of phenylalanine. 2-oxoglutarate dehydrogenase is responsible for converting L-tyrosine into p-hydroxyphenylpyruvate. This metabolic pathway is significant for the production of phenazine compounds. The aromatic portion of phenylalanine is utilized in the phenazine backbone. A possible explanation for the decrease in abundance in DLDH in the cells exposed to *E,E*-farnesol may be that two isoenzymes for DLDH are found in *Pseudomonas* species where one is responsible for activity in central metabolism and the second plays a role in phenazine production (Carothers, *et al.*, 1989). An enzyme assay, such as the one performed to determine activity of PD, would not reflect the global effects of the enzyme subunit as it functions in multiple distinct pathways within the cell in both central and secondary metabolism.

Dacheux *et al.* identified pyruvate dehydrogenase as an important player in the Type III secretion system (TTSS) in *P. aeruginosa*. *P. aeruginosa* relies on export systems to secrete virulence factors that aid in defense against the host immune system and for the infection process. The TTSS is activated by a depletion of calcium *in vitro*. The role of PD in the TTSS was first determined by creating mutants that were deficient in Type III secretion and identifying genes that were disrupted. Based on the results of this assay it was found that in 14 out of the 25

isolated TTSS-mutants the operon for pyruvate dehydrogenase (*aceAB* operon) was affected. It was determined from this result that the role of PD in the induction of the TTSS was to allow expression of the operon *exsA*, which is a part of the operon for the Type III secretion system. This relationship was validated with a plasmid that fused the *exsCBA* promoter to the *gfp* gene. If *exsAB* is expressed there will be detectable fluorescence. In PD mutants the *exsCBA* promoter was not activated in response to calcium depletion. Virulence of PD mutants was tested using rat models of pneumonia to compare the mutant's virulence with that of wild-type PA with intact pyruvate dehydrogenase complexes. Wild type strains resulted in 100% mortality while mutants in both PD and other operons of the TTSS had a 0% mortality rate. A future direction for this project in this area would be to determine if exposure to *E,E*-farnesol could affect the expression of the TTSS genes and the production of secretion products.

ATPase PilB

This protein demonstrated a decrease in abundance (-2.5 fold change) (Figure 16) in planktonic cells of *P. aeruginosa* PAO1 exposed to 25 μ M *E,E*-farnesol. The significance of this finding is based on ATPase's role in facilitating pili assembly by providing the energy required for movement after assembly. Research on *P. aeruginosa* motility in the literature has shown that the presence of *E,E*-farnesol inhibits swarming motility. If the cell is less capable of extending and moving pili twitching motility is not possible because the engine that is essential for movement has run out of gas (O'Toole, 1998; Kohler, 2000; Chiang, 2005).

The importance of a decrease in twitching motility is its role in biofilm formation. O'Toole and Kolter found in a study in 1998 that flagella and pili are very important for the

ability of *P.aeruginosa* to form a biofilm. This finding is interesting in that if exposure to farnesol is able to decrease the ability of *P. aeruginosa* to form functional pili and result in a decreased ability to form a robust biofilm. In light of the data present in the literature and the findings in this study farnesol affects the ability of *P. aeruginosa* to extend and retract pili, thus decreasing motility.

OprF

The proteomics data from the exposure of *P. aeruginosa* to 25 μ M of *E,E*-farnesol did result in the decreased abundance of OprF precursors within the cytosol and also the peptidoglycan-associated proteins that form the channel within the membrane. This finding suggests that the entire complex that forms the OprF porin was present at a lower abundance. The major physiological role of OprF in *P. aeruginosa* is as a major non-specific surface porin. This porin is homologous to the major porin OmpF in *Escherichia coli*. Interestingly, this protein is larger than that of OmpF however diffusion rates through this porin in *P. aeruginosa* are much slower. This is due to the ability of this protein to exist in two different conformations that are temperature sensitive (Sugawara, 2006).

There could be several implications for how and why *E,E*-farnesol would influence the abundance of OprF. One major theory is that by decreasing the abundance of OprF it is possible to make the cell membrane and cell-wall less stable. The physiological experiment performed in this study to test the effect of growth under osmotic stress (Table 9) was performed to determine if a decreased abundance of OprF could impact the ability of the cell to resist osmotic stress and

undergo lysis. The results indicated that there was no significant difference in the ability of *P. aeruginosa* cells grown in the presence or absence of 250 μ M *E,E*-farnesol to have growth affected by osmotic stress. In the literature farnesol has not been shown to impact the growth or survivability of *P. aeruginosa*, so even under osmotic stress the cells are still viable. In 2002, Hassett, *et al* reported that OprF mutants that completely lacked OprF did show susceptibility to osmotic stress when grown in low osmolarity medium. This finding suggests that although *E,E*-farnesol was shown to decrease the abundance of OprF did not affect the ability to withstand osmotic stress.

The ability of *E,E*-farnesol to influence the cell membrane in gram-positive bacteria has been shown in studies performed with *Staphylococcus aureus*. Figure 25A demonstrates the ability of *E,E*-farnesol to inhibit the formation of biofilm in *S. aureus* that is proportionally related to the dose of *E,E* -farnesol. Figure 25B demonstrates the ability of *E,E* -farnesol to disrupt the cell membrane. Increased uptake of ethidium bromide under exposure to greater concentrations of *E,E* -farnesol suggests a destabilization of the cell membrane. Figure 26 demonstrates the ability of *E,E* -farnesol to non-specifically enhance a broad range of antibiotic classes partially thought to be due to the destabilization of the membrane and a disruption of the transport mechanisms used to export antibiotics once they have entered the cell or the ability of large antibiotic molecules to better permeate inside the cell.

Figure 26: Biofilm formation of *S. aureus* and uptake of ethidium bromide when exposed to *E,E* -farnesol.

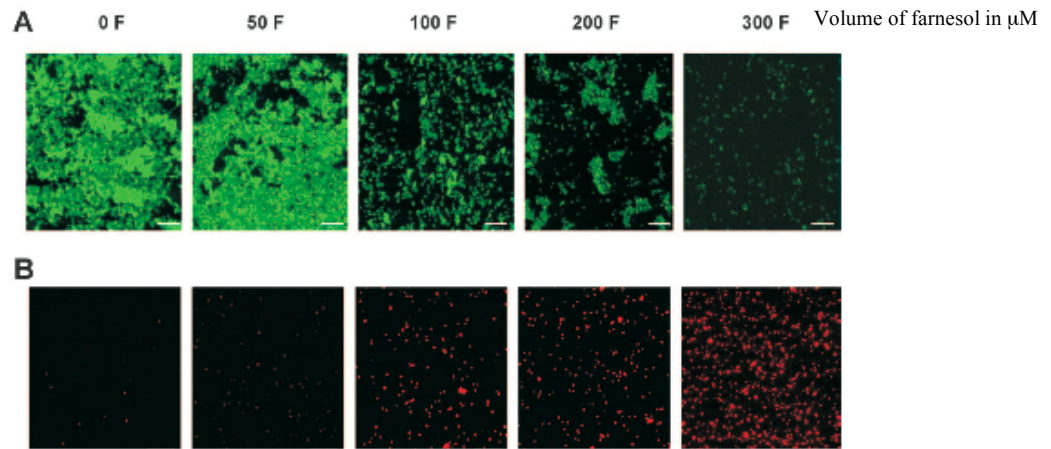


Figure 26: Uptake of ethidium bromide and biofilm formation of *S. aureus* when grown in the presence of varying concentrations of *E,E*-farnesol. (Source: Jabra-Rizk, *et al.*, 2006)

Figure 27: Antibiotic susceptibility patterns when *S. aureus* grown in presence of *E,E*-farnesol

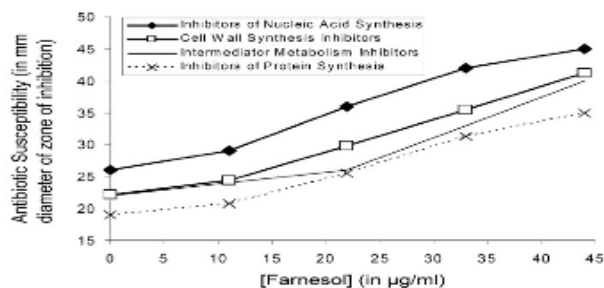


Figure 27: Patterns of antibiotic susceptibility when *S. aureus* is grown in the presence of varying concentrations of *tt*-farnesol. (Source: Jabra-Rizk, *et al.*, 2006)

To test if exposure to *E,E*-farnesol could affect antibiotic susceptibility in *P. aeruginosa* a minimum inhibitory concentration assay was performed with Tobramycin (Table 12). The parameters of the assay tested whether the presence of farnesol in the growth medium and antibiotic could decrease the dose necessary to prevent growth of *Pseudomonas*. The results presented in this study did show that exposure to 250 µM *E,E*-farnesol did decrease the dose necessary for Tobramycin to inhibit growth, as determined by optical density. This assay also showed interesting in colonial morphology in doses of Tobramycin just before complete inhibition. In Figure 24, the cells of *P. aeruginosa* that were exposed to farnesol demonstrated string like structures and were not condensed. One potential reason for this finding is that communication was disrupted and the cells could not orient themselves in a more defensive position. With the cells in a more diffuse orientation it would be possible for more Tobramycin to reach more cells and exhibit an effect. The role that farnesol played in increasing antibiotic

susceptibility could be due to two reasons. The first would be an alteration in permeability of the membrane allowing more of the antibiotic to enter the cell and exert an effect. The second possibility would be that the ability of the cells to communicate were altered so that it was not possible to form a condensed morphology and the number of cells that were exposed to the antibiotic was greater. In Figure 25, there was not farnesol present and the cells formed a tight cluster that would allow fewer cells to be in contact with the tobramycin.

OprF has also been shown in the literature to affect the ability of *P. aeruginosa* to perform surveillance of the activation status of the host immune system. This protein is able to bind to interferon-gamma located outside the cell that is secreted by activated T-cells. Wu *et al.* reported this finding in 2005 where it was shown that OprF in *P. aeruginosa* has a role in binding Interferon gamma (IFN- γ) that is secreted by activated T-cells in the human host. Once OprF binds IFN- γ , a currently undetermined signaling cascade occurs that leads to the induction of genes resulting in production of proteins and secondary metabolites critical to the infection process, for example pyocyanin (Figure 28). A hypothesis to explore based on the results of this study is to test the ability of *E,E*-farnesol to prevent the response of *P. aeruginosa* to IFN- γ by measuring quorum- sensing related gene expression and pyocyanin production.

The significance of a reduction in OprF in *P. aeruginosa* exposed to a fungal quorum sensing compound is the potential to reduce the ability of *P. aeruginosa* to prepare itself for attack by the human host. It is possible to hypothesize that exposure to farnesol has the ability to diminish the virulence of *P. aeruginosa* by decreasing its ability to sense activation of the host immune system and response by secreting pyocyanin.

Figure 28: Schematic for proposed role of OprF in sensing activation of t-cells by the detection of IFN-gamma.

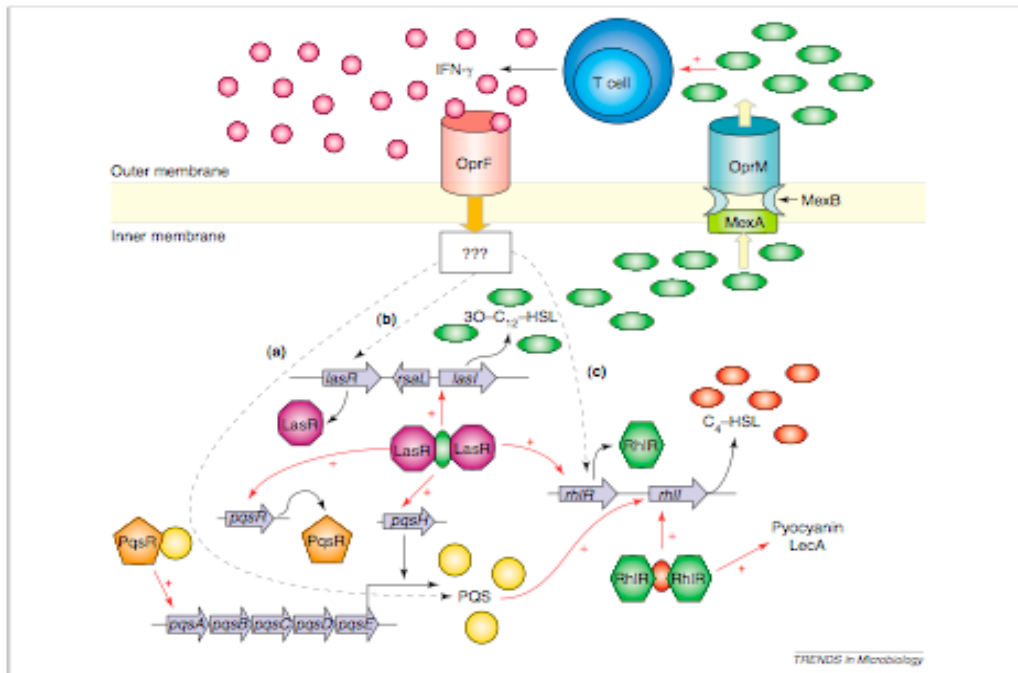


Figure 28: Source (Wagner, *et al.*, 2006) Quorum sensing system and possible role of OprF in the detection of IFN-gamma released from activated T-cells.

The role of OprF within the anaerobic biofilm, which is of great importance to the CF lung infection model, is believed to play a role as a redundant transporter of nitrate and nitrite that does not fall into the classical nitrate transporter category. A second possible function of OprF within the CF lung infection model that was determined using OprF mutants was its role in stabilizing the cell wall. It was found that OprF mutants did not form a biofilm within CF

mucous that was as robust as the wild-type. One theory was that the lack of OprF allowed for the peptidoglycan to become unstable. This was further illustrated by the reduced growth in low salt environments where the cell wall would have been placed under osmotic pressures that lead to cell lysis (Hassett, *et al.*, 2002). Data from the osmotic stress assay (Table 9) did not demonstrate any delay in growth or decrease in growth rate in *P. aeruginosa* cells exposed to *E,E*-farnesol as compared to the control which did not have exposure to *E,E*-farnesol.

It was also shown that the OprF mutant exhibited poor NIR activity, which is thought to recruit normal OprF in the anaerobic biofilm. Although not fully characterized, it is believed that OprF may play a role in denitrification and the maintenance of the global nitrogen cycle (Hassett, *et al.*, 2002). The importance of OprF to the ability of PA to form biofilms under anaerobic conditions was determined using proteomic analysis that revealed in an anaerobic biofilm model the abundance of OprF increased approximately 40 fold as compared to the aerobic biofilm. It was also found that in chronically infected CF patients there was an increase in the titer of OprF antibodies. OprF is a surface-exposed protein that holds great promise as a viable drug target to affect difficult to treat anaerobically growing *P. aeruginosa* cells.

The protein OprF has been implicated in several physiological functions in *P. aeruginosa* that relates to virulence and attachment. This protein holds much promise for future areas of research to identify new methods to combat infection with this organism. One major important factor of OprF is its candidate as a vaccine target for *P. aeruginosa* infections (Price, *et al.*, 2001). This protein is continually presented on the outer surface of the cell and does not exhibit a great deal of variation between strains. OprF has also been implicated in its role for allowing *P. aeruginosa* to adhere to lung epithelial surfaces (Azghani, *et al.*, 2002). This is a significant

finding because the ability of farnesol to influence attachment to inanimate surfaces has been tested in multiple studies and the result has consistently been that no effect was seen. A model system could be used to mimic an epithelium and the ability of farnesol to affect attachment to this surface could be tested. The results presented in this study provide evidence that farnesol could decrease the ability of *P. aeruginosa* to attach to an epithelial surface since it decreases the abundance of OprF.

Summary and Future Directions

The proteins that were identified in this study from *P. aeruginosa* showed a change in abundance in response to exposure to *E,E*-farnesol. ATPase PilB and Flagellin B have a clear role in motility. The importance of motility mediated by the flagella and the pili have documented roles in initiating biofilm formation. The results in this study suggest that there is a decrease in both of these proteins and could potentially affect the ability of *P. aeruginosa* to form a biofilm when in contact with a variety of surfaces. One future direction will be to determine the ability of *P. aeruginosa* exposed to *E,E*-farnesol to attach to different surfaces including medical devices and epithelial surfaces as mediated by the pili and flagella.

The direct role of porins in moderating quorum sensing and the ability of bacteria to detect activation of the host immune system in *P. aeruginosa* is a developing area of research that is gaining greater understanding. Documented interactions between OprF and interferon-gamma produced by the human adaptive immune system illustrate the complexity of the interaction between bacteria and the human host. Future directions to better determine the role

that exposure to *E,E*-farnesol could have include performing assays where *P. aeruginosa* is exposed to both *E,E*-farnesol and interferon-gamma to measure the level of activation of quorum sensing regulated genes and measure the degree of production of virulence factors that are regulated by those genes.

Proteins identified in this study that were shown to change in abundance upon exposure to *E,E*-farnesol have not been directly linked to biofilm formation and quorum sensing as documented in the scientific literature. However, additional experiments are needed to confirm their peripheral role in these processes. Potential experiments include constructing mutants that lack enzymes such as GMP synthase and dihydrolipoamide dehydrogenase to determine if production of quorum sensing regulated virulence factors are affected. These experiments could potentially provide a targeted approach to find the role that these enzymes play, since they are members of larger enzymatic complexes that play multiple roles in the cell for central and secondary metabolism.

References

1. **Adair, C., S. Gorman, B. Feron, L. Byers, D. Jones, C. Goldsmith, J. Moore, J. Kerr, M. Curran, G. Hogg, C. Webb, G. McCarthy, and K. Milligan.** 1999. Implications of endotracheal tube biofilm for ventilator-associated pneumonia. *Intensive care medicine* **25**:1072-6.
2. **Ader, F., K. Faure, B. Guery, and S. Nseir.** 2007. *Pseudomonas aeruginosa* and *Candida albicans* interaction in the respiratory tract: from pathophysiology to a therapeutic perspective. *Pathol Biol.*
3. **Alem, M., M. Oteef, T. Flowers, and L. Douglas.** 2006. Production of tyrosol by *Candida albicans* biofilms and its role in quorum sensing and biofilm development. *Eukaryotic Cell* **5**:1770-9.
4. **Azghani, A., S. Idell, M. Bains, and R. Hancock.** 2002. *Pseudomonas aeruginosa* outer membrane protein F is an adhesin in bacterial binding to lung epithelial cells in culture. *Microb Pathog* **33**:109-14.
5. **Backovic, A., H. Huang, B. Del Frari, H. Piza, L. Huber, and G. Wick.** 2007. Identification and dynamics of proteins adhering to the surface of medical silicones in vivo and in vitro. *J Proteome Res* **6**:376-81.
6. **Balajee, S., M. Lindsley, N. Iqbal, J. Ito, P. Pappas, and M. Brandt.** 2007.

- Nonsporulating clinical isolate identified as *Petromyces alliaceus* (anamorph *Aspergillus alliaceus*) by morphological and sequence-based methods. J Clin Microbiol **45**:2701-3.
7. **Bauman, S., and M. Kuehn.** 2006. Purification of outer membrane vesicles from *Pseudomonas aeruginosa* and their activation of an IL-8 response. Microbes Infect **8**:2400-8.
 8. **Beale, E., G. Li, M. Tan, and K. Rumbaugh.** 2006. *Caenorhabditis elegans* senses bacterial autoinducers. Appl Environ Microbiol **72**:5135-7.
 9. **Bjarnsholt, T., and M. Givskov.** 2006. The role of quorum sensing in the pathogenicity of the cunning aggressor *Pseudomonas aeruginosa*. Analytical and bioanalytical chemistry **387**:409-14.
 10. **Blankenship, J., and A. Mitchell.** 2006. How to build a biofilm: a fungal perspective. Curr Opin Microbiol **9**:588-94.
 11. **Bodilis, J., and S. Barray.** 2006. Molecular evolution of the major outer-membrane protein gene (*oprF*) of *Pseudomonas*. Microbiology (Reading, Engl) **152**:1075-88.
 12. **Bodilis, J., M. Hedde, N. Orange, and S. Barray.** 2006. *OprF* polymorphism as a marker of ecological niche in *Pseudomonas*. Environ Microbiol **8**:1544-51.
 13. **Braun, P.** 2005. The effect of farnesol on amino acid incorporation by a wild-type and cell-wall variant strain of *Candida albicans*. Can J Microbiol **51**:715-8.
 14. **Britigan, B., T. Roeder, G. Rasmussen, D. Shasby, M. McCormick, and C. Cox.**

1992. Interaction of the *Pseudomonas aeruginosa* secretory products pyocyanin and pyochelin generates hydroxyl radical and causes synergistic damage to endothelial cells. Implications for *Pseudomonas*-associated tissue injury. *J Clin Invest* **90**:2187-96.
15. **Burns, J., J. Van Dalfsen, R. Shawar, K. Otto, R. Garber, J. Quan, A. Montgomery, G. Albers, B. Ramsey, and A. Smith.** 1999. Effect of chronic intermittent administration of inhaled tobramycin on respiratory microbial flora in patients with cystic fibrosis. *J Infect Dis* **179**:1190-6.
16. **Calfee, M., J. Coleman, and E. Pesci.** 2001. Interference with *Pseudomonas* quinolone signal synthesis inhibits virulence factor expression by *Pseudomonas aeruginosa*. *Proc Natl Acad Sci USA* **98**:11633-7.
17. **Cao, Y., Y. Cao, Z. Xu, K. Ying, Y. Li, Y. Xie, Z. Zhu, W. Chen, and Y. Jiang.** 2005. cDNA microarray analysis of differential gene expression in *Candida albicans* biofilm exposed to farnesol. *Antimicrob Agents Chemother* **49**:584-9.
18. **Cha, C., and R. Dematteo.** 2005. Molecular mechanisms in hepatocellular carcinoma development. *Best practice & research Clinical gastroenterology* **19**:25-37.
19. **Cheer, S., J. Waugh, and S. Noble.** 2003. Inhaled tobramycin (TOBI): a review of its use in the management of *Pseudomonas aeruginosa* infections in patients with cystic fibrosis. *Drugs* **63**:2501-20.
20. **Chen, H., M. Fujita, Q. Feng, J. Clardy, and G. Fink.** 2004. Tyrosol is a quorum-sensing molecule in *Candida albicans*. *Proc Natl Acad Sci USA* **101**:5048-52.
21. **Chiang, P., M. Habash, and L. Burrows.** 2005. Disparate subcellular localization

- patterns of *Pseudomonas aeruginosa* Type IV pilus ATPases involved in twitching motility. J Bacteriol **187**:829-39.
22. **Christensen, L., C. Moser, P. Jensen, T. Rasmussen, L. Christophersen, S. Kjelleberg, N. Kumar, N. Høiby, M. Givskov, and T. Bjarnsholt.** 2007. Impact of *Pseudomonas aeruginosa* quorum sensing on biofilm persistence in an in vivo intraperitoneal foreign-body infection model. Microbiology (Reading, Engl) **153**:2312-20.
23. **Coignard, C., S. Hurst, L. Benjamin, M. Brandt, D. Warnock, and C. Morrison.** 2004. Resolution of discrepant results for *Candida* species identification by using DNA probes. J Clin Microbiol **42**:858-61.
24. **Cugini, C., M. Calfee, J. Farrow, D. Morales, E. Pesci, and D. Hogan.** 2007. Farnesol, a common sesquiterpene, inhibits PQS production in *Pseudomonas aeruginosa*. Mol Microbiol.
25. **Dacheux, D., O. Epaulard, A. de Groot, B. Guery, R. Leberre, I. Attree, B. Polack, and B. Toussaint.** 2002. Activation of the *Pseudomonas aeruginosa* type III secretion system requires an intact pyruvate dehydrogenase aceAB operon. Infect Immun **70**:3973-7.
26. **Danson, M., K. Conroy, A. McQuattie, and K. Stevenson.** 1987. Dihydrolipoamide dehydrogenase from *Trypanosoma brucei*. Characterization and cellular location. Biochem J **243**:661-5.
27. **Dietrich, L., A. Price-Whelan, A. Petersen, M. Whiteley, and D. Newman.** 2006. The

- phenazine pyocyanin is a terminal signalling factor in the quorum sensing network of *Pseudomonas aeruginosa*. *Mol Microbiol* **61**:1308-21
28. **Diggle, S., K. Winzer, S. Chhabra, K. Worrall, M. Cámara, and P. Williams.** 2003. The *Pseudomonas aeruginosa* quinolone signal molecule overcomes the cell density-dependency of the quorum sensing hierarchy, regulates rhl-dependent genes at the onset of stationary phase and can be produced in the absence of LasR. *Mol Microbiol* **50**:29-43.
 29. **Dörr, J., T. Hurek, and B. Reinhold-Hurek.** 1998. Type IV pili are involved in plant-microbe and fungus-microbe interactions. *Mol Microbiol* **30**:7-17.
 30. **Dosselaere, F., and J. Vanderleyden.** 2001. A metabolic node in action: chorismate-utilizing enzymes in microorganisms. *Crit Rev Microbiol* **27**:75-131.
 31. **Dumitru, R., J. Hornby, and K. Nickerson.** 2004. Defined anaerobic growth medium for studying *Candida albicans* basic biology and resistance to eight antifungal drugs. *Antimicrob Agents Chemother* **48**:2350-4.
 32. **Dumitru, R., D. Navarathna, C. Semighini, C. Elowsky, R. Dumitru, D. Dignard, M. Whiteway, A. Atkin, and K. Nickerson.** 2007. In vivo and in vitro anaerobic mating in *Candida albicans*. *Eukaryotic Cell* **6**:465-72.
 33. **El-Azizi, M., S. Starks, and N. Khardori.** 2004. Interactions of *Candida albicans* with other *Candida* spp. and bacteria in the biofilms. *J Appl Microbiol* **96**:1067-73.
 34. **Enjalbert, B., and M. Whiteway.** 2005. Release from quorum-sensing molecules triggers hyphal formation during *Candida albicans* resumption of growth. *Eukaryotic Cell* **4**:1203-10.
 35. **Farrow, J., and E. Pesci.** 2007. Two distinct pathways supply anthranilate as a precursor

- of the *Pseudomonas* quinolone signal. J Bacteriol **189**:3425-33.
36. **Finnen, R., N. Martin, R. Siehnel, W. Woodruff, M. Rosok, and R. Hancock.** 1992. Analysis of the *Pseudomonas aeruginosa* major outer membrane protein OprF by use of truncated OprF derivatives and monoclonal antibodies. J Bacteriol **174**:4977-85.
 37. **Gallagher, L., and C. Manoil.** 2001. *Pseudomonas aeruginosa* PAO1 kills *Caenorhabditis elegans* by cyanide poisoning. J Bacteriol **183**:6207-14.
 38. **Gerberding, J.** 1998. Nosocomial transmission of opportunistic infections. Infection control and hospital epidemiology : the official journal of the Society of Hospital Epidemiologists of America **19**:574-7.
 39. **Gerberding, J.** 2002. Hospital-onset infections: a patient safety issue. Ann Intern Med **137**:665-70.
 40. **Gilligan, P.** 1991. Microbiology of airway disease in patients with cystic fibrosis. Clin Microbiol Rev **4**:35-51.
 41. **Goto, Y., H. Zalkin, P. Keim, and R. Heinrikson.** 1976. Properties of anthranilate synthetase component II from *Pseudomonas putida*. J Biol Chem **251**:941-9.
 42. **Govan, J., and J. Nelson.** 1993. Microbiology of cystic fibrosis lung infections: themes and issues. Journal of the Royal Society of Medicine **86 Suppl 20**:11-8.

 43. **Hajjeh, R., A. Sofair, L. Harrison, G. Lyon, B. Arthington-Skaggs, S. Mirza, M.**

- Phelan, J. Morgan, W. Lee-Yang, M. Ciblak, L. Benjamin, L. Sanza, S. Huie, S. Yeo, M. Brandt, and D. Warnock.** 2004. Incidence of bloodstream infections due to *Candida* species and in vitro susceptibilities of isolates collected from 1998 to 2000 in a population-based active surveillance program. *J Clin Microbiol* **42**:1519-27.
44. **Hassett, D., J. Cuppoletti, B. Trapnell, S. Lymar, J. Rowe, S. Yoon, G. Hilliard, K. Parvatiyar, M. Kamani, D. Wozniak, S. Hwang, T. McDermott, and U. Ochsner.** 2002. Anaerobic metabolism and quorum sensing by *Pseudomonas aeruginosa* biofilms in chronically infected cystic fibrosis airways: rethinking antibiotic treatment strategies and drug targets. *Adv Drug Deliv Rev* **54**:1425-43.
45. **Hemery, G., S. Chevalier, M. Bellon-Fontaine, D. Haras, and N. Orange.** 2006. Growth temperature and OprF porin affect cell surface physicochemical properties and adhesive capacities of *Pseudomonas fluorescens* MF37. *J Ind Microbiol Biotechnol* **34**:49-54.
46. **Henriques, M., M. Martins, J. Azeredo, and R. Oliveira.** 2007. Effect of farnesol on *Candida dubliniensis* morphogenesis. *Lett Appl Microbiol* **44**:199-205.
47. **Hermann, C., J. Hermann, U. Munzel, and R. Rüchel.** 2000. Bacterial flora accompanying *Candida* yeasts in clinical specimens. *Mycoses* **42**:619-27.
48. **Hogan, D.** 2006. Talking to themselves: autoregulation and quorum sensing in fungi. *Eukaryotic Cell* **5**:613-9.
49. **Hogan, D., and R. Kolter.** 2002. *Pseudomonas-Candida* interactions: an ecological role for virulence factors. *Science* **296**:2229-32.
50. **Hogan, D., A. Vik, and R. Kolter.** 2004. A *Pseudomonas aeruginosa* quorum-sensing

- molecule influences *Candida albicans* morphology. Mol Microbiol **54**:1212-23.
51. **Hornby, J., E. Jensen, A. Lisec, J. Tasto, B. Jahnke, R. Shoemaker, P. Dussault, and K. Nickerson.** 2001. Quorum sensing in the dimorphic fungus *Candida albicans* is mediated by farnesol. Appl Environ Microbiol **67**:2982-92.
 52. **Hornby, J., and K. Nickerson.** 2004. Enhanced production of farnesol by *Candida albicans* treated with four azoles. Antimicrob Agents Chemother **48**:2305-7.
 53. **Jabra-Rizk, M., M. Shirliff, C. James, and T. Meiller.** 2006. Effect of farnesol on *Candida dubliniensis* biofilm formation and fluconazole resistance. FEMS Yeast Res **6**:1063-73.
 54. **Jensen, E., J. Hornby, N. Pagliaccetti, C. Wolter, K. Nickerson, and A. Atkin.** 2006. Farnesol restores wild-type colony morphology to 96% of *Candida albicans* colony morphology variants recovered following treatment with mutagens. Genome **49**:346-53.
 55. **Kaleli, I., N. Cevahir, M. Demir, U. Yildirim, and R. Sahin.** 2007. AntiCandidal activity of *Pseudomonas aeruginosa* strains isolated from clinical specimens. Mycoses **50**:74-8.
 56. **Kanagasabai, R., W. Zhou, J. Liu, T. Nguyen, P. Veeramachaneni, and W. Nes.** 2005. Disruption of ergosterol biosynthesis, growth, and the morphological transition in *Candida albicans* by sterol methyltransferase inhibitors containing sulfur at C-25 in the sterol side chain. Lipids **39**:737-46.
 57. **Kao, A., M. Brandt, W. Pruitt, L. Conn, B. Perkins, D. Stephens, W. Baughman, A.**

- Reingold, G. Rothrock, M. Pfaller, R. Pinner, and R. Hajjeh.** 1999. The epidemiology of candidemia in two United States cities: results of a population-based active surveillance. *Clin Infect Dis* **29**:1164-70.
58. **Kerr, J.** 1994. Inhibition of fungal growth by *Pseudomonas aeruginosa* and *Pseudomonas cepacia* isolated from patients with cystic fibrosis. *J Infect* **28**:305-10.
59. **Kerr, J., G. Taylor, A. Rutman, N. Høiby, P. Cole, and R. Wilson.** 1999. *Pseudomonas aeruginosa* pyocyanin and 1-hydroxyphenazine inhibit fungal growth. *J Clin Pathol* **52**:385-7.
60. **Köhler, T., L. Curty, F. Barja, C. van Delden, and J. Pechère.** 2000. Swarming of *Pseudomonas aeruginosa* is dependent on cell-to-cell signaling and requires flagella and pili. *J Bacteriol* **182**:5990-6.
61. **Kolter, R., and E. Greenberg.** 2006. Microbial sciences: the superficial life of microbes. *Nature* **441**:300-2.
62. **Kretzschmar, U., M. Schobert, and H. Görisch.** 2001. The *Pseudomonas aeruginosa* *acsA* gene, encoding an acetyl-CoA synthetase, is essential for growth on ethanol. *Microbiology (Reading, Engl)* **147**:2671-7.
63. **Kruppa, M., B. Krom, N. Chauhan, A. Bambach, R. Cihlar, and R. Calderone.** 2004. The two-component signal transduction protein Chk1p regulates quorum sensing in *Candida albicans*. *Eukaryotic Cell* **3**:1062-5.
64. **Kurnasov, O., L. Jablonski, B. Polanuyer, P. Dorrestein, T. Begley, and A.**

- Osterman.** 2003. Aerobic tryptophan degradation pathway in bacteria: novel kynurenine formamidase. *FEMS Microbiol Lett* **227**:219-27.
65. **Larsen, M., S. Cordwell, and P. Roepstorff.** 2002. Graphite powder as an alternative or supplement to reversed-phase material for desalting and concentration of peptide mixtures prior to matrix-assisted laser desorption/ionization-mass spectrometry. *Proteomics* **2**:1277-87.
66. **Lau, G., D. Hassett, H. Ran, and F. Kong.** 2004. The role of pyocyanin in *Pseudomonas aeruginosa* infection. *Trends in molecular medicine* **10**:599-606.
67. **Li, M., P. Ho, S. Yao, and K. Shimizu.** 2005. Effect of *lpdA* gene knockout on the metabolism in *Escherichia coli* based on enzyme activities, intracellular metabolite concentrations and metabolic flux analysis by ¹³C-labeling experiments. *J Biotechnol* **122**:254-66.
68. **Lisacek, F., S. Cohen-Boulakia, and R. Appel.** 2006. Proteome informatics II: bioinformatics for comparative proteomics. *Proteomics* **6**:5445-66.
69. **Lyczak, J., C. Cannon, and G. Pier.** 2000. Establishment of *Pseudomonas aeruginosa* infection: lessons from a versatile opportunist. *Microbes Infect* **2**:1051-60.
70. **MacEachran, D., S. Ye, J. Bomberger, D. Hogan, A. Swiatecka-Urban, B. Stanton, and G. O'Toole.** 2007. The *Pseudomonas aeruginosa* secreted protein PA2934 decreases apical membrane expression of the cystic fibrosis transmembrane conductance regulator. *Infect Immun* **75**:3902-12.
71. **Martin, S., L. Douglas, and J. Konopka.** 2005. Cell cycle dynamics and quorum

- sensing in *Candida albicans* chlamydozoospores are distinct from budding and hyphal growth. Eukaryotic Cell **4**:1191-202.
72. **Mavrodi, D., R. Bonsall, S. Delaney, M. Soule, G. Phillips, and L. Thomashow.** 2001. Functional analysis of genes for biosynthesis of pyocyanin and phenazine-1-carboxamide from *Pseudomonas aeruginosa* PAO1. J Bacteriol **183**:6454-65.
73. **Mosel, D., R. Dumitru, J. Hornby, A. Atkin, and K. Nickerson.** 2005. Farnesol concentrations required to block germ tube formation in *Candida albicans* in the presence and absence of serum. Appl Environ Microbiol **71**:4938-40.
74. **Mullick, A., Z. Leon, G. Min-Oo, J. Berghout, R. Lo, E. Daniels, and P. Gros.** 2006. Cardiac failure in C5-deficient A/J mice after *Candida albicans* infection. Infect Immun **74**:4439-51.
75. **Navarathna, D., J. Hornby, N. Hoerrmann, A. Parkhurst, G. Duhamel, and K. Nickerson.** 2005. Enhanced pathogenicity of *Candida albicans* pre-treated with subinhibitory concentrations of fluconazole in a mouse model of disseminated candidiasis. J Antimicrob Chemother **56**:1156-9.
76. **Navarathna, D., J. Hornby, N. Krishnan, A. Parkhurst, G. Duhamel, and K. Nickerson.** 2007. Effect of farnesol on a mouse model of systemic candidiasis, determined by use of a DPP3 knockout mutant of *Candida albicans*. Infect Immun **75**:1609-18.
77. **Navarathna, D., K. Nickerson, G. Duhamel, T. Jerrels, and T. Petro.** 2007.

- Exogenous Farnesol Interferes with the Normal Progression of Cytokine Expression during Candidiasis in a Mouse Model. *Infect Immun* **75**:4006-11.
78. **Nickerson, K., A. Atkin, and J. Hornby.** 2006. Quorum sensing in dimorphic fungi: farnesol and beyond. *Appl Environ Microbiol* **72**:3805-13.
79. **Niyogi, K., and G. Fink.** 1992. Two anthranilate synthase genes in *Arabidopsis*: defense-related regulation of the tryptophan pathway. *Plant Cell* **4**:721-33.
80. **Nouwens, A., S. Beatson, C. Whitchurch, B. Walsh, H. Schweizer, J. Mattick, and S. Cordwell.** 2003. Proteome analysis of extracellular proteins regulated by the las and rhl quorum sensing systems in *Pseudomonas aeruginosa* PAO1. *Microbiology (Reading, Engl)* **149**:1311-22.
81. **Nunn, D., S. Bergman, and S. Lory.** 1990. Products of three accessory genes, pilB, pilC, and pilD, are required for biogenesis of *Pseudomonas aeruginosa* pili. *J Bacteriol* **172**:2911-9.
82. **O'Toole, G., and R. Kolter.** 1998. Initiation of biofilm formation in *Pseudomonas fluorescens* WCS365 proceeds via multiple, convergent signalling pathways: a genetic analysis. *Mol Microbiol* **28**:449-61.
83. **O'Toole, G., and R. Kolter.** 1998. Flagellar and twitching motility are necessary for *Pseudomonas aeruginosa* biofilm development. *Mol Microbiol* **30**:295-304.
84. **Otto, M.** 2004. Quorum-sensing control in *Staphylococci* -- a target for antimicrobial drug therapy? *FEMS Microbiol Lett* **241**:135-41.
85. **Overhage, J., S. Lewenza, A. Marr, and R. Hancock.** 2006. Identification of genes

- involved in swarming motility using a *Pseudomonas aeruginosa* PAO1 mini-Tn5-lux mutant library. J Bacteriol **189**:2164-9.
86. **Palagi, P., P. Hernandez, D. Walther, and R. Appel.** 2006. Proteome informatics I: bioinformatics tools for processing experimental data. Proteomics **6**:5435-44.
87. **Payne, R., E. Bulloch, A. Abell, and C. Abell.** 2005. Design and synthesis of aromatic inhibitors of anthranilate synthase. Org Biomol Chem **3**:3629-35.
88. **Perham, R., L. Packman, and S. Radford.** 1987. 2-Oxo acid dehydrogenase multi-enzyme complexes: in the beginning and halfway there. Biochem Soc Symp **54**:67-81.
89. **Perumal, P., S. Mekala, and W. Chaffin.** 2007. Antifungal drug resistance in *Candida albicans* biofilms: a role for cell density. Antimicrob Agents Chemother.
90. **Pierce, G.** 2005. *Pseudomonas aeruginosa*, *Candida albicans*, and device-related nosocomial infections: implications, trends, and potential approaches for control. J Ind Microbiol Biotechnol **32**:309-18.
91. **Plebani, M.** 2005. Proteomics: the next revolution in laboratory medicine? Clin Chim Acta **357**:113-22.
92. **Price, B., D. Galloway, N. Baker, L. Gilleland, J. Staczek, and H. Gilleland.** 2001. Protection against *Pseudomonas aeruginosa* chronic lung infection in mice by genetic immunization against outer membrane protein F (OprF) of *P. aeruginosa*. Infect Immun **69**:3510-5.
93. **Price-Whelan, A., L. Dietrich, and D. Newman.** 2006. Rethinking 'secondary' metabolism: physiological roles for phenazine antibiotics. Nat Chem Biol **2**:71-8.
94. **Prithiviraj, B., H. Bais, T. Weir, B. Suresh, E. Najarro, B. Dayakar, H. Schweizer,**

- and J. Vivanco.** 2005. Down regulation of virulence factors of *Pseudomonas aeruginosa* by salicylic acid attenuates its virulence on *Arabidopsis thaliana* and *Caenorhabditis elegans*. *Infect Immun* **73**:5319-28.
95. **Probst, C., H. Njapau, and P. Cotty.** 2007. Outbreak of an acute aflatoxicosis in Kenya in 2004: identification of the causal agent. *Appl Environ Microbiol* **73**:2762-4.
96. **Rae, J., J. Cutfield, and I. Lamont.** 1997. Sequences and expression of pyruvate dehydrogenase genes from *Pseudomonas aeruginosa*. *J Bacteriol* **179**:3561-71.
97. **Ramage, G., S. Saville, B. Wickes, and J. López-Ribot.** 2002. Inhibition of *Candida albicans* biofilm formation by farnesol, a quorum-sensing molecule. *Appl Environ Microbiol* **68**:5459-63.
98. **Rasmussen, T., and M. Givskov.** 2006. Quorum-sensing inhibitors as anti-pathogenic drugs. *Int J Med Microbiol* **296**:149-61.
99. **Rasmussen, T., and M. Givskov.** 2006. Quorum sensing inhibitors: a bargain of effects. *Microbiology (Reading, Engl)* **152**:895-904.
100. **Rawling, E., F. Brinkman, and R. Hancock.** 1998. Roles of the carboxy-terminal half of *Pseudomonas aeruginosa* major outer membrane protein OprF in cell shape, growth in low-osmolarity medium, and peptidoglycan association. *J Bacteriol* **180**:3556-62.
101. **Rossignol, T., M. Logue, K. Reynolds, M. Grenon, N. Lowndes, and G. Butler.** 2007. Analysis of the transcriptional response of *Candida parapsilosis* following exposure to farnesol. *Antimicrob Agents Chemother*.
102. **Rüegg, T., A. Calderón, E. Queiroz, P. Solís, A. Marston, F. Rivas, E. Ortega-**

- Barría, K. Hostettmann, and M. Gupta.** 2005. 3-Farnesyl-2-hydroxybenzoic acid is a new anti-*Helicobacter pylori* compound from *Piper multiplinervium*. *Journal of ethnopharmacology* **103**:461-7.
103. **Saidi, S., C. Luitaud, and M. Rouabhia.** 2006. In vitro synergistic effect of farnesol and human gingival cells against *Candida albicans*. *Yeast* **23**:673-87.
104. **Sato, T., T. Watanabe, T. Mikami, and T. Matsumoto.** 2004. Farnesol, a morphogenetic autoregulatory substance in the dimorphic fungus *Candida albicans*, inhibits hyphae growth through suppression of a mitogen-activated protein kinase cascade. *Biol Pharm Bull* **27**:751-2.
105. **Sauer, S., J. Okun, M. Schwab, L. Crnic, G. Hoffmann, S. Goodman, D. Koeller, and S. Kölker.** 2005. Bioenergetics in glutaryl-coenzyme A dehydrogenase deficiency: a role for glutaryl-coenzyme A. *J Biol Chem* **280**:21830-6.
106. **Schooling, S., and T. Beveridge.** 2006. Membrane vesicles: an overlooked component of the matrices of biofilms. *J Bacteriol* **188**:5945-57.
107. **Semighini, C., J. Hornby, R. Dumitru, K. Nickerson, and S. Harris.** 2006. Farnesol-induced apoptosis in *Aspergillus nidulans* reveals a possible mechanism for antagonistic interactions between fungi. *Mol Microbiol* **59**:753-64.
108. **Seow, T., R. Liang, C. Leow, and M. Chung.** 2001. Hepatocellular carcinoma: from bedside to proteomics. *Proteomics* **1**:1249-63.
109. **Shchepin, R., R. Dumitru, K. Nickerson, M. Lund, and P. Dussault.** 2005. Biologically active fluorescent farnesol analogs. *Chem Biol* **12**:639-41.
110. **Shea, J., and M. Del Poeta.** 2006. Lipid signaling in pathogenic fungi. *Curr Opin*

- Microbiol **9**:352-8.
111. **Smith, A., H. Roche, M. Trombe, D. Briles, and A. Håkansson.** 2002. Characterization of the dihydrolipoamide dehydrogenase from *Streptococcus pneumoniae* and its role in pneumococcal infection. *Mol Microbiol* **44**:431-48.
 112. **Smith, R., and B. Iglewski.** 2003. *P. aeruginosa* quorum-sensing systems and virulence. *Curr Opin Microbiol* **6**:56-60.
 113. **Sriramulu, D., H. Lünsdorf, J. Lam, and U. Römling.** 2005. Microcolony formation: a novel biofilm model of *Pseudomonas aeruginosa* for the cystic fibrosis lung. *J Med Microbiol* **54**:667-76.
 114. **Stone, J., M. Gabriel, and D. Ahearn.** 1999. Adherence of *Pseudomonas aeruginosa* to inanimate polymers including biomaterials. *J Ind Microbiol Biotechnol* **23**:713-7.
 115. **Sugawara, E., E. Nestorovich, S. Bezrukov, and H. Nikaido.** 2006. *Pseudomonas aeruginosa* porin OprF exists in two different conformations. *J Biol Chem* **281**:16220-9.
 116. **Tan, M., and F. Ausubel.** 2000. *Caenorhabditis elegans*: a model genetic host to study *Pseudomonas aeruginosa* pathogenesis. *Curr Opin Microbiol* **3**:29-34.
 117. **Tan, M., L. Rahme, J. Sternberg, R. Tompkins, and F. Ausubel.** 1999. *Pseudomonas aeruginosa* killing of *Caenorhabditis elegans* used to identify *P. aeruginosa* virulence factors. *Proc Natl Acad Sci USA* **96**:2408-13.
 118. **Totten, P., J. Lara, and S. Lory.** 1990. The rpoN gene product of *Pseudomonas aeruginosa* is required for expression of diverse genes, including the flagellin gene. *J Bacteriol* **172**:389-96.
 119. **Trautner, B., and R. Darouiche.** 2004. Role of biofilm in catheter-associated urinary

- tract infection. American journal of infection control **32**:177-83.
120. **Tripathi, R., and D. Gottlieb.** 1969. Mechanism of action of the antifungal antibiotic pyrrolnitrin. J Bacteriol **100**:310-8.
 121. **Turner, P., S. Moore, A. Hall, A. Prentice, and C. Wild.** 2003. Modification of immune function through exposure to dietary aflatoxin in Gambian children. Environ Health Perspect **111**:217-20.
 122. **Uppuluri, P., S. Mekala, and W. Chaffin.** 2007. Farnesol-mediated inhibition of *Candida albicans* yeast growth and rescue by a diacylglycerol analogue. Yeast **24**:681-693.
 123. **Van Alst, N., K. Picardo, B. Iglewski, and C. Haidaris.** 2007. Nitrate Sensing and Metabolism Modulate Motility, Biofilm Formation, and Virulence in *Pseudomonas aeruginosa*. Infect Immun **75**:3780-90.
 124. **Varghese, S., Y. Tang, and J. Imlay.** 2002. Contrasting sensitivities of *Escherichia coli* aconitases A and B to oxidation and iron depletion. J Bacteriol **185**:221-30.
 125. **Wagner, V., J. Frelinger, R. Barth, and B. Iglewski.** 2006. Quorum sensing: dynamic response of *Pseudomonas aeruginosa* to external signals. Trends Microbiol **14**:55-8.
 126. **Walter, T., and A. Aronson.** 1999. Specific binding of the E2 subunit of pyruvate dehydrogenase to the upstream region of *Bacillus thuringiensis* protoxin genes. J Biol Chem **274**:7901-6.
 127. **Wargo, M., and D. Hogan.** 2006. Fungal--bacterial interactions: a mixed bag of mingling microbes. Curr Opin Microbiol **9**:359-64.
 128. **Wargo, M., and D. Hogan.** 2007. Examination of *Pseudomonas aeruginosa* lasI

- regulation and 3-oxo-C12-homoserine lactone production using a heterologous *Escherichia coli* system. FEMS Microbiol Lett **273**:38-44.
129. **Wendland, J., D. Hellwig, A. Walther, S. Sickinger, Y. Shadkchan, R. Martin, J. Bauer, N. Osherov, A. Tretiakov, and H. Saluz.** 2006. Use of the Porcine Intestinal Epithelium (PIE)-Assay to analyze early stages of colonization by the human fungal pathogen *Candida albicans*. J Basic Microbiol **46**:513-23.
130. **Westwater, C., E. Balish, and D. Schofield.** 2005. *Candida albicans*-conditioned medium protects yeast cells from oxidative stress: a possible link between quorum sensing and oxidative stress resistance. Eukaryotic Cell **4**:1654-61.
131. **Wu, L., O. Estrada, O. Zaborina, M. Bains, L. Shen, J. Kohler, N. Patel, M. Musch, E. Chang, Y. Fu, M. Jacobs, M. Nishimura, R. Hancock, J. Turner, and J. Alverdy.** 2005. Recognition of host immune activation by *Pseudomonas aeruginosa*. Science **309**:774-7.
132. **Wu, L., C. Holbrook, O. Zaborina, E. Ploplys, F. Rocha, D. Pelham, E. Chang, M. Musch, and J. Alverdy.** 2003. *Pseudomonas aeruginosa* expresses a lethal virulence determinant, the PA-I lectin/adhesin, in the intestinal tract of a stressed host: the role of epithelia cell contact and molecules of the Quorum Sensing Signaling System. Ann Surg **238**:754-64.
133. **Yu, L., K. Lee, R. Hodges, W. Paranchych, and R. Irvin.** 1994. Adherence of

Pseudomonas aeruginosa and *Candida albicans* to glycosphingolipid (Asialo-GM1) receptors is achieved by a conserved receptor-binding domain present on their adhesins. Infect Immun **62**:5213-9.

Appendix

Protocol: Buffers and Reagents for 2D DIGE proteomics

Protocol: Cell Lysis and Crude Protein Extract

Protocol: First-dimension strip reswelling for cup or paper bridge loading

Protocol: First-dimension strip reswelling for in-gel rehydration

Protocol: Casting Analytical Gels

Protocol: Casting Preparative Gels

Protocol: Pyruvate Dehydrogenase Assay

Protocol: *C. elegans* Virulence Assay

Protocol : Buffers and Reagents

Stock solutions

0.75% acetic acid – 4L

____4L ddH₂O)

____30ml acetic acid

1% Contrad 70 – 20L

____ 200ml Contrad 70

____ 20L ddH₂O

1.0M magnesium acetate – 50ml

____ add 10.73g MgAcetate to 30ml ddH₂O

____ make up to 50ml and filter into autoclaved cent bottle

10% SDS – 250ml

____ 25g SDS to 200ml ddH₂O

____ make up to 250ml and filter into clean, rinsed bottle

1.0M Tris, not pH'd – 100ml

____ add 12.1g Tris to 80ml ddH₂O

____ make up to 100ml and filter into clean, rinsed bottle

____ store at 4°C

1.0M Tris, pH 8.0 – 500ml

____ add 60.6g Tris to 400ml ddH₂O

____ pH to 8.0 with concentrated HCl

____ make up to 500ml and filter into clean, rinsed bottle

____ store at 4°C

1.5M TrisCl, pH 8.8 – 2L

___ 1.5L ddH₂O into rinsed flask

___ 363g Tris

___ pH to 8.8 with concentrated HCl

___ make up to 2L and filter into clean, rinsed 2L bottle

___ store at 4°C

Sample preparation

10mM Lysine – 10ml

___ 10ml ddH₂O

___ 18mg lysine (MW 182.6)

___ filter into sterile tube and store at 4°C.

Lysis buffer #1 (30mM Tris, 7M urea, 2M thiourea, 4% CHAPS, Complete) – 25ml

___ make 50ml 8M urea, 2.3M thiourea

___ 24ml ddH₂O

___ 24g urea

___ 9g thiourea

___ make up to 50ml with ddH₂O

___ add 500mg amberlite and stir for 1 h

____ filter into clean, rinsed bottle
____ 22 ml deionized urea/thiourea solution
____ 750 ul 1M Tris, not pH'd
____ 150 ul protector reagent (or 250 ul nuclease mix for #2)
____ 3 min-Complete tablets (or 500 ul protease inhibitor for #2)
____ 1g CHAPS
____ pH to 8.6 with HCL
____ make up to 25 ml
____ 1ml aliquots and store at -70°C

2X Lysis buffer (7M urea, 2M thiourea, 4% CHAPS, 2% DTT, 2% IPG) – 5 ml

____ 4.4 ml urea/thiourea solution
____ 200 mg CHAPS
____ 100 mg DTT (or 8 mg for Destreak rehydration solution)
____ 100 µl IPG 3-11NL
____ make up to 5 ml, aliquot 500 ul, and store at -70°C

Up to 150 ul diluent for cup loading and destreak (7M urea, 2M thiourea, 4% CHAPS, 0.1% DTT, 1% IPG 3-11NL)

____ 4.4 ml urea/thiourea solution
____ 200 mg CHAPS
____ 4 mg DTT

___ 50 ul IPG 3-11NL

___ make up to 5 ml, aliquot 500 ul, store at -70°C

1st dimension

Rehydration buffer (7M urea, 2M thiourea, 4% CHAPS, 0.4% DTT, 1% IPG)

___ 22 ml urea/thiourea solution

___ 1g CHAPS

___ 100 mg DTT

___ 250 ul IPG 3-11NL

___ make up to 25 ml and store 1 ml aliquots at -70°C.

Casting

Bind-silane working solution (prepare fresh) – 10 ml

___ 8 ml 200 proof ethanol

___ 1.8 ml ddH₂O

___ 200 ul glacial acetic acid

___ 12.5 ul bind-silane

Monomer solution (40% T, 3% C) – 1L

___ add 12 g Bis to 1L 40% acrylamide in the supplied bottle

___ dissolve and store at 4°C

Gel solution (12.5%) – 900ml

___ 280 ml 40% monomer solution (12% 270ml)

___ 225 ml 1.5M TrisCl pH8.8

___ 382 ml ddH₂O (12% 392)

___ 9 ml 10% SDS

___ 450 ul TEMED

___ mix and degas for at least 10 min

___ add 3.6 ml 10% APS

Gel solution (12.5%) – 450 ml

___ 140 ml 40% monomer solution

___ 113 ml 1.5M TrisCl, pH8.8

___ 191 ml ddH₂O

___ 4.5 ml 10% SDS

___ 225 ul TEMED

___ mix and degas for 20 min

___ 1.8 ml 10% APS

Gel solution (12.5%, Protogel) – 450 ml

___ 188 ml Protogel monomer solution

___ 113 ml TrisCl pH 8.8

___ 142 ml ddH₂O

- ___ 4.5 ml SDS
- ___ 225 ul TEMED
- ___ mix and make 10% APS (2ml ddH2O and 200mg APS)
- ___ add 1.8 ml 10% APS prior to pouring

Displacing solution (0.375M TrisCl pH 8.8, 50% glycerol, 0.002% bromophenol blue) – 120 ml

- ___ 20 ml ddH2O
- ___ 30 ml 1.5M TrisCl pH 8.8
- ___ 70 ml glycerol
- ___ 240 ul 1% bromophenol blue

Water saturated butanol – 110 ml

- ___ 100 ml butanol
- ___ 10 ml ddH2O

2nd dimension

Agarose sealing solution (0.5% agarose and 0.01% bromophenol blue in electrophoresis buffer)

– 50ml

- ___ 50 ml 1X electrophoresis
- ___ 250 mg
- ___ 5 mg bromophenol blue

2X SDS running buffer ([final] 15mM Tris, 192mM glycine, 0.2% SDS) – 10L

____ transfer 1.5L ddH₂O to flask

____ add 60.5 g Tris

____ add 288 g glycine

____ add 40 g SDS

____ dissolve and make up to 2 L

____ add 2 L concentrate to 8 L ddH₂O in 15 L carboy and store at room temp

Equilibration stock solution (50mM TrisCl pH 8.8, 6M urea, 30% glycerol, 2% SDS, 0.01%

bromophenol blue – 1L

____ 250 ml ddH₂O

____ 352 ml glycerol

____ 34 ml 1.5M TrisCl pH 8.8

____ 360 g urea

____ dissolve and make up to 1L

____ 20 g SDS and dissolve

____ 100 mg bromophenol blue

____ 50 ml aliquots in 50ml centrifuge tubes and store at -20C

Protocol: Cell Lysis and Crude Protein Extract

Crude protein extract

- 1) Remove cell pellets and solubilization buffer (1 tube per pellet) from -80°C and allow solubilization buffer to thaw at room temperature. Solubilization buffer should be vortexed until all components are fully in solution. No precipitated urea should be visible. The cell pellets should be placed in an ice bucket until ready for use.
- 2) Remove one cell pellet from ice bucket and add one aliquot of solubilization buffer to the cell pellet tube.
- 3) Vortex the slurry until the pellet is fully in suspension.
- 4) Transfer slurry to sonication vessel, such as 15ml sterile Falcon tube, and incubate on ice for five minutes.
- 5) Clean sonication tip with three rounds of ethanol and water. Set up beaker on a stir plate with ice water to submerge the sonication vessel into.

- 6) Fix probe into sonication vessel. The tip should be at the center of the vessel and at the midpoint of the sample slurry.

- 7) Sonicate sample for a total process time of two minutes. The cycle should be one second pulse on and .5 seconds pulse off time. Pause the sonication every 30 seconds to allow the sample to cool on ice for approximately one minute. Replace ice to the ice bath beaker as needed.

- 8) Transfer lysate to a low-bind Eppendorf tube and place the tube on ice until all samples have been processed.

- 9) Place samples into an Eppendorf centrifuge and spin at maximum speed (13,500 RPM) for ten minutes.

- 10) Transfer clarified lysate to fresh low-bind Eppendorf tube.

Protocol: First-dimension Strip Reswelling for Cup or Paper-bridge Loading

**IPG strip rehydration with reswelling tray for cup or paper-bridge loading
only**

- 1) Using a toothbrush, clean the reswelling tray with IPG detergent (or other non-ionic detergent). Rinse thoroughly with ddH₂O and air dry (if needed, use crewipes to dry).
- 2) Remove appropriate amount of Destreak rehydration solution from -20°C. Bottle contains 3 ml of solution and should be thawed at room temperature. A total of 450 µl is required per well per strip. Once thawed, vortex vigorously until white solid urea dissolves.
- 3) Add IPG buffer (or other ampholytes) to 0.5% v/v (15ul to 3ml, 60ul to 6ml).
Note: Ampholyte range should match that of the strip. However, many prefer 3-11NL ampholytes when using 3-7NL or 4-7 strips.
- 4) For right-handed persons, orient the reswelling tray so that the acidic (+) end is to the left. Acidic end has the little circular well. Pipet 450 ul of rehydration solution along the length of the channel. Do not go beyond the length of the strip.
- 5) Remove one strip at a time from the packaging. Place the remaining strips in the freezer until ready for use. Once the packaging is opened remove the strip with curved forceps.

Then use fingers to separate the protective plastic strip from the gel. Once the two have separated use the forceps to grasp the cover strip. Hold onto the back strip with fingers. Once protective strip is removed grasp the back strip (with the gel) with the forceps. Ensure that the gel side of the strip is facing down when placed in the reswelling tray. Introduce the basic end first into the channel at the furthest point where the Destreak solution was added. Then gradually introduce the strip into the channel making sure that the Destreak solution is evenly distributed along the strip. The acidic end should be over the small well holes.

- 6) Cover each strip with 3.4 ml of Drystrip cover fluid (mineral oil).
- 7) Insert cover and balance with black knobs and balance indicator in the reswelling tray.
- 8) Incubate strips for 20-30 hours at room temp.

Protocol: Casting Analytical Gels

(Analytical: gels not bound to plate; used for imaging only)

14 gels in large gel box: for smaller gel box (6 gels) use volumes in parenthesis.

Reagent prep:

Gel solution (12.5%) – 900ml; mix in flask with spout for vacuum tube

____ 280 ml (147ml) 40% monomer solution

____ 225 ml (117.5ml) 1.5M TrisCl pH8.8

____ 382 ml (196ml) ddH₂O

____ 9 ml (4.7ml) 10% SDS

____ 450 μ l (188 μ l) TEMED

____ mix and degas for at least 10 min (place clean mouse pad over mouth, attach vacuum tube to spout and turn on. Vacuum is adequate when mouse pad dimples into mouth of flask)

10% APS – 4ml

____ add 1g APS to 9.6ml ddH₂O

____ add 9.4 ml (4.7 ml) fresh 10% APS (**add immediately prior to pouring**)

Displacement solution – 120 ml

____ 20 ml ddH₂O

____ 30 ml 1.5M TrisCl pH 8.8

____ 70 ml glycerol

____ 240 ul 1% bromophenol blue

Protocol

- 1) Clean plates and dry with Kimwipes or allow to air dry
- 2) Prepare solutions
- 3) Load gel box and level. Place thin spacer first in the box, push as far as possible to the left of the box with the “wonder wedge.” Then place the back plate with the spacer and push to the left. Finally, place the top plate and push as far to the left. Place another thin spacer. Repeat this until six complete sandwiches are in place. Then fill the remainder of the box with the thick spacers until they are flush with the edge of the box. Place gel-seal around the perimeter of the caster on the grey gasket. Gently smear with single gloved finger. Place the front of the caster onto the back. Gently tighten the screws on the bottom of the caster. Place the red and black clamps, and then fully tighten the screws on the bottom. Ensure that the seal is tight (the gel-seal will spread).
- 4) Add 10% APS to gel solution and mix gently; prevent formation of bubbles (There is SDS in this solution!!!)
- 5) Pour gel solution directly from the flask slowly until 1cm below top of front plate Add displacement solution to large gel caster only
- 6) Overlay each gel with 1ml water saturated butanol with a 1ml pipette. Be sure to introduce between the plates of the gel sandwich. Drag pipette smoothly from one end of the sandwich to the other. Be consistent in application for each sandwich!

- 7) Allow to polymerize for at least 1.5 hours
- 8) Remove sandwiches, trim excess acrylamide, rinse thoroughly with double deionized water, and lay clean gels on plastic wrap. Fold plastic wrap over the bottom half of the gel to create a pocket. Then add gel storage solution (approximately 10 ml total) to the bottom, the notch on the top and the sides. Fold plastic wrap to enclose all of the gel solution.
- 9) Allow to polymerize overnight at room temperature lying horizontally. Then in the morning place at 4°C until ready for use. Make sure that the gel is moist and that the gel storage solution was not lost. If they gels dry out they are useless.

Protocol: Casting Preparative Gels

(preparative: gels bound to plate. To be used for spot picking and MS analysis)

- 1) Prepare 2L of 1% HCL
- 2) Pour 1.5L 1% HCL into staining bucket

- 3) Insert plates to have gels bound to (decide if top or back plate. Must be consistent!!!)
stack carefully on top of each other
- 4) Incubate at 30 rpm for 2h
- 5) Wash top plates with 1% Decon Labs detergent (Do not use excessive detergent or time-
the plates will become etched and ruined). Rinse with deionized water, then double
deionized water and shake off excess water and leave to dry protected from dust
contamination
- 6) Repeat (5) with acid-treated plates
- 7) Prepare 4 ml bind solution per gel
Bind-silane working solution – 10 ml
 ___ 8 ml 200 proof ethanol
 ___ 1.8 ml ddH₂O
 ___ 200 ul glacial acetic acid
 ___ 12.5 ul bind-silane
- 8) Place dried plate on clean surface with face to have gel attached facing up.
- 9) Evenly spread 4 ml bind solution over each plate and allow Bind solution to cure before
covering. Then cover to protect from dust and let sit for one hour.
- 10) Place markers two cm away from spacers and 10.5 cm from bottom and allow plates to
sit for an additional hour. When placing the markers be sure to be consistent on each
plate. If placing markers on the top plate make sure to accommodate for the space that
the spacers on the back plate will take up. Make a template to follow to ensure that the
markers are placed consistently.

11) Prepare solutions according to **Casting (analytical)** protocol

12) Wipe treated plates with 200 proof ethanol before loading caster and let them sit several minutes before placing in the caster. The bind solution will volatilize and stick to the opposite plate if not allowed to vent properly. If binding to the top plate make sure that the face with the bind solution is placed on the inside of the gel sandwich (facing the back plate).

Protocol: Pyruvate Dehydrogenase Assay

Read absorption at 500 nm at 25°C

Reagents:

Reaction solution: (2.5 mM NAD, 0.2 mM thiamine pyrophosphate, 0.1 mM Coenzyme A, 0.3 mM DTT, 1 mM Magnesium chloride, .6 mM INT) Make up in 10X solution to accommodate small masses of additives. Make reaction solution up to a total volume of 10 ml

First add 7 ml of double deionized water then add the following components

17 mg of NAD (MW 685.41)

.9 mg of Thiamine Pyrophosphate (MW 460.77)

.767 mg of Coenzyme A (MW 767.53)

.462 mg of DTT (MW 154.25)

.952 mg of Magnesium Chloride (MW 95.21)

3.03 mg of INT (MW 505.70)

Then store the reaction solution at 4°C until ready for use.

Make up fresh pyruvate (MW 110.04) prior to use. Start with a 4X solution of 5mM pyruvate by adding .55 mg into 10 ml of double deionized water.

Cell prep:

Disrupt the cells to be assayed into appropriate lysis buffer (50 mM PBS) and centrifuge at 10,000 x g for 10 minutes to pellet any cellular debris. Collect the supernatant and discard the pellet. Remove 10 µl to use in quantification of the amount of protein present in the lysate.

Adjust the final concentration of all samples to 1 µg/µl with 50 mM PBS.

Add the same volume of crude enzyme extract into each reaction vial (3 replicates per sample).

Then take a base line OD before the pyruvate is added. This value will be subtracted from each sample to determine the difference in slope between the control and experimental conditions.

To start the reaction mixture add an appropriate volume of 5 mM pyruvate (MW 110.04) to start the reaction. Then read the OD at 500 nm at 25°C

In order to obtain the correct concentration of reaction mixture, pyruvate solution, and protein concentration make up the solution in the following manner:

Total volume in each reaction vial 1.5 ml

Make up a 10x solution of the reaction mixture and add 150 µl

Then make up a 4x solution of pyruvate and add 375 μ l

Then calculate the volume of crude sample needed to add the same concentration to each vial x and subtract from (150 + 375 = 525). Take that value and add that volume of water

$$525 - (X \mu\text{l of crude lysate}) = \text{vol. of water}$$

* This gives you 975 ml to work with

The goal is to have the total volume in the vial at 1.5 ml

Then remove 300 μ l and assay in the Victor at 490nm and take 1 ml and assay in the Turner at 500nm.

Protocol overview:

1. disrupt cells
2. quantify and adjust concentration to 1 μ g/ μ l with 50 mM PBS
3. Add lysate and reaction mixture without pyruvate and take OD
4. Add pyruvate and measure color change
5. Calculate the difference between the two slopes (with and without pyruvate) to determine the rate of activity

Protocol: *C. elegans* Virulence Assay

Assay for fast killing (based on high salt medium use high osmolarity PGS media). The fast killing assay should be scored 8 hours post inoculation.

Grow *P. aeruginosa* and *E. coli* 0P50 control overnight in LB medium to an approximate OD₆₀₀ nm of 1.

Inoculate assay Petri plates (5.5 cm) with 10 µl of cell suspension and spread over plate with glass spreader incubate for 16 hours at 37°C and 24 hours at 25°C

Seed plate with 20-30 L4 stage *C. elegans* once seeded incubate at 25°C

Score after 8 hours (% live organisms compared to survival on the *E. coli* 0P50 control strain. Considered dead when touched by a metal probe and no response)

Assay for slow killing (based on low salt medium use NG medium) follow protocol above but score after 3 days.

Media

NG: Nematode growth medium source US biologicals

Agar 17.5 g/L

Sodium Chloride 3.0 g/L

Peptone 2.5 g/L

Cholesterol 0.005 g/L

Total:

23.005g/L

500g makes 21.7 liters

Directions per Liter:

Dissolve 23.005 grams per liter of distilled/deionized (DDI) water. Heat with stirring until completely solubilized. Adjust pH as necessary. Dispense into appropriate containers. Loosen caps or cover with foil. Autoclave for 15 minutes at 121°C (15psi).

Cooling the N1000 solution:

Place the sterile N1000 solution into the water bath

N1000 solution needs 31 hour to cool to the desired temperature (58°C). If the media is not properly cooled when the CaCl₂, MgSO₄ and K₂PO₄ are added, crystals will form in the agar.

Further preparing the media:

Once the N1000 solution has cooled to 58°C, place flask(s) onto stir plate(s). Maintain temperature at 58°C Add the following:

- a) 1M K₂PO₄, pH 6.0: 25ml/liter N1000 solution
- b) 1M CaCl₂: 1ml/liter N1000 solution
- c) 1M MgSO₄: 1ml/liter N1000solution

Allow the solution to mix for five minutes before starting to pour plates to ensure that a

homogeneous mixture has been achieved.

Storage and Stability:

Store powdered media at RT. Opened bottles should be capped tightly and kept in a dark, low humidity environment. Prepared media should be kept at 4°C and used within a short period of time

PGS medium per Liter

1% Bacto peptone

1% NaCl

1% glucose

0.15M sorbitol

1.7% Bacto agar

LB medium

* grow on 5 g NaCl in place of 10 g NaCl